

Design of 42V/3000W PERMANENT MAGNET SYNCHRONOUS GENERATOR

By

Guruprasad Mahalingam , M.S. Student

Prof. Ali Keyhani

Mechatronics System Laboratory

DEPARTMENT OF ELECTRICAL ENGINEERING

THE OHIO STATE UNIVERSITY

Keyhani.1@osu.edu

Phone: 614-292-4430

December, 2000

Acknowledgments

I wish to thank my adviser, Professor Ali Keyhani, for his insight, support and guidance which made this work possible.

This work was supported in part by the Delphi Automotive Systems, The National Science Foundation: Grant ESC 9722844, 9625662, Department of Electrical Engg., The Ohio State University. I also wish to thank Ford Motor Company, TRW, AEP which support the work at Mechatronics Systems Lab.

I wish to acknowledge Mongkol Konghirun, Coy Brian Studer whose earlier work in the field was a ready reference to my work.

My sincere thanks to Dr. Tomy Sebastian, Delphi Saginaw Steering Systems for his support, advice, and interest in my research; Mr. Philippe Wendling from Magsoft Corporation for his technical assistance.

CHAPTER 1

Machine Design - Introduction And Basics

1.1 Background

Transforming the classical mechanical and hydraulic systems into electric systems to provide better performance and customer satisfaction is the current trend in the automotive industry. Eg. electric power steering systems, electric brakes etc.. The penalty is the increase in demand for electrical power. It is estimated that the steady state power requirement in the typical luxury class vehicle would rise from the current level of 1500 W to about 3000 W and to about 7000 W for a hybrid electric vehicle by the year 2005 [16,17,2]. The requirements of increased electrical power, improved fuel economy and reduced emissions have imposed the necessity of developing more efficient power systems for the future applications. At this level of power demand, the current 12V bus voltage becomes inefficient and a new voltage standard is needed in order to enable an efficient operation of the system.

The Consortium for Advanced Automotive Electrical/Electronic Components and Systems, organized and coordinated by MIT and having members from about 30 Companies have been working to establish the level of 42 V as the new voltage standard [16,17,2]. In fact, the close future electric system will be a dual voltage one (42 V and 12V), this is mainly due to the time that must be allowed for the car manufacturers to adapt and redesign all their systems based on the new voltage level [16].

The level of dual voltage is 14/42 V for two 12-V and 36-V batteries rather than 14 V in single voltage system. The first advantage is associated with the wire cost in the system. With delivering the same power, the 42-V system supply only one-third of the current required at 14-V system. Consequently, the wire size can be reduced in the 42-V system, causing decrease in cost, weight of wire. However, the minimum wire size is constrained in order to provide sufficient mechanical strength. As a result, with the same wire size, the wire/copper loss in the 42-V system is decreased three times that in the 14-V system [16,17,2]. The second advantage is related to the electrical load flexibility in rated voltage. The electrical loads are separated with their power consumption. The high-power loads are generally allocated to the 42-V bus, while the incandescent lamps and low-power electronics loads are allocated to the 14-V bus.

1.2 Electric machines for automotive applications

Lundell alternator, a three phase claw poles synchronous machine has been the traditional generator in vehicles. Although relatively inefficient, this solution has met the requirements in a cost-effective manner, mostly due to the low level of power demand (approx. 1.2 KW). An attempt to adopt a more efficient machine was not justified from the cost point of view because the machine had a low absolute value loss (a couple hundred watts). With the power demand at the level of 3 KW, the value of the losses in the machine becomes important and performance improvement is necessary. The attempt to improve the performance of the Lundell machine has proved to be ineffective [16,17,2]. The claw pole alternator has almost reached its limits in terms of efficiency and output power.

In view of the above problems, the idea of replacing it with a more efficient and compact machine has become apparent. In order to meet the requirements of fuel economy and affordable cost at the power level mentioned before (3-7 KW), the designer of such a system should consider constraints as: high efficiency, small size, light weight and safety. There were several candidates to be considered as replacements for the lundell generator and they are:

- ❖ switched reluctance machine
- ❖ induction machine
- ❖ permanent magnet machine
- ❖ permanent magnet hybrid machine

Each of the above specified solutions provide specific characteristics and have their own positive and negative points in their favor.

This research addresses the problem of designing a system using a permanent magnet machine, similar to that presented in Fig 1.2.

A choice of unidirectional AC/DC power converter is presented and the PM synchronous machine is designed to fit the loads on the DC side by using this converter topology.

1.3 Power system in a vehicle

1.3.1 Current Power System

The current power system is presented in Fig 1.1 :

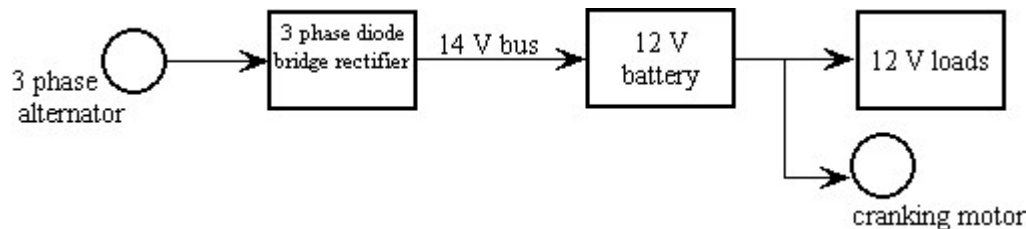


Figure 1.1 present automotive electrical power system [17]

This consists of a three phase alternator, a three phase diode bridge and a 12 V battery. The diode bridge converts the AC power generated by the alternator into 12 V DC power which is supplied to the loads through the battery. The output voltage of the machine is regulated by controlling the field current of the alternator.

1.3.2 Future Power System

The block diagram of the future power system is presented in Fig 1.2:

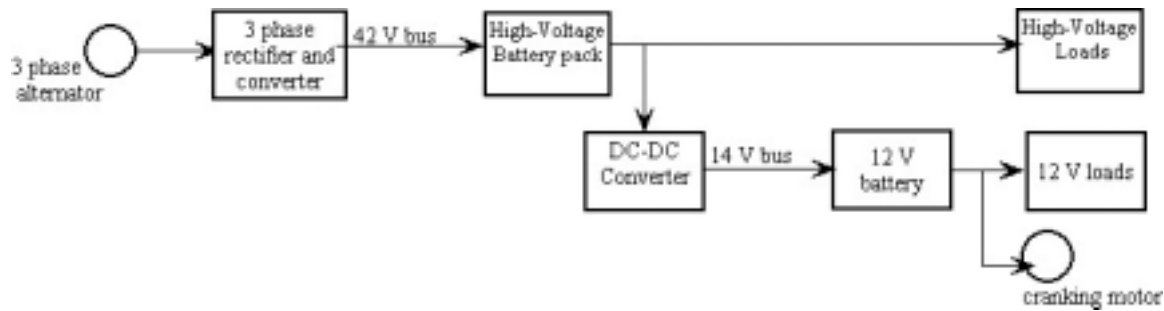


Figure 1.2 : Future automotive electrical power system [17]

This system consists of a three phase alternator, rectifier, high voltage battery packs (36V), a DC/DC converter and a low voltage battery (12V). The rectifier (AC /DC converter) is fed by the alternator and is connected to the high voltage loads and is charging the 36 V battery. A DC/DC converter supplies the low voltage loads and also charges the 12 V battery. The 12V battery is used to crank the motor and also to supply the low voltage loads, examples of such loads are: lights, clocks and radio - some of which require continuous supply in order to keep their memories alive. This dual voltage system is flexible for future expansion.

1.4 Problem statement

1.4.1 Speed of the Generator

At what running speed do we design the generator is the question which is to be answered for a successful design . Generally we know the voltage developed in a generator, E is $E \propto \omega$ or $E = k_1 \omega$ (1.1)

where ω = speed of revolution

k_1 = constant of proportionality

Equation 4.1 implies that if we design the generator at higher speed , then for the same voltage E to be developed , k_1 the constant which depends on sizing and other constants can be made less. ie. Higher the operating speed ,lower the size of generator , for the same output voltage.

Consider the following case, where the driver "switches on" all the loads at idle speed. This would drain the power from battery necessitating the need to charge the battery even at idle speed. *Taking into consideration this worst case also, we design the generator to generate at optimal efficiency at idle speed.* This would make sure we charge the battery even at idle speed. Since we know $P = V * I$ (1.2)

This design of required potential E to be developed at idle speed, would mean , we already have the highest current and therefore the highest current density in the winding. At this highest current density, we design the coil insulation . this gives no possibility of increase in current density and therefore no more increase in I^2R losses and hence we could assume the insulation to be intact always. At higher speed, for the same power P, we have lesser current because we develop more E. this would imply lesser I^2R losses.

Thus by designing the generator for idle speed we ensure

- We always charge the battery
- We support all loads even at idle speed without draining the battery

- Insulation would stay intact for all speeds, because we have designed it for the highest current density and hence highest I^2R losses.

The idle speed of IC engine = 600 rpm. We use a gear ratio of 3/3.1 and feed it into the shaft of generator. Hence idle shaft speed (generator) = 1800 rpm.

Hence we design the generator to supply 3000 W /50 V at 1800 rpm.

1.4.2 System Topology

1.4.2.1 Present Topology

The proposed structure has a rectifier (6 diode bridge, not commanded) which converts a 3 phase square wave voltage with a line to neutral voltage $V_{LN} = 22V$.the system of 50 V is designed assuming the lowest power factor for the rectifier/ converter. Thus we assume a low power factor of 0.84. If the power factor for the rectifier/converter be increased we could feed a lower voltage which implies a smaller machine. But the current design is made for all the worst cases ie (1) low power factor , (2) idle running speed .

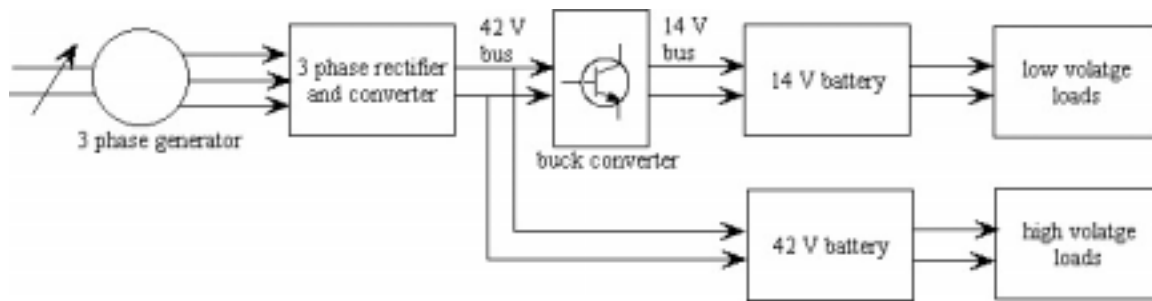


Figure 1.3 : Present Topology

The shaft of the generator is rotating at speeds between 1800- 18000 rpm. The output phase voltage of the machine varies directly in proportion to the speed of the shaft. This has some potential drawbacks which are stated below

Since the output voltage of machine can be very high at very high speeds the diodes of the 3 phase bridge and semi-conductor devices of DC-DC converter have to be rated for higher break-down voltages. The semiconductor devices that are rated for high break-down voltages have high losses and lower system efficiency. They also are very costly.

The diode switching frequency varies from 60-600 Hz (speed range of 1: 10). At a speed of 18000 rpm we have $f = \frac{p * n}{120} = \frac{4 * 18000}{120} = 600\text{Hz}$. Using one bridge only to regulate the voltage over the entire engine speed range (1: 10) results in pulsed currents associated with ohmic losses in both alternator and the regulator (rectifier & converter) at very high switching frequency.

The converter supply voltage varies in the range of 1:10 , hence its time period for conduction to maintain same output voltage must be in the range of 1:0.1 at a constant switching frequency.

Both conditions at diode and at converter will give rise to lot of transients and more losses. Also output voltage may not be steady voltage because of transients.

1.4.2.2 Changes In Topology For Optimal Design

To overcome the above mentioned drawbacks the following remedy could be applied as mentioned in [21].

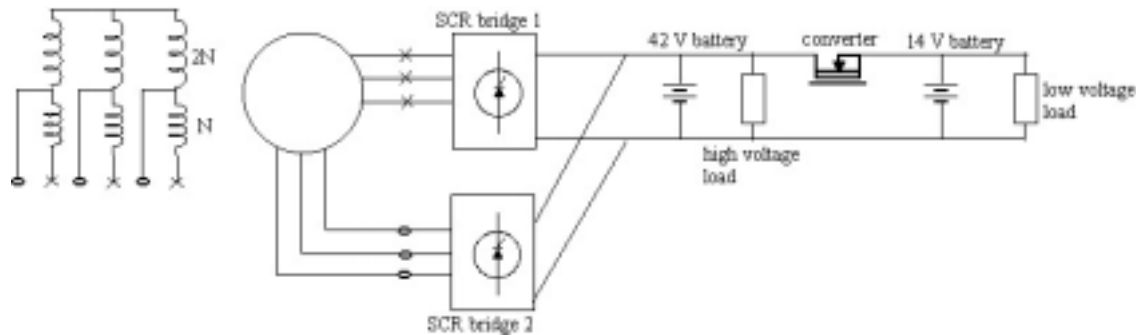


Figure 1.4 : Changes in Topology for Optimal Design [21]

Instead of the diode rectifier a dual-SCR could be used which could function as a rectifier. SCR bridge which is connected to the winding set with higher number of turns is activated to control the output voltage from idle speed n_j to a speed $n_i = 3 * n_j$. Above n_i the bridge is connected to the winding set with lower number of turns, which is sufficiently high to provide the system voltage. Beyond n_i this bridge (lower) is activated while deactivating the other bridge simultaneously. The switching of bridges is done automatically in a fraction of a second without any impact on the electrical system and completely transparent to the passengers. After switching, the currents flow through only small part of stator windings ($1/3$) thus producing only $1/3^{\text{rd}}$ copper loss.

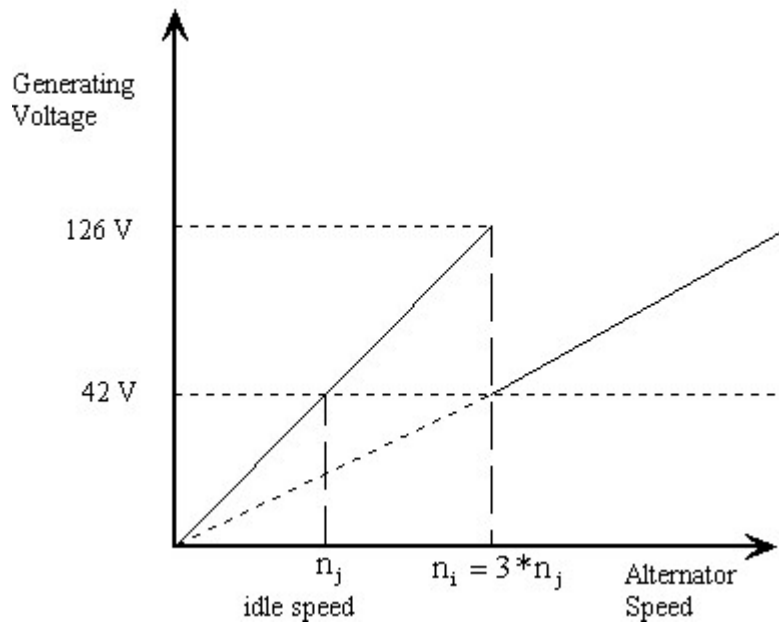


Figure 1.5 : Voltage Generated Vs Speed Range [21]

Further speed range covered by each bridge is approximately 3:1 only instead of 10:1 and as a result currents are less pulsed generating less heat.

1.4.2.3 Problem Statement

The optimal design of permanent magnet synchronous generator in the single-excitation PMSG system is mainly addressed in this thesis. The optimal machine geometry which generates the required power at stated voltage is to be designed at minimum power losses and minimum power weight is provided. The studied structure of PMSG is 3-phase, 4-pole, and 12-slot machine. The full pitched stator windings result in square waveform of output ac voltage. The parallel coils for each phase would be designed because the high current capability of loads. The Nd-Fe-B permanent magnet is selected because of its properties of high both H_c and $(B \times H)_{max}$. The machine parameters are solved by the use of a Matlab function, *fmincon*, an inequality constrained multi-objective optimization function. *fmincon* uses medium scale Sequential Quadratic Programming (SQP), Quasi-Newton, Line-search algorithms. The electrical parameters the temperature rises, maximum output current and efficiency of the machine are evaluated in this thesis.

When looking at the single-excitation PMSG system, the PMSG with a three-phase diode bridge rectifier can be shown in Figure 1.6. If the output dc voltage and output dc current of three-phase diode bridge rectifier are $2E$ and I , respectively.

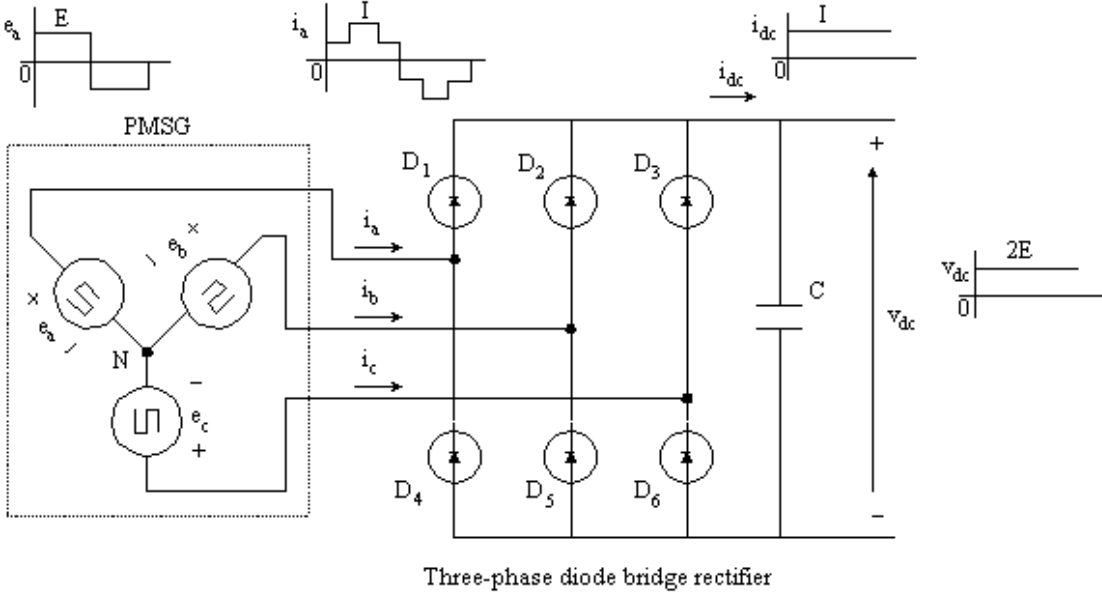


Figure 1.6 : PMSG with a three-phase diode bridge rectifier [2]

Since the dc/dc buck converter is employed to regulate dc voltage from the speed variation, that is supposed to be 1800-18000 rpm, the rated speed of PMSG would be specified at the lowest speed, that is 1800 rpm.

(A) Determination of Machine Rated Values

The variable frequency variable magnitude of 3 phase system voltages from the PM machine (Square Wave Excited) is rectified by an uncontrolled rectifier. The presence of the

inductor with the rectifier on the DC side allows us to have a constant current at the output of the rectifier. The circuit topology we use is given below

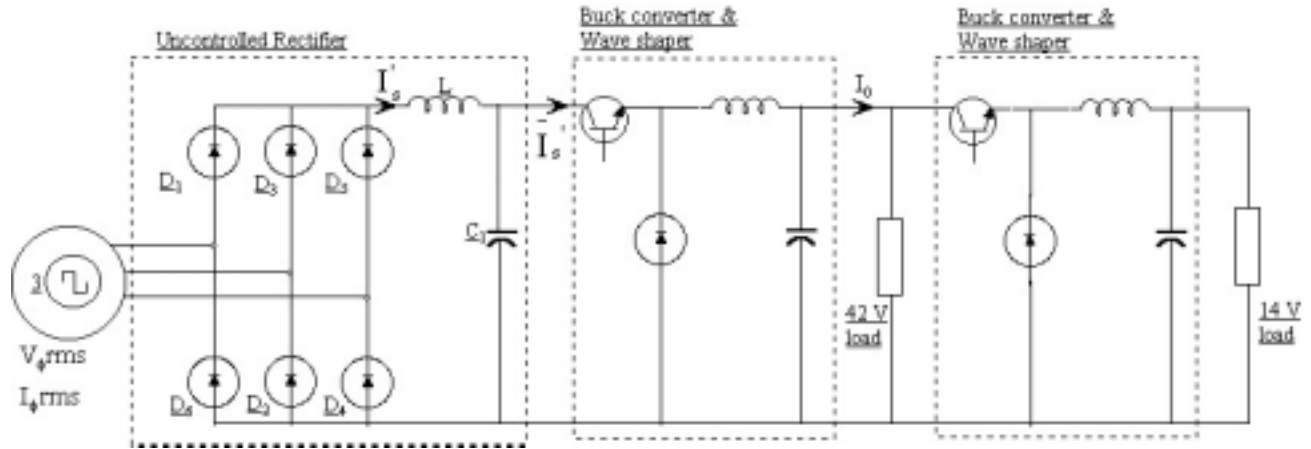


Figure 1.7 : Power System in the automobile [21]

The output rectified voltage of the machine is a function of machine speed (n) at the generator shaft. This is to be converted to a 42 V DC level through a step-down (buck) converter whose duty cycle is varied as a function of shaft speed to get the required $V_0 = 42$ V output. We therefore should have the basic criteria as

- Output voltage $V_0 = 42$ V.
- Power consumed by the load $P=3000$ W.
- The aim then is to find
- Machine phase rms value of voltage and current
- Apparent power to be developed by the machine.

(B) Assumptions

- ❖ Minimum speed of piston = 600 rpm. Gear ratio used = 3:1 .
- ❖ Therefore minimum speed at the shaft of the machine = 1800 rpm.
- ❖ At minimum speed the converter duty cycle, $D = 1$.
- ❖ The converter output voltage $V_0 = D V_{in}$.
- ❖ The current fed into the converter is (I'_s) continuous .
- ❖ Efficiency of step down converter is $\eta = 0.95$

(C) V_ϕ , I_ϕ , Apparent Power Of Machine

We know at the converter

$$P_{in} = P_{out} \tag{1.3}$$

$$P_{out} = V_0 I_0 = 3000W \tag{1.4}$$

$$P_{in} = \frac{V_s I_s}{\eta_{buck}} = \frac{V_0 I_0}{D \eta_{buck}} \tag{1.5}$$

For $D=1$ and $\eta_{buck}= 0.95$, we compute;

$$V_s = \frac{V_o}{D} = 42V$$

$$I_s = \frac{P_{out}}{V_s} = 75.18A$$

For a square wave voltage , we know $V_{\phi rms} = V_{\phi peak}$ (1.6)

Also from the rectifier structure $V_s = V_{LL} - V_{is} - V_r$ (1.7)

where: $V_{LL} = 2 * E =$ line-line voltage at the input of the rectifier.

V_{is} = voltage drop due to phase inductance , assumed to be 4V.

V_r = voltage drop on switches in conduction , assumed to be 4V.

$$V_s = 42 = 2E - 8 \Rightarrow E = 25V \quad (1.8)$$

Hence we have $V_{\phi rms} = V_{\phi peak} = 25V;$ $I'_s = 75.18A$ (1.9)

The PM machine considered here has 4 poles ie 2 pole pairs

$$\omega = 2\pi f = \frac{2\pi p n}{60} = \frac{2\pi * 2 * 1800}{60} = 120 * \pi \quad (1.10)$$

For a square wave machine , we know $I_{\phi rms} = \frac{I'_s}{\sqrt{2}}$ (1.11)

$$I_{\phi rms} = \frac{75.18}{\sqrt{2}} = 53.16 \quad A \quad (1.12)$$

The apparent power of the machine

$$S = 3V_{\phi rms} I_{\phi rms} = 3 * 25 * 53.18 \quad A \quad (1.13)$$

$$S = 3987.02 \quad VA$$

(D) Power factor seen by the PM machine

We can determine the power factor imposed by the converter circuit to the AC line:

$$pf = \frac{P}{S} = \frac{V_s I_s}{S} = \frac{42 * 75.18}{3987.02} = 0.79 \quad (1.14)$$

In our design of a 4 pole/ 12 slot machine we would be looking at double layered windings. Therefore Number of coils/phase = 4. For an ideal voltage and current sharing among these coils , we feel the following circuit would help to reduce losses.

Each coil handle only half the voltage and current requirement.

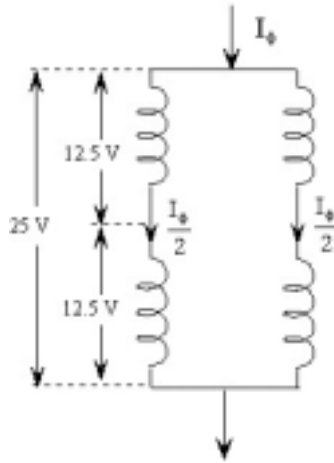


Figure 1.8 : Arrangement of coil in one phase

Finally, the specification of PMSG can be summarized as follows. To design the high voltage side of an automotive power system using a PM synchronous machine. The system has the following characteristics

- ✓ Voltage level on the high voltage bus $V_{DC} = 42$ V
- ✓ Speed range at the generator shaft $n = 1,800 - 18,000$ rpm
- ✓ Square wave output voltage/phase of 25 volt (peak).
- ✓ Quasi-square wave output current/phase of 53.18 amp (rms).
- ✓ Uniformly distributed winding with full coil pitch.
- ✓ Minimum power losses and minimum machine weight.

Reference

- [1] J.R. Hendershot Jr. and T.J.E. Miller, 'Design of brushless Permanent Magnet Motors', *Magna Physics Publishing and Clarendon Press, Oxford, 1994.*
- [2] Mongkol Konhirun, 'Optimal Design of Permanent Magnet Synchronous Generator', *a Master's Thesis in the Dept. of Electrical Engineering, The Ohio State University, 1999*
- [15] Huang S., Luo J, Leonardi F., Lipo T.A. , 'A General Approach to Sizing and Power Density Equations for Comparison of Electrical Machines', *IEEE Transactions on Industry Applications, vol. 34 NO 1, January/February 1998.*
- [16] J.M. Miller, D. Goel, D. Kaminski, H.P. Schoner and T.M. Jahns 'Making the case for a next Generation Automotive Electrical System', *Ford Motor Co. .*
- [17] I.A. Khan, 'Automotive Electrical : Architecture and Components' *Delphi Automotive Systems.*
- [21] M. Naidu, N. Boules and R. Henry, ' A High-efficiency, High Power Generation system for Automobiles' , *IEEE Transactions on Industry Applications Society, 1995.*

CHAPTER 2

Two Dimensional Finite Element Analysis

2.1 Overview of the Maxwell 2D Field Simulator from Ansoft

This section provides an overview of the Maxwell 2D Field Simulator from Ansoft. It includes a general discussion of the steps needed for analysis as well as the theory used for solving the magnetostatic field problem. Refer [6] for further details.

2.2 General Procedure

Figure 2.1 displays the procedure used to perform an analysis using the Maxwell 2D Field Simulator from Ansoft. The theory involved with magnetostatic fields is further discussed in section 2.3.

Solid object modeling is used to create the geometry. This basically entails combining and subtracting cubes and cylinders of various dimensions from one another until the desired geometry is achieved. The units, co-ordinates, and problem region are also established during this step. Material properties, from either a pre-existing database or user-created input, are assigned to the various geometric regions of the model.

Boundary conditions are automatically assigned to the interfaces between objects in the model and to the outer boundary of the problem region. The Maxwell 2D Field Simulator from Ansoft must be supplied with information concerning the type of solution desired as well as solution accuracy before we solve the problem.

The Maxwell 2D Field Simulator from Ansoft adaptively solves the problem until the specified stopping criteria are met. During the computation, data involving the executive parameters, mesh, convergence, and system demands is continually updated. Plots relating to the magnetic field can be obtained from the post processor.

2.3 Theory

For magnetostatic field problems, the Maxwell 2D Field Simulator creates an initial mesh, solves the field problem using this mesh, performs an error analysis, refines the mesh, and repeats the process until the stopping criteria are met. The current density solution is used as an input for the magnetic field computation. The energy and residual associated with the magnetic field are also computed. The energy and residual determine when the field solution has converged.

2.3.1 The Finite Element Mesh

The Maxwell 2D Field Simulator from Ansoft uses triangular for its mesh elements. For a magnetostatic problem, the magnetic field is divided into its homogeneous and particular solution. A scalar potential associated with the homogeneous solution is stored at the nodes of

each element . When the convergence, or stopping, criteria are not met, the elements having the largest energy error are further subdivided into smaller tetrahedral elements. The percent refinement per pass that the user specifies in the solution criteria module determines the amount the mesh is refined.

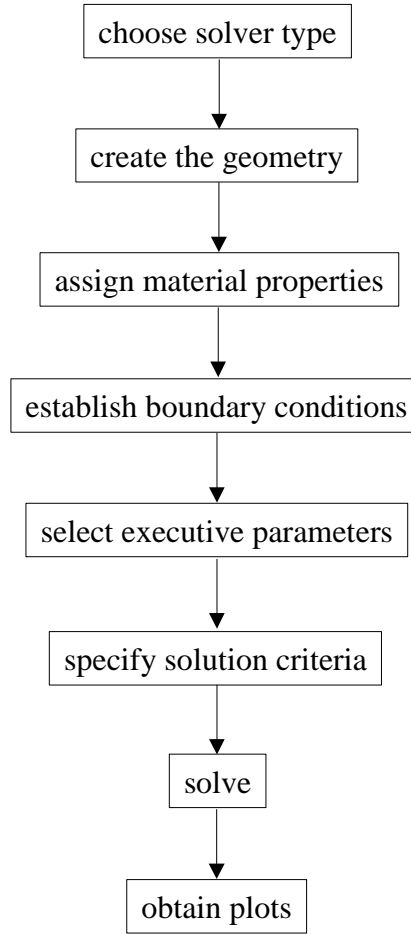


Figure :2.1 General Steps Required for the Three Dimensional Analysis Using the Maxwell 2D Field Simulator from Ansoft [6]

2.3.2 The Current Density Calculation

The current density is given by:

$$\mathbf{J} = \sigma \mathbf{E} = -\sigma \nabla \phi, \quad (2.1)$$

where \mathbf{J} is the current density in Amperes per meter, σ is the conductivity in Siemens per meter, \mathbf{E} is the electric field in volts per meter, and ϕ is the electric potential in volts. By Gauss' law (in an infinitely small region the amount of charge leaving is equal to the amount of charge entering that region), the charge density, $\rho(x,y,z)$, is time invariant:

$$\nabla \cdot \mathbf{J} = \frac{\partial \rho}{\partial t} = 0. \quad (2.2)$$

Substituting equation 2.1 into 2.2:

$$\nabla \cdot (\sigma \nabla \phi) = 0. \quad (2.3)$$

Equation 2.3 is solved in the solution process for the current density. Refer [6] for further details.

2.3.3 The Magnetic Field Calculation

The magnetic field from Ampere's Law and Maxwell's equation for flux using the current density as an input:

$$\nabla \times \mathbf{H} = \mathbf{J}, \quad (2.4)$$

$$\nabla \cdot \mathbf{B} = 0, \quad (2.5)$$

where $\mathbf{H}(x,y,z)$ is the magnetic field in Amperes per meter, $\mathbf{B}(x,y,z)$ is the magnetic flux density in Tesla, and $\mathbf{J}(x,y,z)$ is the previously calculated current density in Amperes per meter. The magnetic flux density and magnetic field are related by:

$$\mathbf{B} = \mu_r \mu_o \mathbf{H}, \quad (2.6)$$

where $\mu_r(x,y,z)$ is the relative permeability, and μ_o is the permeability of free space ($\mu_o = 4\pi \cdot 10^{-7}$ H/m).

2.3.4 The Boundary Conditions

Boundary equations are needed to solve the partial differential equations given by equation 2.1 through 2.6. A Neumann boundary condition is automatically assigned to the outer boundary of the problem region because the magnetic field does not penetrate the surface of a Neumann boundary.

Natural boundary conditions are automatically assigned to the interface of objects in the model. This type of boundary has a continuous tangential component of the magnetic field given by:

$$\mathbf{H}_{T1} = \mathbf{H}_{T2} + \mathbf{J}_s, \quad (2.7)$$

where \mathbf{H}_{T1} and \mathbf{H}_{T2} are the tangential component of the magnetic field in Amperes per meter for region 1 and 2 respectively, and \mathbf{J}_s is the surface current density in Amperes per square meter at the interface between region 1 and 2. Likewise, the normal component of the magnetic flux density is continuous for a natural boundary. Periodic boundaries can also be simulated with appropriate boundary conditions.

2.3.5 The Solution Process

The Maxwell 2D Field Simulator first solves for the current density then uses it as input for the magnetic field calculation. Once the current density is computed, it is used as an input, as are the boundary conditions, for the magnetic field calculation. Recall, the magnetic field is computed at the nodes of the triangular elements making up the mesh for the problem. For nonlinear materials, the Newton-Raphson method is used to compute the magnetic field. The Newton-Raphson method uses the slope of the BH curve to obtain a linear approximation of the field within the nonlinear material. As with the current density calculation, the mesh is refined until the specified stopping criteria for the magnetic field energy are met.

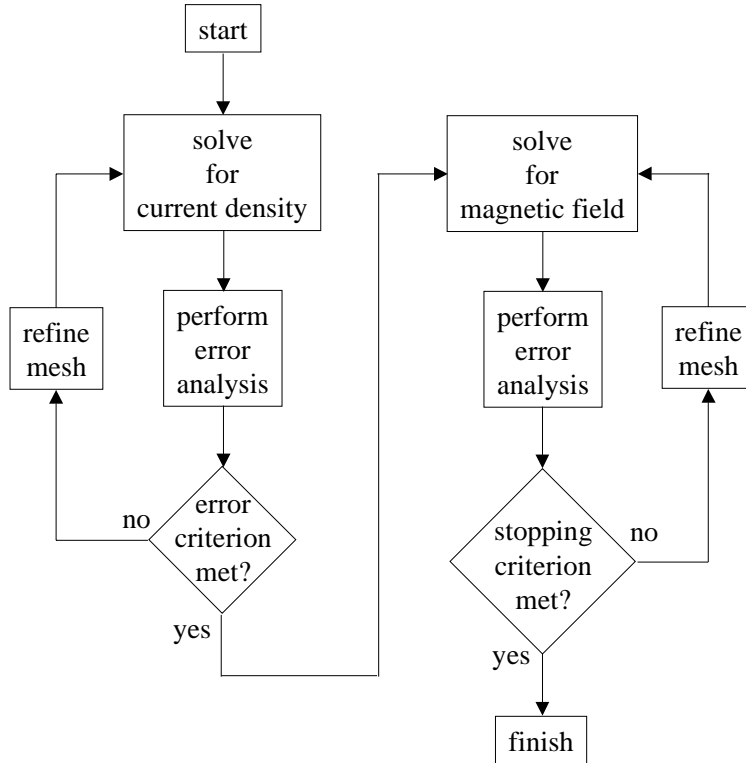


Figure :2.2 Maxwell 2D Field Simulator Magnetostatic Solution Process [6]

2.3.6 The Energy and Co-energy of the Magnetic Field

The magnetic field energy is given by:

$$U = \frac{1}{2} \int_V (\mathbf{B} \cdot \mathbf{H}) dV, \quad (2.8)$$

for linear materials and:

$$U = \frac{1}{2} \int_V (d\mathbf{B} \cdot \mathbf{H}) dV, \quad (2.9)$$

for nonlinear materials where U is the magnetic field energy in Joules, \mathbf{B} is the magnetic flux density in Tesla, \mathbf{H} is the magnetic field in Amperes per meter, and V is the volume in cubic meters.

The co-energy of the magnetic field is given by:

$$W = \frac{1}{2} \int_V (\mathbf{B} \cdot \mathbf{H}) dV, \quad (2.10)$$

for linear materials and:

$$W = \int_V (\mathbf{B} \cdot d\mathbf{H}) dV, \quad (2.11)$$

for nonlinear materials where W is the co-energy of the magnetic field in Joules. Comparing equation 2.8 to 2.10, the energy and co-energy of the magnetic field in linear materials are equal.

2.3.7 The Solution Criteria

The solution criteria consists of two groups: the residual values and the adaptive analysis data. The residual values, determine the tolerance for the residuals in the energy calculation. The adaptive analysis data consists of the percent refinement per pass and stopping criteria subgroup. The percent refinement per pass determines how the mesh is modified during the adaptive analysis when the stopping criteria are not satisfied.

The stopping criteria subgroup contains information used to determine when the iterative process is complete. The stopping criteria consists of the number of requested passes and the percent error. The percent error is the percentage of total energy contributed by the energy residual. Since the residual corresponds to the energy error, the percent error determines the accuracy of the solution. The percent error also corresponds to the percent change in energy between subsequent iterations. This indicates the solution has converged.

Criterion	Default value	
	Conduction Current	Magnetic Field
Residual:	-	-
solver	-	1×10^{-8}
linear	1×10^{-6}	-
nonlinear	0.01	-
Adaptive analysis:	-	-
Percent refinement per pass	30	30
Stopping criteria:	-	-
Number of requested passes	10	10
Percent error	2	2

Table :1 Default Values for the Solution Criteria of the Maxwell 3D Field Simulator [6].

Overall, there are four ways in which the solution process can be stopped.

1. The user can abort the process manually.
2. The solution diverges and the system aborts the process due to inadequate memory.
3. The number of specified passes have been reached.
4. The solution converges.

Reference

- [5] Magsoft Corporation, 'Finite Element Analysis Software Reference Manuals', *Magsoft Corporation, Troy, NY, April 1995.*

- [6] Coy Brian Studer, 'Study Of Cogging Torque In Permanent Magnet Machines', a Master's Thesis in the Dept. of Electrical Engineering, The Ohio State University, 1998.

- [7] S.J. Salon, 'Finite Element Analysis of Electrical Machines', *Kluwer Academic Publisher, 1995.*

- [10] Ansoft Corporation, 'Finite Element Analysis Software Reference Manuals', Ansoft Corporation, Pittsburgh, PA, September 1996.

CHAPTER 3

Linear Reluctance Model For Permanent Magnet Machines

3.1 Introduction

This chapter presents the fundamentals and mathematical formulations of developed modeling approach for permanent magnet machines. This model is based on the Reluctance Model developed for Synchronous Machines by M.L.Awad for his PhD thesis [6]. The equivalent reluctance model is developed from the dimensions and material properties of the machine. It has the inherent flexibility for representing magnetic saturation. Sectoral model of the machine are developed. A linear reluctance matrix is used to relate the flux and magnetomotive force throughout the different sectors of the machine. The saturation effects are evaluated according to the iron section properties and dimensions and then used to adjust the flux distribution

Here in this chapter we initially present the basics of reluctance modeling for some basic shapes which are rectangular where the direct substitution of formulae is possible. We then present the reluctance of complex structures with some formulae. But in actual case the machine structure is complex with lots of curvature ie magnet, stator ,rotor etc are all curved . Hence some stress is laid on how to calculate reluctance of each part and then model stator, rotor etc. individually and then how to interface them and arrive at the complex reluctance model for the entire machine.

A case study of the machine when projected on to 2-Dimension is studied first and then the permanent magnet motor is modeled.

3.2 Magnetic Circuit Concepts

3.2.1 Why Magnetic Circuit Analysis ?

In a permanent magnet machine a central role is played by magnetic energy in the conversion of energy from electrical to magnetic to mechanical, in case of a motor or mechanical to magnetic to electrical, in case of a generator. Hence it is necessary to formulate methods to compute it accurately.

There are numerous ways to find magnetic field distribution within the machine. In Finite Element Analysis the machine discretized geometrically and the magnetic field is numerically found at such discrete points. In the other case approximated values magnetic field distribution can be found analytically. This involves two steps. In the first step the direction of the field everywhere within the machine is assumed. This leads to magnetic circuit analysis which is analogous to electric circuit analysis.

Of the two methods Finite Element Analysis gives the most accurate results if the geometric discretization is fine enough. This accuracy however comes only with significant computational cost and in addition to many hours or days of effort to generate the initial discretized model. Also geometric parameters and resulting change in magnetic field distribution are not linked. The great disadvantage with this method is that we need to develop many Finite Element solutions to develop basic insight into the effect of various design parameters on the

field distribution. Hence Finite Element Analysis is used mostly to confirm or improve the results of analytical design work.

The simplicity and analytic properties of the magnetic circuit analysis make it most commonly used magnetic field approximation method. Also in this method geometry of the machine is related to the field distribution giving substantial design insight.

3.2.2 Basic Concepts

Two vector quantities magnetic flux density B and flux intensity H describe the field.

The flux density B is defined as field flowing through the unit area of the material with units : Wb/m^2 .

The field intensity H is defined as the resulting change in the intensity of the magnetic field due to interaction of B and the material with units : Wb .

Both B and H are oriented in the same direction within a given material. For many materials the relationship between B and H is linear or nearly linear over a sufficiently large operating range. This dependency could be written as

$$B = \mu_0 \mu_r H \quad (3.1)$$

where μ_0, μ_r are the permeability of vacuum and relative permeability of the material respectively.

Some of the basic formulae used in the magnetic circuit analysis are well illustrated through the figure 3.1

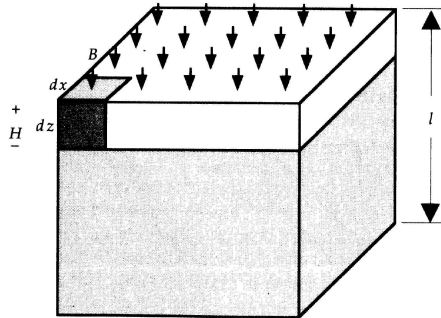


Figure 3.1 A block of magnetic material [3]

From the figure, when $dz=1$; $\phi = \int B_z(x, y) dx dy$ (3.2)

and when $B_z(x, y) = B$ is constant over the cross section , integral simplifies to

$$\phi = B * A \quad (3.3)$$

where ϕ is flux in Webers (Wb), B is flux density in Wb/m^2 , and A is area in m^2 respectively . Also F , the mmf is linked to H , the flux intensity by

$$F = \int H dz = Hl \quad (3.4)$$

where F is in amperes, H in A/m , length l in m .

substituting 3.3 and 3.4 in 3.1 and rearranging gives

$$\phi = PF \quad (3.5)$$

$$\text{where } P = \frac{\mu A}{l} \quad (3.6)$$

P is the permeance of the material having cross sectional area A , length l , permeability μ .

Reluctance , which is the inverse of permeance is given by

$$R = \frac{l}{\mu A} \quad (3.7)$$

giving the relation $F = \phi * R$ (3.8)

Equation (3.5) and (3.8) are analogous to Ohm's law, $I=GV$ and $V=IR$ respectively, with reluctance analogous to resistance, flux analogous to current and magneto motive force (mmf) analogous to voltage (emf) .

Magnetic Circuit Parameter		Electric Circuit Parameter	
Flux	[Wb]	Current	[A]
MMF	[A-t]	Voltage	[V]
Reluctance	[A-t/Wb]	Resistance	[ohms]

Table 3.1 Magnetic/Electric Circuit Analogy [3]

3.2.2.1 Magnetic Field Sources

There are 2 common sources of magnetic fields, one being current coil and the other being the permanent magnet.

Current Coil : Current flowing through the coil produces a magnetic field that can be found by applying Ampere's law.

$$\oint \mathbf{H} \cdot d\mathbf{l} = \begin{cases} I, & \text{if } C \text{ encloses } I \\ 0, & \text{if } C \text{ does not enclose } I \end{cases} \quad (3.9.a)$$

where C is any closed path or contour.

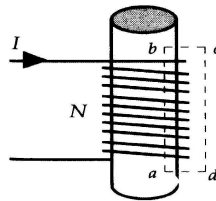


Figure 3.2 A coil wound over a piece of magnetic material

The direction of H with respect to the current I is related by the direction of right hand screw rule: Positive current is defined as flowing in the direction of advance of a right hand screw turned in the direction in which the closed path is traversed . If there were N turns enclosed

$$NI = \int_a^b \mathbf{H} dz = Hl \quad (3.9.b)$$

where $l = |b-a|$ is the length of coil in dz direction . Since Hl is modeled as an mmf source according to equation (2.4) above equation implies that coil of wire is modeled as an mmf source of value $F=NI$ with ampere -current as conventional units and just ampere in SI units. The cylinder carrying the coil is modeled as a reluctance or permeance.

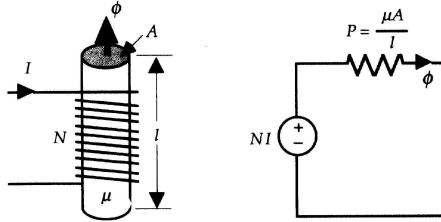


Figure 3.3 Magnetic Source Model of a coil [3]

Permanent Magnet : This can be represented as a Thevenin equivalent circuit comprising an MMF source, F_c , in series with an internal reluctance ; or by a Norton equivalent comprising a flux source, F_m , in parallel with an internal permeance, known as magnetic leakage permeance. Which of the two equivalent circuits we use is a matter of convenience.

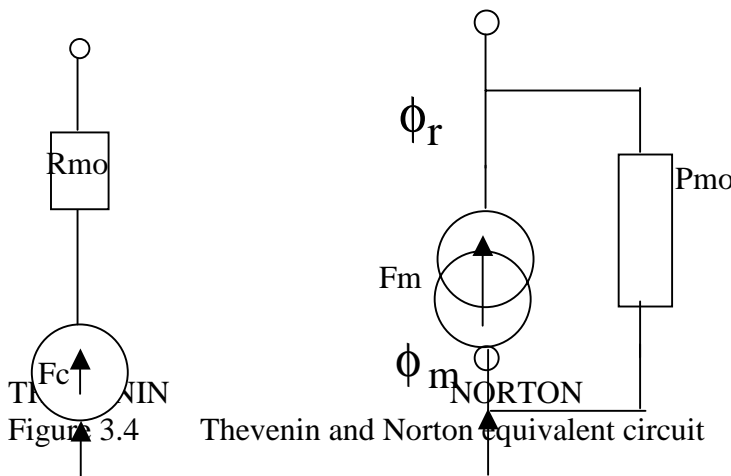


Figure 3.4 Thevenin and Norton equivalent circuit

The value of the mmf is given by

$$\phi_r = B_r A_m \tag{3.10.a}$$

$$F_c = H_c L_m \tag{3.10.b}$$

- where ϕ_r is the remanent flux
- B_r is the remanent flux density
- A_m is the magnet pole area
- F_c is the coercive mmf
- H_c is the coercive magnetizing force or coercivity
- L_m is the length of the magnet

3.3 Reluctance Modeling

The general formula of reluctance for the flow of flux lines through a material is

$$\mathfrak{R} = \frac{L}{\mu_o \mu_r * A} \quad (3.11)$$

\mathfrak{R} = reluctance of the material for flow of flux lines

L = length of the part which the flux has to traverse

A = cross sectional area of the part

μ_o, μ_r = are the permeability of air and relative permeability of material respectively

The above is the general formula which is used to find reluctance for flow of flux through any material. We assume the flux usually traverses perpendicular to the cross sectional area.

3.3.1 Air-Gap Modeling

It is important to model the reluctance of air-gap because flux passes between rotor and stator which are highly permeable, through an air-gap.

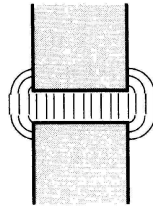


Figure 3.5 Fringing of flux in the air-gap when it flows between 2 highly permeable material [3]

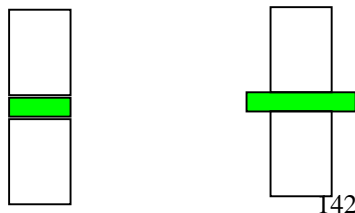
There are numerous methods for modeling reluctance of air-gap depending on the degree of accuracy required. Refer [3] for further details. Simplest model neglects fringing fully and gives giving

$$P_g = \frac{\mu A_g}{g} \quad (3.12)$$

where g is the length of air-gap as shown in figure 3.6 (a) . A refinement to this when g/A_g is small lets

$$P_g = \frac{\mu A_g'}{g} \quad (3.13)$$

where length g is added to the perimeter of A to obtain A' as shown in figure 3.6 (b) . The figure below shows the cases discussed.



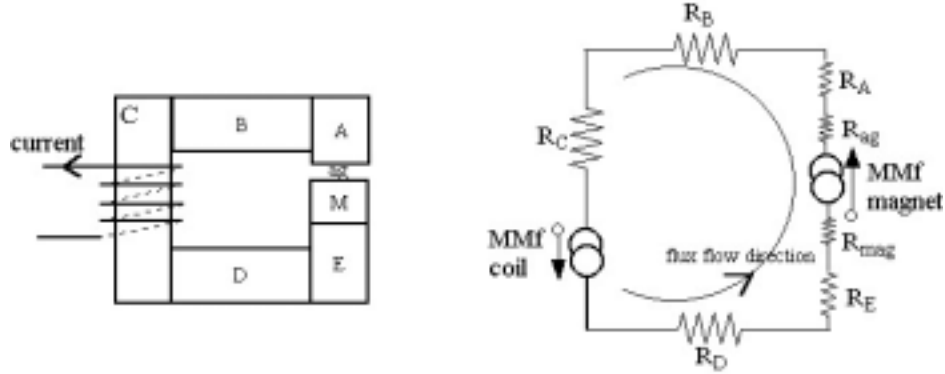


Figure 3.7 Single Loop Structure with magnet and current coil as mmf sources

The above figure shows the structure with magnet and current coil as mmf sources and the corresponding reluctance model diagram for the same. The structure is split into various arms A,B,C through to g as marked in the figure 3.7.

There are 2 sources for mmf in this structure

Magnet (marked M in the figure):- It's a permanent magnet with $B_r = 1 \text{ T}$ and $\mu_r = 1.1$.

Coil :- It carries a current and establishes a flux on its own which either opposes or aids the magnetic flux.

We assume the two sources to be in series and hence find the resultant mmf and reluctance for the flux path using the equation (2.28) and (2.29).

The core is steel with $\mu_r = 4000$ which is assumed to be a constant in the linear reluctance model.

The individual reluctances of each arm is found using the general equation (2.11). The flux flows through each arm of the structure in series and so the total reluctance is the sum of individual reluctance's of each arm.

$$\mathcal{R}_{eq} = \mathcal{R}_A + \mathcal{R}_B + \mathcal{R}_C + \mathcal{R}_D + \mathcal{R}_E + \mathcal{R}_M + \mathcal{R}_{ag} \quad (3.17)$$

The mmf is the algebraic sum of mmf from the magnet and current coil.

$$\sum_{mmf} = mmf_{mag} + mmf_{coil} \quad (3.18)$$

The flux ϕ and flux density B in the structure are given by

$$\phi = \frac{\sum_{mmf}}{\mathcal{R}_{eq}} \text{ webers} \quad ; B = \frac{\phi}{A} \text{ Tesla} ; \quad (3.19)$$

where $A = 20 \text{ mm}^2$

All these calculations are based on the assumption that flux through each arm flows in series which is well depicted in Finite Element Analysis.

3.4.2.1 Cases considered for the structure

We have analysis for 2 cases in the structure

Case 1: only magnetic source for mmf.

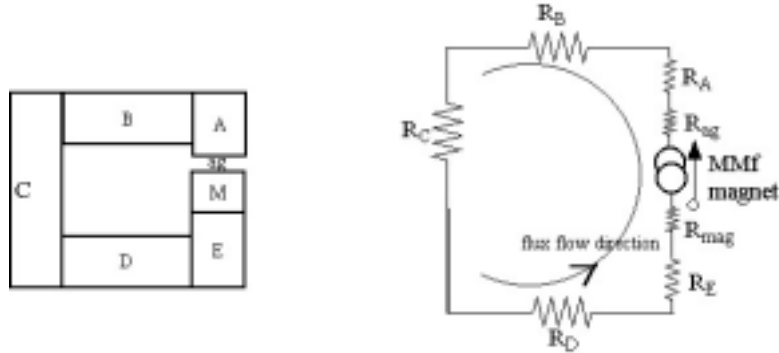


Figure 3.8 Single Loop structure with magnet source only

the equations used in this case are

$$\mathcal{R}_{eq} = \mathcal{R}_A + \mathcal{R}_B + \mathcal{R}_C + \mathcal{R}_D + \mathcal{R}_E + \mathcal{R}_M + \mathcal{R}_{ag} \quad (3.20)$$

The mmf is the algebraic sum of mmf from the magnet and current coil.

$$\sum_{mmf} = mmf_{mag} \quad (3.21)$$

The flux ϕ and flux density B in the structure are given by

$$\phi = \frac{\sum_{mmf}}{\mathcal{R}_{eq}} \text{ webers} \quad ; B = \frac{\phi}{A} \text{ Tesla} \quad (3.22)$$

where $A=20 \text{ mm}^2$

Case 2: current source of mmf aids the magnetic source .

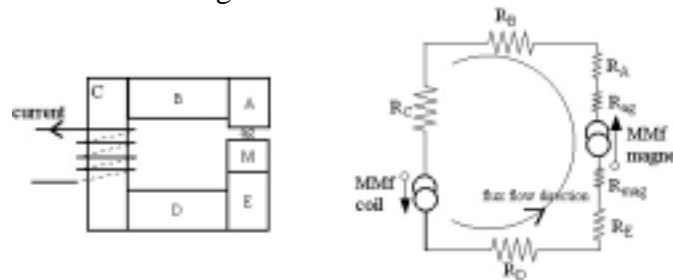


Figure 3.9 Structure with Current Source of mmf which aids the magnet mmf .

The equations used in this case

$$\mathcal{R}_{eq} = \mathcal{R}_A + \mathcal{R}_B + \mathcal{R}_C + \mathcal{R}_D + \mathcal{R}_E + \mathcal{R}_M + \mathcal{R}_{ag} \quad (3.23)$$

The mmf is the algebraic sum of mmf from the magnet and current coil.

$$\sum_{mmf} = mmf_{mag} + mmf_{coil} \quad (3.24)$$

The flux ϕ and flux density B in the structure are given by

$$\phi = \frac{\sum_{mmf}}{\mathcal{R}_{eq}} \text{ webers} \quad ; B = \frac{\phi}{A} \text{ Tesla} \quad (3.25)$$

where $A=20 \text{ mm}^2$

The figure below shows how we split each arm into various planes. We find the average values of ϕ, B along the planes. Then mean of these values are found to get the average value of ϕ, B for the entire arm.

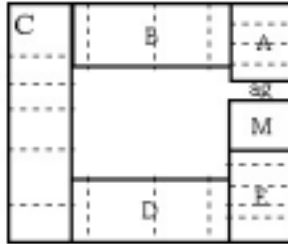


Figure 3.10 Structure split into various planes

3.4.2.2 Results of Single Loop Structure

Case 1 : Only magnet as a source of mmf , there is no current in the coil

From Analytical Model

Average $\phi = 1.4595 * 10^{-5}$ Wb: Average $B = .7298$ T in all arms of the structure .

From Finite Element Analysis

Average value of B in

Arm A=0.6673 T ; Arm E= 0.7432 T; Arm C = 0.7283 T .

Case 2 : when the mmf source due to current in coil (1000 A.Turns) aids the magnetic source.

From Analytical Model

Average $\phi = 2.13199 * 10^{-5}$ Wb: Average $B = 1.0659$ T in all arms of the structure .

From Finite Element Analysis

Average value of B in

Arm A=1.0298 T ; Arm C = 0.98645 T .

From the 2 cases we find our results from Analytical model closely matches with that of Finite Element Analysis. This validates the model developed so far. The small difference in values between the analytical model and finite element analysis is due to the fact that we average the values at some planes only in each arm. If we were to find the values at each cut plane of the arm then our results would match more closely. Since infinite such planes could be cut in each arm and finding the average value at each plane is a very time consuming task , we restrict the planes where the average values are found. A direct effect for this approximation is found in the average value of the arm that we find for the Finite Element Results.

Considering the above stated facts , we find the results from the two models closely match and the assumed direction of flow of flux is in analytical model is correct which is verified from the plots of finite element analysis.

3.4.3 Two Loop Structure

3.4.3.1 Structure

The results from the two loop structure are more important to validate our analytical model of the machine. Hence more effort is put for the structure.



Figure 3.11 Two Loop Structure with current and magnet as mmf sources

The materials in the structure

- 1) Magnet : Magnet :- It's a permanent magnet with $B_r = 1$ T and $\mu_r = 1.1$.
- 2) Coil :- It carries a 1A current and establishes a flux on its own which either opposes or aids the magnetic flux.
- 3) Airgap
- 4) Iron core with $\mu_r = 4000$.

The iron core structure is split into various arms : A through H and magnet M, air-gap (ag). We follow Maxwell loop current method to solve for the flux and flux density at each arm. There are two loops in the structure.

An equivalent diagram showing the reluctances and mmf sources is shown below

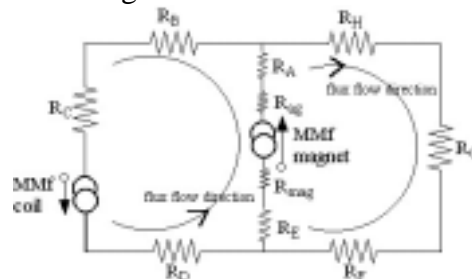


Figure 3.12 Reluctance Model for the 2 Loop structure

Here the magnet is modeled as a mmf source with reluctance. But we assume coil to be an ideal mmf source. We assume a constant value of μ_r for the magnet and iron core for the linear model. As was the case for a single loop structure , we use average value of ϕ and B calculated from the Finite Element Analysis for comparison with the results of analytical model.

The figure below shows various planes in each arm of the structure.

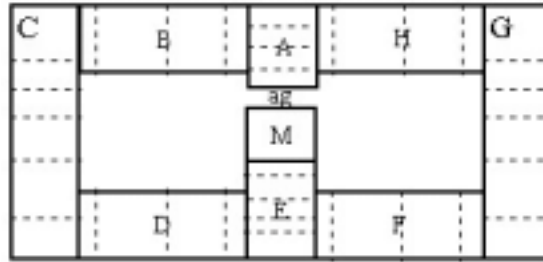


Figure 3.13 2 loop structure with each arm split into various planes

3.4.3.2 Comparison of Results

Here we compare the results obtained from the Analytical model and that of the Finite Element Analysis (Ansoft). The value of reluctances of each arm as obtained from the formula (2.11)

$$R_A = 4.97e+002 ;$$

$$R_B = R_D = R_F = R_H = 9.95e+002 ;$$

$$R_C = R_G = 1.49e+003 ;$$

$$R_E = 5.97e+002 ;$$

$$R_M = 1.09e+006 ;$$

$$R_{ag} = 3.99e+005$$

The solution for the following cases are obtained using the Maxwell's Loop Current method because of the analogy that exists between magnetic circuit and electric circuit.

Case 1: when the current coil produces mmf aiding the magnet in the central branch.

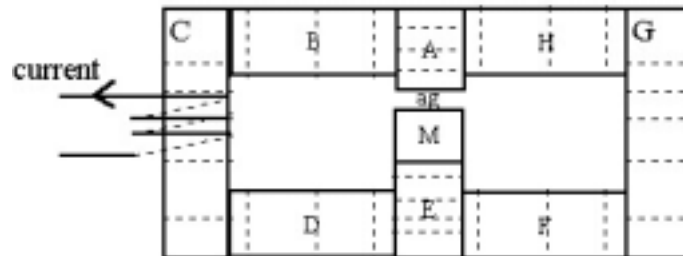


Figure 3.14 Structure with mmf due to current in coil aiding the magnetic mmf

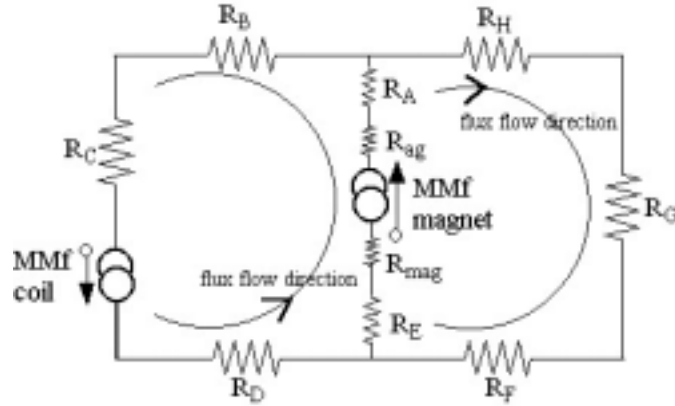


Figure 3.15 Reluctance Model for the case: 1

Comparison of the results from the two methods

ARM	Average value of flux density from Analytical model in Tesla (T)	Average value of flux density from Ansoft in Tesla (T)
A	0.7304	0.6598
B	0.4370	0.46268
H	0.2934	0.32735
G	0.2934	0.2942

Table : 3.2 Table which shows the results from the two methods for case 1
Case 2: when the current coil produces mmf opposing the magnet in the central branch.

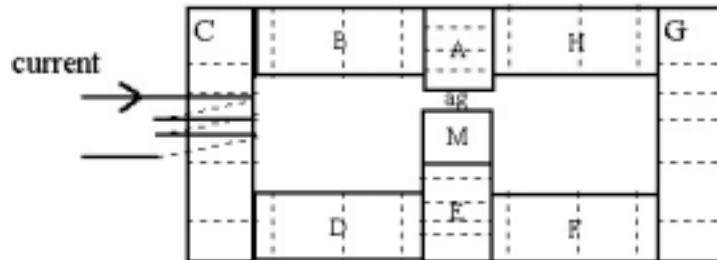


Figure 3.16 Structure with mmf due to current in coil opposing the magnetic mmf

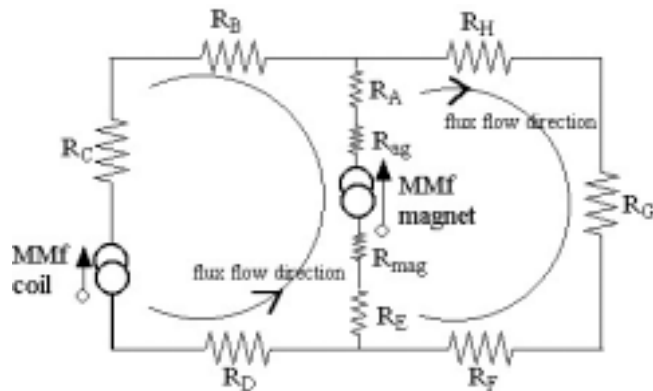


Figure 3.17 Reluctance Model for the case: 2

Comparison of values obtained from the 2 methods

ARM	Average value of flux density from Analytical model in Tesla (T)	Average value of flux density from Ansoft in Tesla (T)
A	0.7304	0.6592
B	0.2932	0.3174
C	0.2932	0.29236
H	0.4369	0.3961
G	0.4369	0.4008

Table :3.3 Table which shows the results from the two methods for case 2

From the above results we close co-relation between Analytical model and Ansoft solution indicating correctness of the developed model.

3.5 Linear Reluctance Model For Permanent Magnet Machines

3.5.1 Model Assumptions

- Permeability of the iron sections are high but not infinite. We assume a value for permeability (μ_r) of iron to be 4000. This value is used only for linear reluctance model. For nonlinear reluctance model we calculate various values of permeability from the values of Flux density (**B**) and flux intensity (**H**) in the iron path. Therefore reluctances of the iron path consists of iron, air gap and leakage reluctance.
- Initially saturation effects are neglected . Also we try to fix the saturation flux density for iron path and try to restrict the actual iron flux density well below this value ie. $\mathbf{B}_{actual,iron\ path} < \mathbf{B}_{sat, iron\ path}$.
- The effect of tooth ripples are neglected.

3.5.2 Machine Sectionalizing

3.5.2.1 Radial Direction

In the radial direction , the machine can be regarded as 3 consecutive layers as shown in [4]

- ❖ Stator : windings, stator yoke and teeth as the first layer.
- ❖ Air-gap.
- ❖ Rotor : core and the magnets.

3.5.2.2 Circumferential Direction

In circumferential direction, the machine is sectored according to the number of stator slots (N_s) which implies N_s sectors of the machine exist long the circumference. The rotor is similarly split into corresponding sections based on the stator sections ie. same angle between sections as of the stator sections.

The stator and rotor sections are linked together by a set of linear air-gap reluctance. The following machine has been split into 12 sectors along the circumference with each sector spanning $\Delta\theta_{ks}$ radians, which is equal to the stator slot pitch.

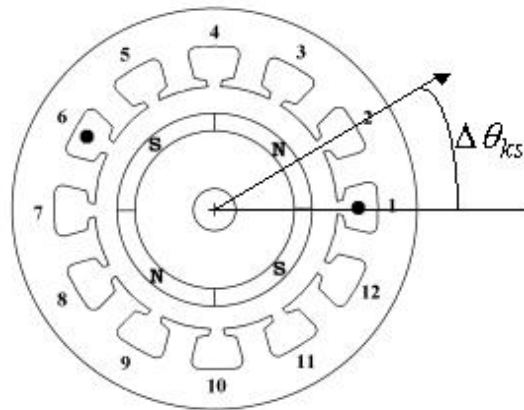


Figure 3.18 Machine split into 12 sectors

The above machine has been split into 12 sectors with each slot and a tooth constituting the sector in the stator. Corresponding portion in the air-gap and rotor make the entire sector for the machine. Each sector spans a full slot pitch.

3.5.3 Reluctance Modeling

The reluctance for the flux lines at stator, air-gap, rotor is calculated from the general

formula
$$\mathfrak{R} = \frac{L}{\mu_o\mu_r * A} \quad (3.26)$$

\mathfrak{R} = reluctance of the material for flow of flux lines

L = length of the part

A = area of the part concerned

$\mu_o\mu_r$ = are the permeability of air and material (relative) respectively

3.5.3.1 Stator Reluctances

(A) Yoke

The reluctance of stator yoke is given by

$$\mathfrak{R}_y = \frac{L_y}{\mu_o\mu_r * A_y} \quad (3.27)$$

L_y = length of the yoke per sector = $r_y * \Delta\theta_{ks}$

A_y = Area of the stator yoke per sector

$$r_y = \text{radius of yoke} = \frac{(OD - y_t)}{2}$$

$\Delta\theta_{ks}$ = span of each sector

OD = outer diameter of the stator

Y_t = yoke thickness

$$A_y = y_t * L_{stk} \tag{3.27a}$$

L_{stk} = length of the stator stack

(B) Teeth

$$\mathfrak{R}_t = \frac{d_s}{\mu_0 \mu_r * t_t * L_{stk}} \tag{3.28}$$

d_s = depth of the tooth

t_t = width of the tooth

(C) Slot Modeling

Since house the windings which are non magnetic flux crossing the air-gap containing air-gaps will avoid air-gaps due to its low relative permeability. There are several ways to approximate slot permeance , some of which are discussed here. Refer [3] for detailed discussion on slot modeling.

The crudest method is to assume the slot contains material of permeability equal to the rest of the block. In this case $P_g = \mu_0 A / g$ where A is the total area of cross section facing the gap. Obviously this would yield a very crude value because permeability of slot is much lower than the material. Ignoring the flux crossing the air-gap over the slot , we have $P_g = \mu_0 (A - A_s) / g$, where A_s is the cross sectional area of the slot facing the air-gap.

Observing that flux crossing the air-gap over the slot travels a further distance before reaching the highly permeable material, we have $P_g = \mu_0 A / g_e$ (3.29)

where $g_e = g * k_c$ is an effective air-gap length. Here $k_c > 1$, is the Carter's co-efficient. Three different expressions of Carter's are listed below.

$$k_{c1} = \left[1 - \frac{1}{\frac{\tau_s}{w_s} \left(5 \frac{g}{w_s} + 1 \right)} \right]^{-1} \quad (3.30)$$

$$k_{c2} = \left(1 - \frac{2w_s}{\pi\tau_s} \left\{ \tan^{-1} \left(\frac{w_s}{g} \right) - \frac{g}{2w_s} \ln \left[1 + \left(\frac{w_s}{g} \right)^2 \right] \right\} \right)^{-1} \quad (3.31)$$

$$k_{c3} = \left[1 - \frac{w_s}{\tau_s} + \frac{4g}{\pi\tau_s} \ln \left(1 + \frac{\pi w_s}{4g} \right) \right]^{-1} \quad (3.32)$$

We use the last method discussed with correction in air-gap length based on Carter's coefficient.

(D) Peripheral Leakage

Some amount of the flux flows entirely through peripheral region rather than radial direction in the air-gap of the machine [4].

$$\mathfrak{R}_{pl} = \frac{r_s * \Delta\theta k_s}{\mu_0 L_{stk} * ge} \quad (3.33)$$

r_s = inner radius of the stator

ge = air-gap length

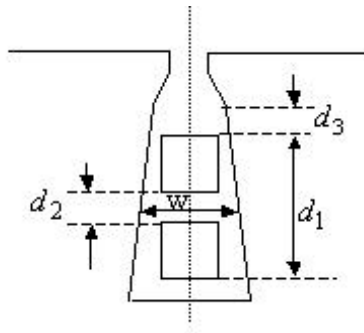
Usually the peripheral air gap leakage is shared between the stator and rotor .

$$\mathfrak{R}_{spl} = \mathfrak{R}_{rpl} = \frac{1}{2} \mathfrak{R}_{pl} \quad (3.34)$$

\mathfrak{R}_{spl} = peripheral leakage associated with stator

\mathfrak{R}_{rpl} = peripheral leakage associated with rotor

(E) Slot Leakage



$$\text{Slot permeance ratio (SPR)} = \frac{k_s}{w} \left(d_3 + \frac{d_1}{3} \right) + \frac{d_1}{12w} (1 - k_s) - \frac{d_2}{4w} \left(k_s - \frac{2}{3} \right) \quad (3.35)$$

$$k_s = \frac{1 + \cos\theta}{2} \quad \text{where } \theta = \text{phase difference between top and bottom coils}$$

$$P_{ls} = L_{stk} * \text{SPR} * \mu_0 \quad (3.36)$$

P_{ls} = leakage permeance

$$\text{Slot leakage permeance} = \frac{1}{P_{ls}} \quad (3.37)$$

(F) STATOR SECTOR MODEL For MMF

Winding : In a sine wave machine the effective sine distributed number of turns of each phase is

$$N_{se} = \frac{4 * K_w N_s}{\pi} \quad (3.38)$$

N_s = actual number of turns of each phase

K_w = stator winding factor

Therefore the number of turns of each phase per pole per slot is

$$N_{tq} = \frac{N_{se}}{q * P} \quad (3.39)$$

N_{tq} = number of turns of each phase per pole per phase

N_{se} = effective sine distributed number of turns of each phase

q = number of slots per pole per phase

P = number of poles

In a square wave machine

$$N_{tq} = N_s$$

N_s = number of turns of each phase per pole per phase

Stator MMF : Stator MMF per slot is the product of the Rmf value of the current flowing in the slot and the number of turns of each phase per pole per phase .

$$\text{Tau}_{\text{slot}} = N_{tq} * I_{\text{rms}} \quad (3.40)$$

3.5.3.2 Air-Gap Reluctance

$$\mathfrak{R}_{ag} = \frac{ge}{\mu_0 r_s * \Delta\theta k_s * L_{stk}} \quad (3.41)$$

$r_s * \Delta\theta k_s$ = span of the air-gap/ sector

3.5.3.3 Rotor Reluctance

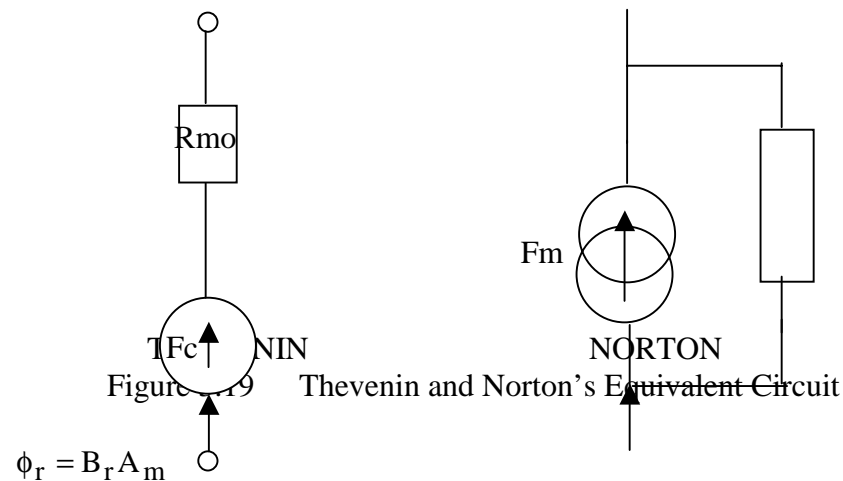
(A) Core

$$\mathfrak{R}_{\text{core}} = \frac{y_{\text{rc}}}{\mu_0 \mu_r * \frac{D_r}{2} * \Delta\theta_{\text{ks}} * L_{\text{stk}}} \quad (3.42)$$

y_{rc} = core width

D_r = radius of the rotor

(B) Magnet In A Sector



$$\phi_r = B_r A_m$$

$$\mathfrak{R}_m = \frac{l_m}{\mu_0 \mu_r A_m} \quad (3.43 \ \& \ 3.44)$$

$$\text{Tau}_m = \phi_r * \mathfrak{R}_m \text{ where} \quad (3.45)$$

$\text{Tau}_m, \phi_r, \mathfrak{R}_m$ are the MMF of the magnet, flux from the magnet, Reluctance of the magnet material under the sector.

(C) Magnet Reluctance

The reluctance of the magnet material under the slot is

$$\mathfrak{R}_m = \frac{l_m}{\mu_0 \mu_r A_m} \quad (3.46)$$

Here we find the Area under the slot differs from slot to slot based on whether the slot is fully covered by magnet or just partially covered by the magnet. This is mainly because people have found that to produce the magnetic flux in the air-gap, it is always not necessary to have the magnetic span to be equal to magnetic pole pitch.

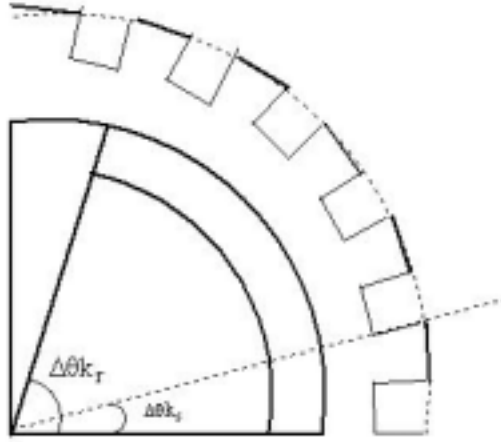


Figure 3.20 Machine Quadrant with slots and pole

$$\text{Angle covered by one slot, } \Delta\theta_{Ks} = \frac{2\pi}{N_s} \quad (3.47)$$

$$\text{Angle covered by one pole, } \Delta\theta_{Kr} = \frac{\pi D_r * \alpha_m}{P} \quad (3.48)$$

Where N_s = number of stator slots

P = total number of poles

α_m = magnetic coverage factor

$$\text{Width of the magnet that partially covers the slot} = \frac{2\pi}{N_s} - \left(\Delta\theta_{Ks} * \frac{N_s}{P} - \Delta\theta_{Kr} \right) \quad (3.49)$$

$$\text{Area of the magnet that fully covers the stator sector} = L_{stk} * \left(\frac{D_r - l_m}{2} \right) * \Delta\theta_{Ks} \quad (3.50)$$

Area of the magnet that partially covers the sector =

$$L_{stk} * \left(\frac{D_r - l_m}{2} \right) * \left(\frac{2\pi}{N_s} - \left(\Delta\theta_{Ks} * \frac{N_s}{P} - \Delta\theta_{Kr} \right) \right) \quad (3.51)$$

3.5.4 Linear Reluctance Model Of The Sector

The flux analysis when done for a pole pair (a north pole and a south pole constitute a pair) will effectively give us the entire pattern of the flux density in the machine because the flux density pattern in the rest of the machine will be a repetition of the same. This is based on the assumption that the machine parts involved (stator, rotor, magnet, coils air-gap, etc.) are homogeneously spread in the machine

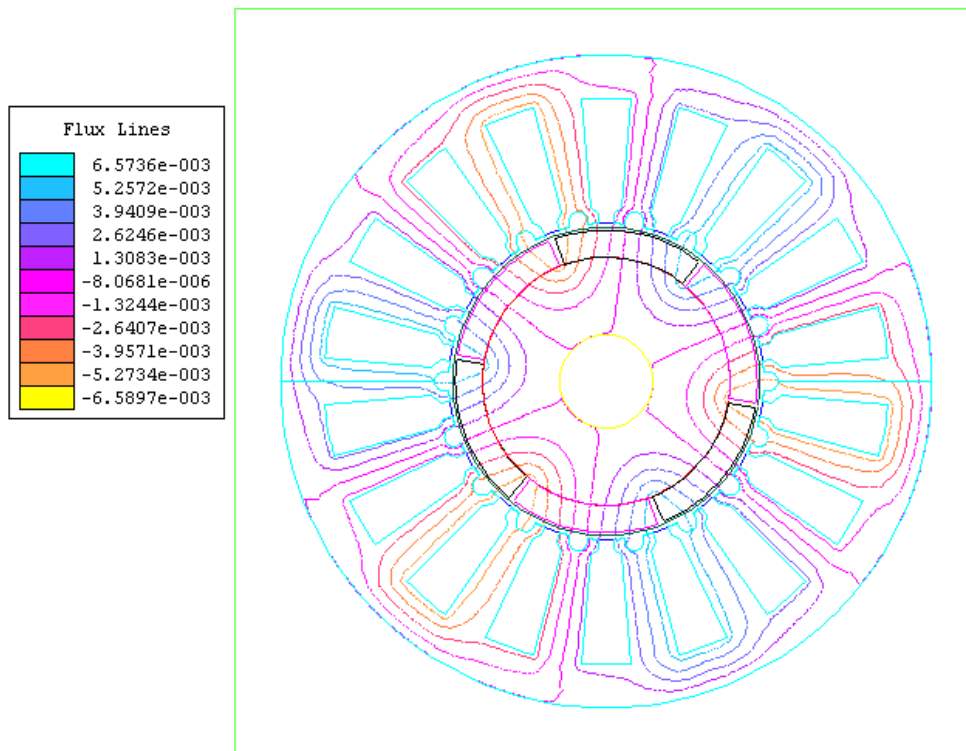


Figure 3.21 Flux Flow in the Machine validating Symmetry

The above figure which is the representation of the flow of flux lines as calculated from the Finite Element Method, clearly proves our assumption to be correct in that flux lines repeat's itself for every pole pair.

3.5.5 Magnet Source (mmf) Under Each Teeth

- ✓ Usually we assign negative sign to mmf from south pole and positive sign to mmf from north pole.
- ✓ Magnets extend beyond the teeth and hence to equate the reluctance of magnet and also mmf of magnet part which influences a particular loop section we need to make some simple approximations.
- ✓ From our experience we know only a small portion of magnet extending beyond the teeth on either side influence the teeth and not the entire length of magnet in each section (in case of permanent magnet machine , each section width is equal to stator slot pitch). Hence we choose approximately 80-85 % of magnet under the section to influence the teeth - length of magnet under each section is equal to stator slot pitch with the center of tooth being the center of magnet ie if τ_m was the magnetic mmf of whole section , we allocate only 80-85 % of τ_m as magnetic source of mmf to the section because the rest of magnetic mmf is either lost as leakage or has no significant influence on the tooth.

- ✓ Also on some teeth are under influence of both north and south pole magnets. In such case τ_m for that tooth is equal to the algebraic sum of the mmf due to north and south pole.

3.5.6 Simplified Machine Structure

3.5.6.1 Structure

Having studied some of the loops involving the magnet, current coils and airgap etc we now shift to the following structure is a simplified structure of the actual Permanent Magnet machine, when spread in 2-D. The following structure could be equated to a permanent magnet machine with just a pole pair and spread in 2-D.

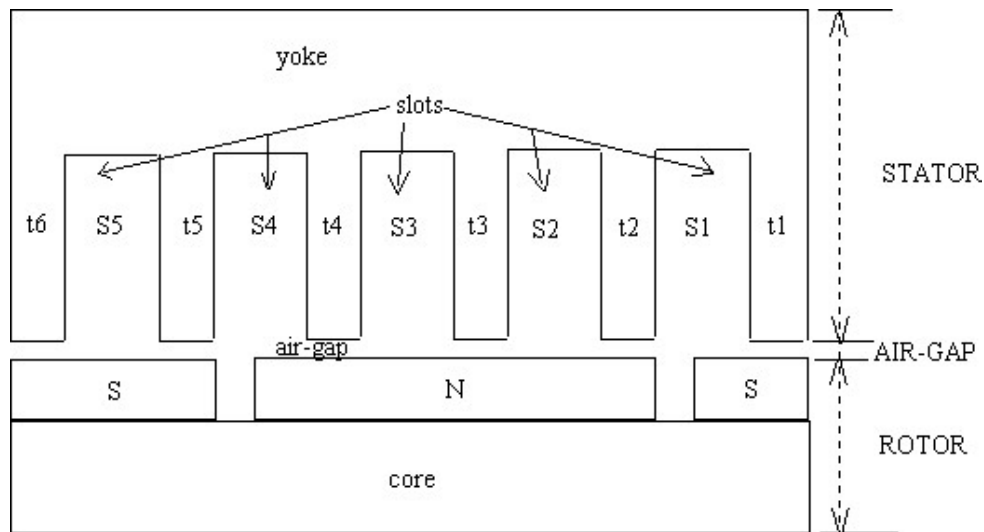


Figure 3.22 P.M. Machine spread in 2-D

The importance of the above structure is that once we prove our analytical model that is developed for the P.M.Machines on this we prove the model as such . The following case we study has no current flowing in the conductors which are placed in the slots ie we prove the reluctance model for the machine with no stator current. Also we assume the slots are filled with vacuum.

3.5.6.2 Sectionalizing

Radial direction

In the radial direction, the machine is regarded as 3 layers [4]

- 1) Stator :- yoke and teeth (Iron core with $\mu_r = 4000$.)
- 2) Rotor :- magnets (permanent magnet with $B_r = 1$ T and $\mu_r = 1.1$) and core (Iron core with $\mu_r = 4000$.)

3) Air-gap :- the stator and rotor sections are linked together by a set of linear air-gap reluctance.

Circumferential direction

The structure is split into 5 sections along the length. All the parts between any two teeth constitute a section.

3.5.6.3 Network of sections

The combination of radial and circumferential sections with the reluctance of each part included with their sources etc. constitute a complex reluctance network. Considering just the cut portion of the machine as seen below, we build the reluctance model for each sector at first and then network them to get the final model for the entire structure considered in figure 3.23

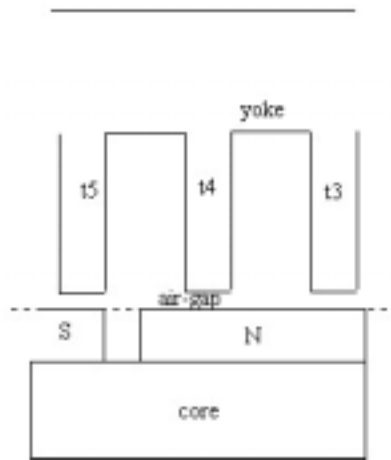


Figure 3.23 Structure showing the sector

(A) STATOR

Consider just the section in the stator with teeth t3, t4, and the yoke connecting them. The corresponding reluctance model for the same is given below

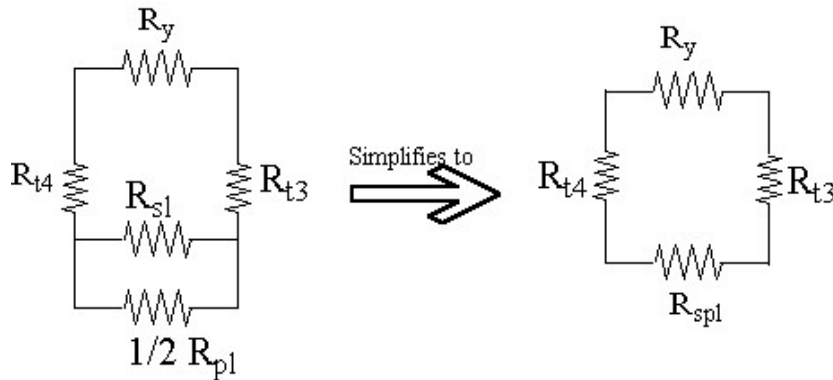


Figure 3.24 Reluctance model of stator

where $R_y, R_{t3}, R_{t4}, R_{sl}, R_{pl}$ stand for reluctances of yoke, tooth3, tooth4, slot leakage, peripheral leakage.

Also $R_{spl} = R_{sl} \parallel R_{pl}$

All sections of stator can be modeled in the same way.

(B) ROTOR

The rotor model for the corresponding section just consists of the magnet and the core connecting them. The mmf from magnet associated with each tooth is found by the method we had discussed earlier in the introduction part (3.6) .

We have width of each section to be equal to stator slot pitch's value.

Stator slot pitch = width of tooth + average width of each slot

Hence the portion of magnet influencing the teeth with its mmf will have a width equal to slot pitch value, with its center being the center of tooth at it's base. Taking the leakage into cognizance we choose approximately 80-85 % of magnet under the section to influence the teeth ie if τ_m was the magnetic mmf of whole section , we allocate only 80-85 % of τ_m as magnetic source of mmf to the section because the rest of magnetic mmf is either lost as leakage or has no significant influence on the tooth.

Incases where both north pole and south pole is active within the distance where it can influence the tooth , then mmf under the tooth is the algebraic sum of the mmf due to north and south poles (north poles are assigned positive mmf and south poles negative mmf).

The value of magnetic reluctance is calculated based on the above mentioned width of magnet. The width of core for calculating its reluctance will be equal to that of slot pitch because all of this length is used by the flux for its propagation.

The figure below shows the reluctance of the rotor part of a section.

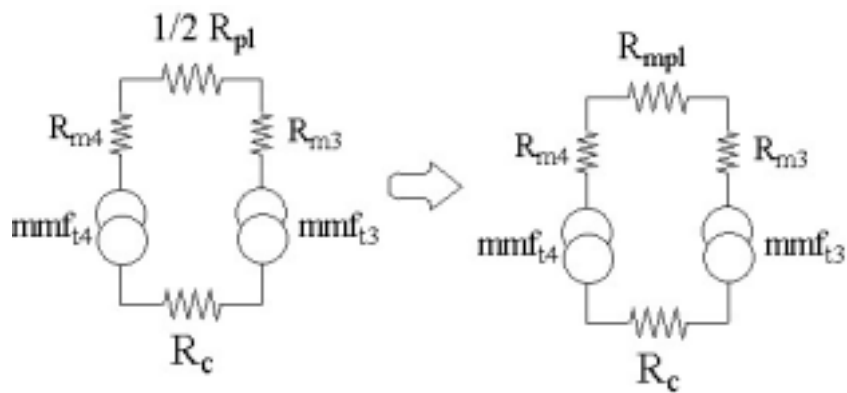


Figure 3.25 Reluctance model for rotor

(C) AIR-GAP

This is just a reluctance part that connects a stator loop with that of rotor loop of a section. The width of air-gap which is equal to the slot pitch the center of which is the center of the tooth usually assigned an equivalent reluctance and is assumed to be connecting the stator and rotor portions of the section.

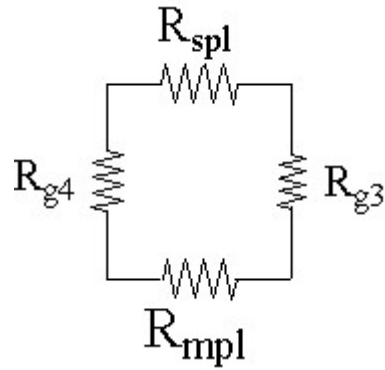


Figure 3.26 Reluctance Model of air-gap

(B) RELUCTANCE MODEL FOR THE ENTIRE SECTION

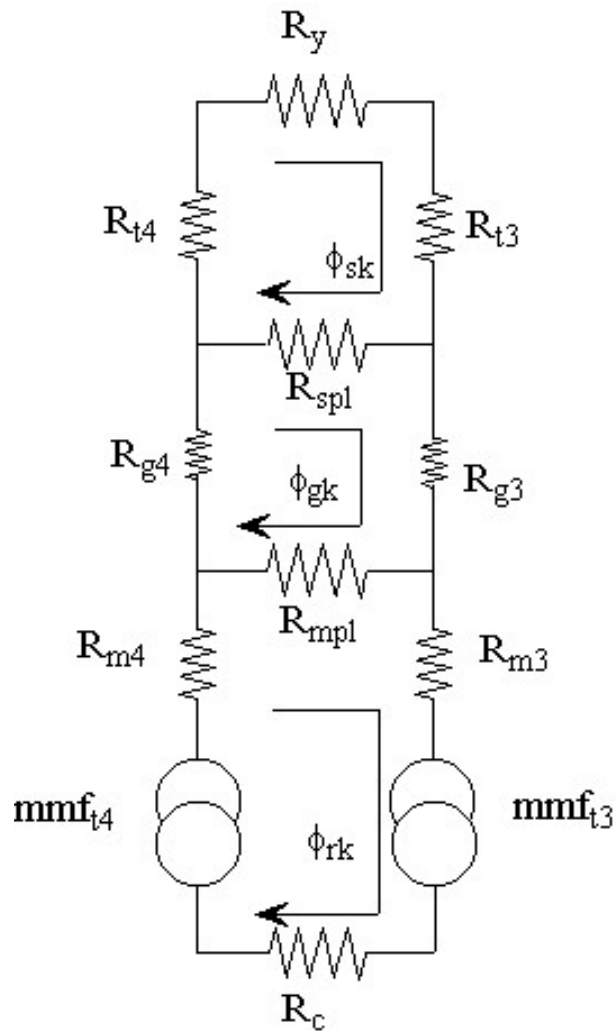


Figure 3.27 Reluctance Model for a Sector

(C) SECTION OF RELUCTANCE MODEL OF PERMANENT MAGNET MACHINE

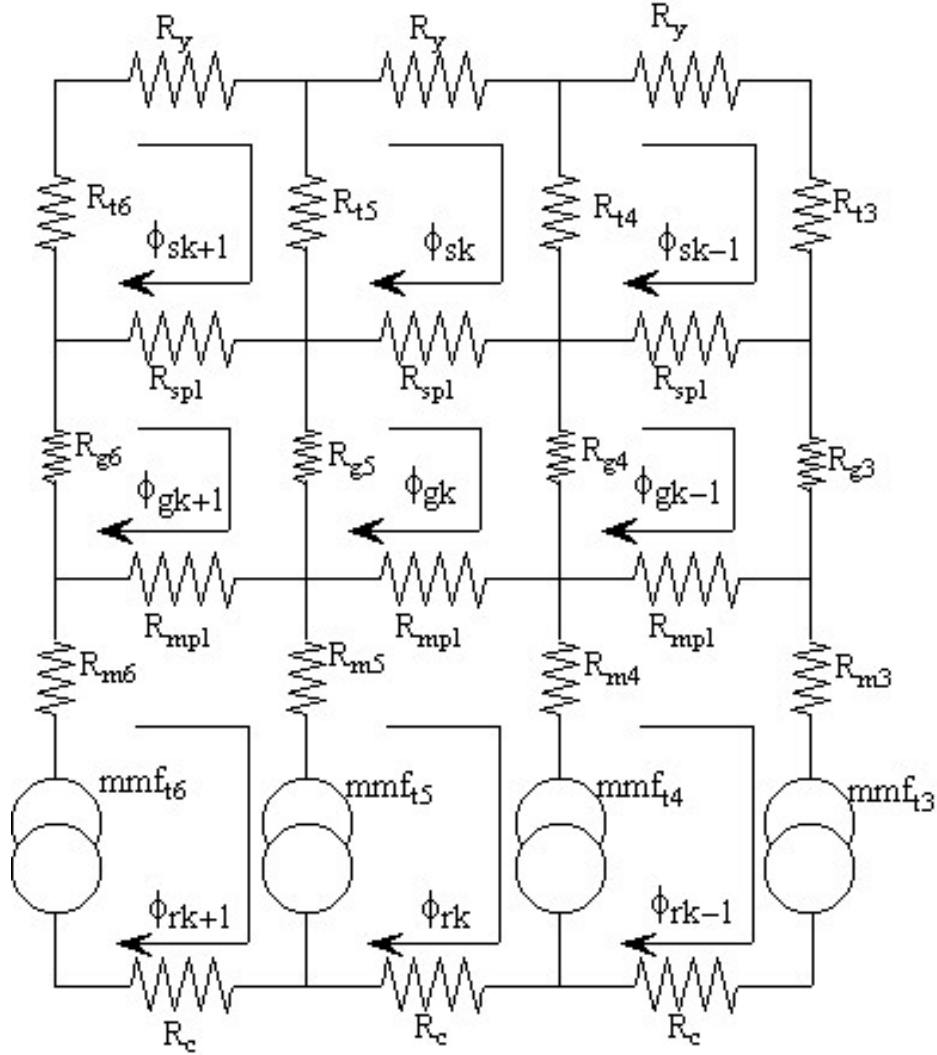


Figure 3.28 Network of reluctance Model for Sectors

$\phi_{sk}, \phi_{gk}, \phi_{rk}$ = the fluxes in the stator loop, air-gap loop and rotor loop ,
 where k is for sector of the machine being considered and
 $k = 1$ to the total number of sectors in the machine.

For the different sections of the machine, flux-mmF relation can be described as follows

➤ Stator

$$-\phi_{sk} R_y - (\phi_{sk} - \phi_{s(k-1)}) R_t - (\phi_{sk} - \phi_{gk}) R_{spl} - (\phi_{sk} - \phi_{s(k+1)}) R_t = 0 \quad (3.52)$$

$$0 = \phi_{sk} (R_y + R_t + R_{spl} + R_t) - \phi_{s(k-1)} R_t - \phi_{s(k+1)} R_t - \phi_{gk} R_{spl} \quad (3.53)$$

When the current in the coil at stator is zero, the mmf due to it is zero and hence here the left side of the equation is zero. If the current in the coils existed, then the LHS must be algebraic sum of the mmf due to current in the coil.

➤ Air-gap

$$-(\phi_{gk} - \phi_{sk})R_{spl} - (\phi_{gk} - \phi_{g(k-1)})R_g - (\phi_{gk} - \phi_{rk})R_{mpl} - (\phi_{gk} - \phi_{g(k+1)})R_g = 0 \quad (3.54)$$

$$\phi_{gk}(R_{spl} + R_g + R_{mpl} + R_g) - \phi_{sk}R_{spl} - \phi_{g(k-1)}R_g - \phi_{rk}R_{mpl} - \phi_{g(k+1)}R_g = 0 \quad (3.55)$$

➤ Rotor

$$\begin{aligned} & -(\phi_{rk} - \phi_{gk})R_{mpl} - (\phi_{rk} - \phi_{r(k-1)})R_{m(k-1)} - \tau_{m(k-1)} \\ & -\phi_{rk}R_c - (\phi_{rk} - \phi_{r(k+1)})R_m + \tau_{mk} = 0 \end{aligned} \quad (3.56)$$

$$\begin{aligned} \tau_{mk} - \tau_{m(k-1)} &= \phi_{rk}(R_{mpl} + R_{m(k-1)} + R_c + R_m) - \phi_{gk}R_{mpl} \\ & -\phi_{r(k-1)}R_{m(k-1)} - \phi_{r(k+1)}R_m = 0 \end{aligned} \quad (3.57)$$

Here we have $R_{m(k-1)}, R_m$ which are the reluctances of the magnet in the previous and current loop respectively. These are algebraic sum of the magnetic mmf that influence a tooth. They might have different or same values based on the extent of magnet coverage under the tooth.

Setting these equations for each mesh, the overall *Reluctance Model* could be constructed as shown in [4]

$$\begin{bmatrix} \tau_{s1} \\ \tau_{s2} \\ \tau_{s3} \\ \vdots \\ \vdots \\ 0 \\ 0 \\ 0 \\ \vdots \\ \vdots \\ \tau_{r1} \\ \tau_{r2} \\ \tau_{r3} \\ \vdots \\ \vdots \end{bmatrix} = \begin{bmatrix} \begin{bmatrix} Stator \\ Reluctance \end{bmatrix} & \begin{bmatrix} Stator to Gap \\ Reluctance \end{bmatrix} & [0] \\ \begin{bmatrix} Stator to Gap \\ Reluctance \end{bmatrix} & \begin{bmatrix} Gap \\ Reluctance \end{bmatrix} & \begin{bmatrix} Rotor to Gap \\ Reluctance \end{bmatrix} \\ [0] & \begin{bmatrix} Rotor to Gap \\ Reluctance \end{bmatrix} & \begin{bmatrix} Rotor \\ Reluctance \end{bmatrix} \end{bmatrix} \begin{bmatrix} \phi_{s1} \\ \phi_{s1} \\ \phi_{s1} \\ \vdots \\ \vdots \\ \phi_{g1} \\ \phi_{g2} \\ \phi_{g3} \\ \vdots \\ \vdots \\ \phi_{r1} \\ \phi_{r2} \\ \phi_{r3} \\ \vdots \\ \vdots \end{bmatrix} \quad (3.58)$$

or simply it can be written as shown in [4]

$$[\tau] = [R][\phi] \quad (3.59)$$

$$\text{or } [\phi] = [R]^{-1}[\tau] \quad (3.60)$$

In the equation (3.58) the suffixes s, g, r, stand for stator, air-gap and rotor respectively. The Reluctance matrix $[R]$ is a square matrix whose dimensions equal the total number of meshes considered. The total number of meshes will be equal to 3 times the number of slots in the pole-pair. For example if there were 6 slots in a pole pair, the reluctance matrix $[R]$ will be 18×18 ie $[R]_{18 \times 18}$.

3.5.6.4 Comparison of Results from Ansoft and Analytical model

Structure

The structure of interest is shown below which could be equated to 2-D spread of the pole-pair of a permanent magnet machine.

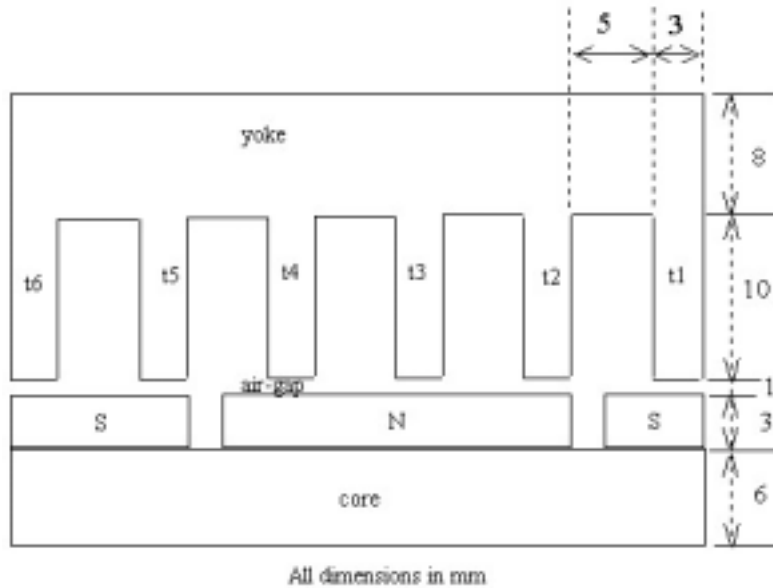


Figure 3.29 P.M.Machine in 2-D with all dimensions

Reluctance Model

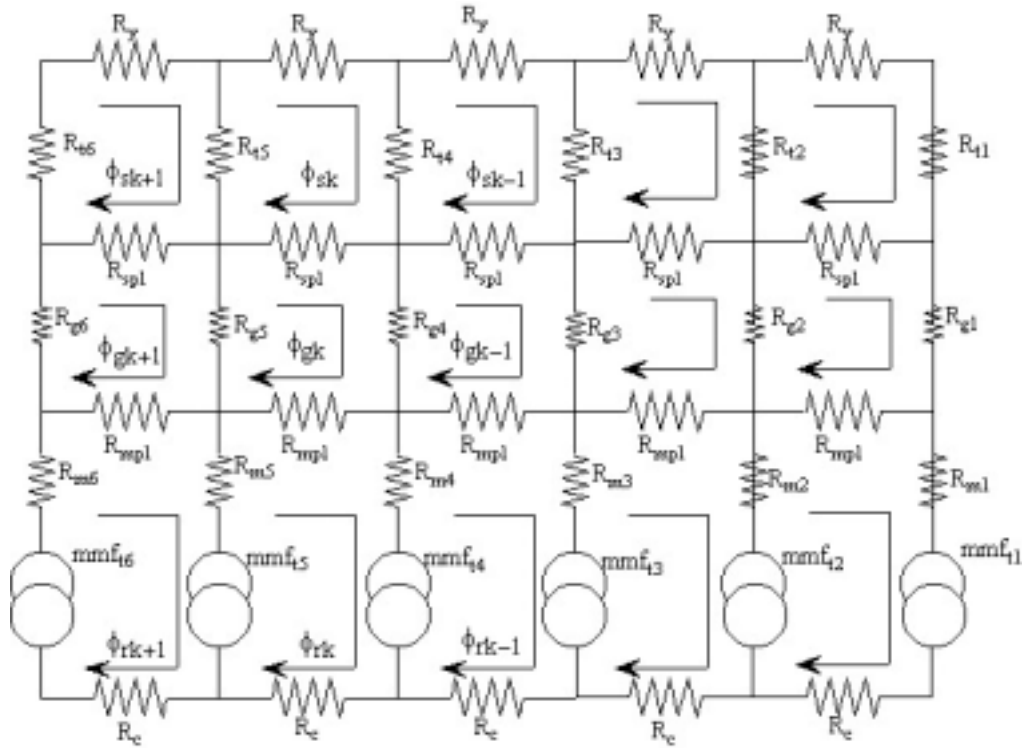


Figure 3.30 Network of reluctance model for the structure

Results

The figure below show the flux density distribution and flux contour on the structure studied from the finite element analysis.

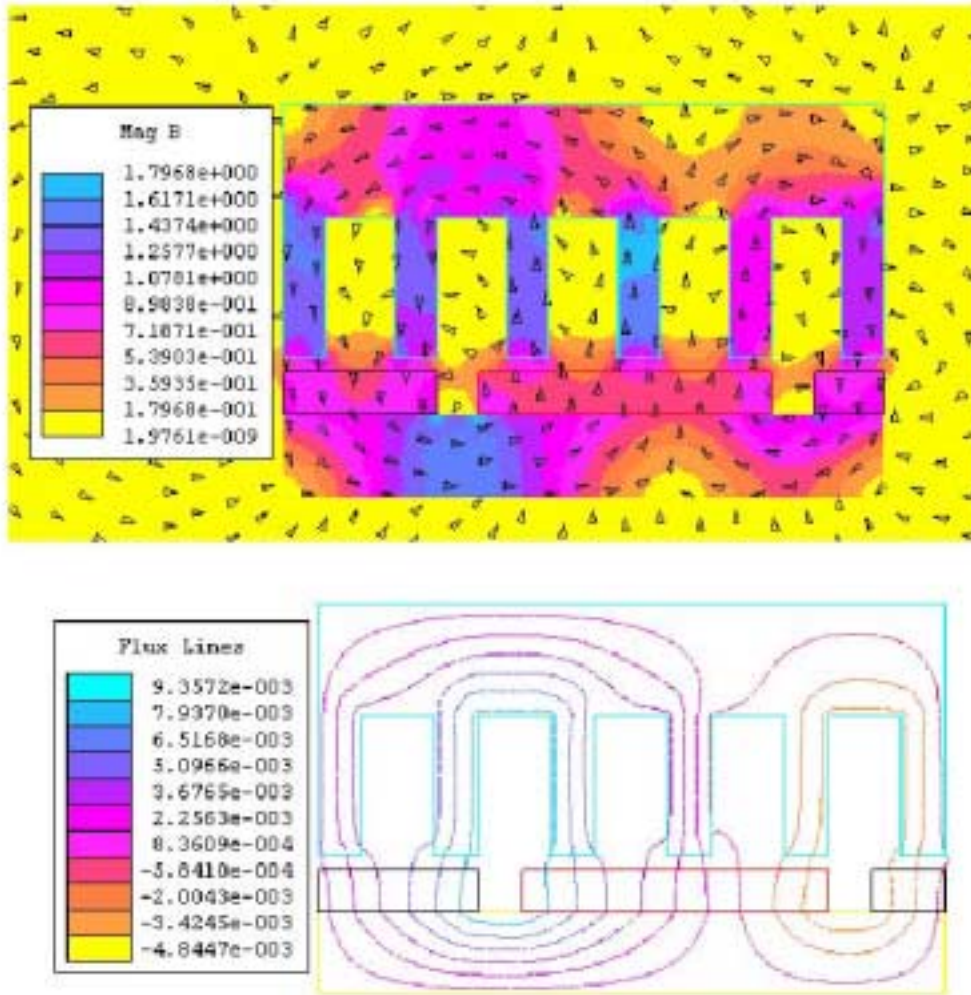


Figure 3.31 Figures from the finite element software showing the flux density distribution and flux flow path

Results that we give is the average of the values of flux density got at different planes at a particular arm or part of the structure which is of interest

SECTION	ANSOFT RESULT In tesla (T),	ANALYTICAL MODEL RESULT in tesla (T)
Tooth 1	1.1911	1.2773
Tooth 2	0.9575	0.9557
Tooth 3	1.5045	1.5189

Tooth 4	1.41	1.4657
Tooth 5	1.1987	1.266
Tooth 6	1.357	1.397
Yoke 1	0.4924	0.48
Yoke 2	0.1199	0.1206
Yoke 3	0.499	0.449
Yoke 4	1.0398	0.9986
Yoke 5	0.59	0.53
Core 1	0.67445	0.6790
Core 2	0.1693	0.171
Core 3	0.448	0.59
Core 4	1.376	1.3809
Core 5	0.7565	0.7014

Table 3.4 Comparison of Flux Density values (magnitude only) obtained for various sections

The value of flux density got from the analytical model closely resembles those from the Finite Element Analysis clearly indicating the correctness of the model.

3.5.7 Study on an actual Permanent Magnet Machine

In this section we apply the reluctance model developed to the *Permanent Magnet Motor* that is currently used by Delphi Saginaw in the steering wheel applications. In the current case reluctance model is applied only to a pole-pair of the machine, because we had earlier proved that flux pattern is usually repeated for every pole-pair. Also in this case we do not split every section that is analysed into various planes and then average the flux density in that section to be compared with that of analytical model results. Because the geometry is complex, splitting them into various planes is avoided. Instead the flux density distribution curve that we obtain from ansoft is visually compared with the results we obtain from analytical model. This is because we have already proved the validity of the model developed from the previous cases.

3.5.7.1 Structure

The machine structure that is to be studied is given below

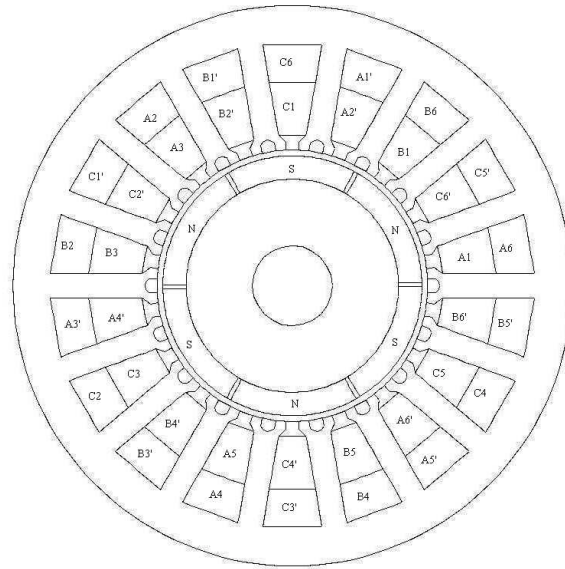


Figure 3.32 The machine structure

3.5.7.2 Reluctance Model for the actual P.M. Machine

The reluctance model for the same is given below.

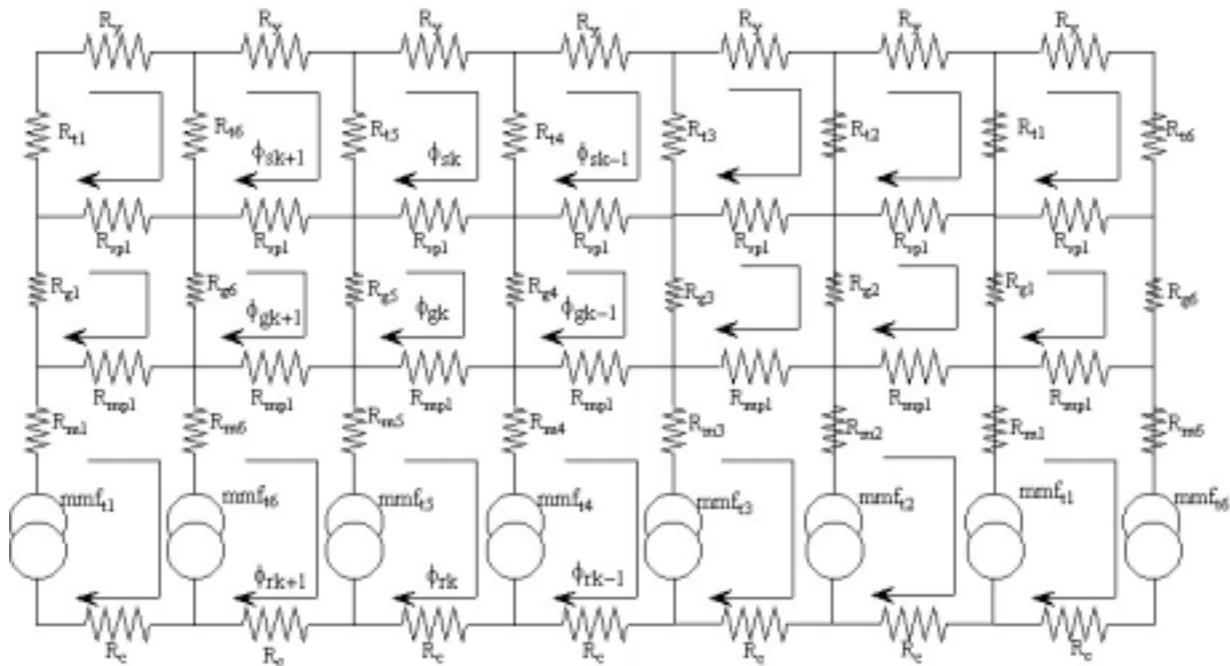


Figure 3.33 Reluctance Model of the P.M. Machine (pole-pair only)

From the figure we see ends of the pole-pair being flanked by the sectors of another pole-pair.

sector 1 : is flanked by sector 6 of preceding pole-pair on its right.
 sector 6 : is flanked by sector 1 of following pole-pair on its left.

This is done taking into account that sectors of preceding and following pole-pairs will have an influence in the pole-pair being studied. This is clearly shown by the loop fluxes as marked. To get to the individual fluxes in each tooth, air-gap etc. we have to find the individual branch flux from which the flux density is found when the branch flux is divided by the corresponding area. The arrows in the flux path indicate the assumed direction of flow of flux in the corresponding loop. The rules we follow are the same as followed in Maxwell's loop current method.

For eg : the flux in the branch of tooth 4 = $\phi_{sk} - \phi_{s(k-1)}$.

Similarly the flux in air-gap 5 = $\phi_{g(k+1)} - \phi_{gk}$.

3.5.7.3 Results from Analytical Model

The value of flux density at various sections that were calculated from the Analytical Model for the actual P.M. Machine is tabulated below.

Section	Analytical Model Result Flux density in Tesla (T)
Tooth 1	1.013
Tooth 2	1.31
Tooth 3	.93
Tooth 4	-1.013
Tooth 5	-1.31
Tooth 6	-.93
Airgap1	0.54
Airgap2	0.698
Airgap3	0.495
Airgap4	-0.54
Airgap5	-0.698
Airgap6	-0.495
Rotor core 1	1.051
Rotor core 2	1.314
Rotor core 3	0.9665
Rotor core 4	-1.051
Rotor core 5	-1.314
Rotor core 6	-0.9665

Table 3.5 Flux Density of various parts as obtained from analytical model

Because the geometry is complex, splitting them into various planes is avoided. Instead the flux density distribution curve that we obtain from ansoft is visually compared with the results we obtain from analytical model.

The number of slots /pole/phase in this machine is 1. The following figure shows the flux flow in the machine when rotor is placed so that the north pole is under the teeth 1 to 3 and the

south pole under the teeth 4 to 6. The horizontal axis is the reference axis for angle measurements

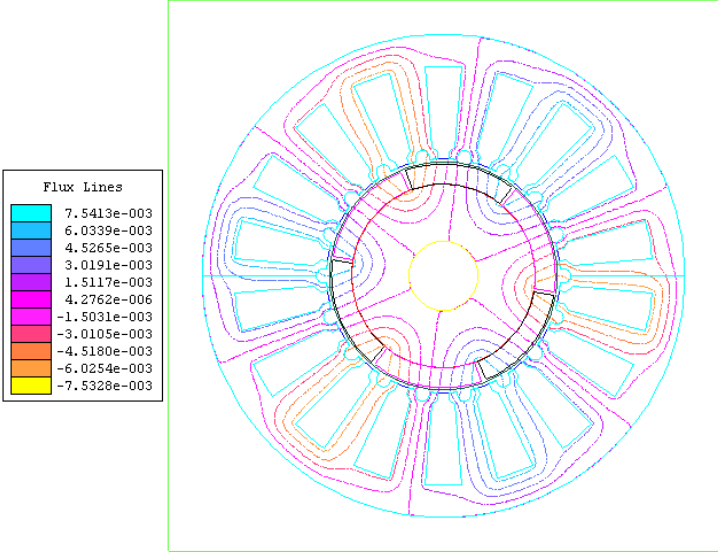


Figure 3.34 Flux flow path for the P.M.Machine (from Delphi) obtained through finite element analysis

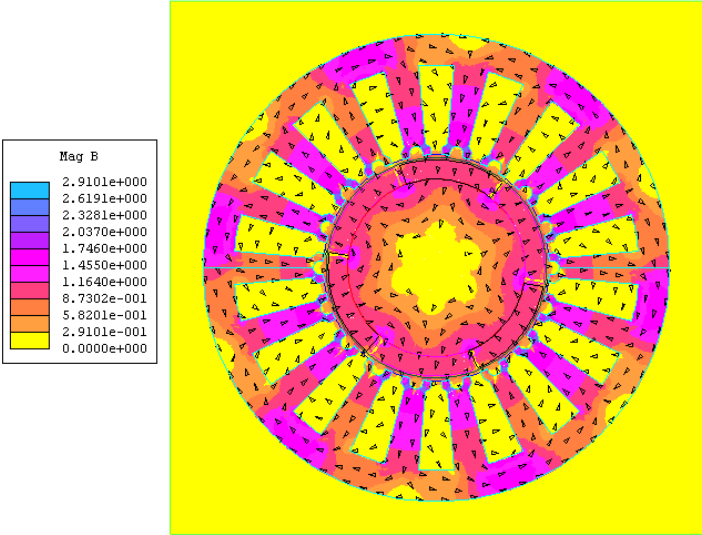


Figure 3.35 Flux density distribution of the P.M.Machine (from Delphi) obtained through finite element analysis

The above figure clearly validates our assumption that flux pattern repeats itself with every pole-pair. Also our assumption in the flux flow direction is validated.

Reference

- [1] J.R. Hendershot Jr. and T.J.E. Miller, 'Design of brushless Permanent Magnet Motors', *Magna Physics Publishing and Clarendon Press, Oxford, 1994.*
- [2] Mongkol Konhirun, 'Optimal Design of Permanent Magnet Synchronous Generator', *a Master's Thesis in the Dept. of Electrical Engineering, The Ohio State University, 1999.*
- [3] D.C. Hanselman, 'Brushless Permanent-Magnet Motor Design', *McGraw-Hill, 1994.*
- [4] M.L. Awad, "Modeling of Synchronous Machines for system studies", *PhD thesis in the Dept. of Electrical Engineering, University of Toronto, 1998.*
- [5] Magsoft Corporation, 'Finite Element Analysis Software Reference Manuals', *Magsoft Corporation, Troy, NY, April 1995.*
- [22] G.R. Slemon and M.L. Awad, "On Equivalent Circuit Modeling for Synchronous Machines", *PE-129-EC-0-06-1998.*
- [23] G.R. Slemon, "Modeling of Induction Machines for Electric Drives", *IEEE Trans., vol.IA-25, No.6, pages 1126-1131, 1989.*
- [24] G.R. Slemon, "Circuit Models for Polyphase Machines", *Electric Machines and Power Systems, vol.8, No.4/5 pages 369-379, 1983.*
- [27] Sebastian, T., Slemon, G. R., and Rahman, M. A., "Modelling of Permanent Magnet Synchronous Motors", *IEEE Transactions on Magnetics, vol. MAG-22, no. 5, pp. 1069-1071, September 1986.*

CHAPTER 4

Electric And Magnetic Design of Generator

4.1 Design philosophy

4.1.1 Sizing Equations

4.1.1.1 Introduction

For the generator, we could represent the various power losses as shown below,

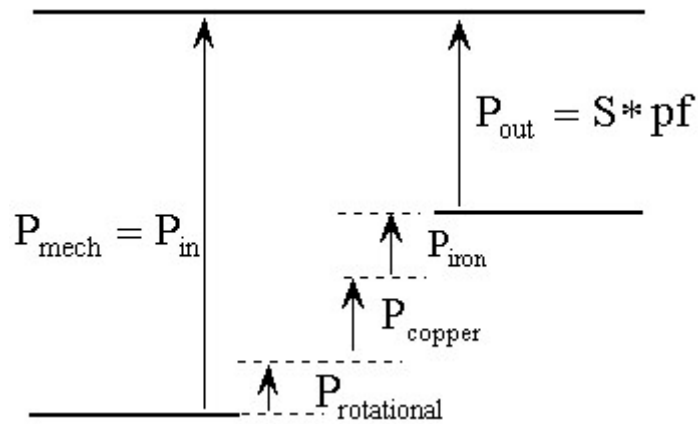


fig : 4.1 Various Power associated with a Generator

Here $P_{out} = S * pf$, (4.1)

is the apparent power fed into the rectifier-converter topology by the machine.

P_{iron} = iron losses ; P_{copper} = copper losses ; $P_{rotational}$ = rotational losses

For the design algorithm to be iterated to obtain a machine with maximum power density and minimum weight, we would try to establish various power in terms of D^2L ie $P_g = D^2L$, where D is the inner diameter of stator and L is the length of stack.

$$\text{Also Power Density} = \frac{\text{Power Generated}}{\text{Volume of machine}} \quad (4.2)$$

4.1.1.2 Loading

Total Magnetic Loading : the total flux around the armature (or stator) periphery at the air-gap is called **total magnetic loading**.

$$\text{T.Magnetic Loading} = p\phi \quad (4.3)$$

where p = number of poles ; ϕ = flux at the air-gap

Specific Magnetic Loading : the average flux density over the air-gap of the machine.

$$\text{Sp. Mag. Loading, } B_{av} = \frac{\text{T.flux around air-gap}}{\text{area of flux path at air-gap}} = \frac{p\phi}{\pi DL} \quad (4.4)$$

Total Electric Loading : the number of ampere conductors around the armature (or stator) periphery is called total electric loading.

$$\text{T. Electric Loading} = I_s Z \quad (4.5)$$

where I_s = rms value of current per phase ;

Z = total number of conductors around the stator .

Specific Electric Loading :

The number of armature ampere conductors per meter of armature periphery at air-gap

$$\text{Sp. Electric Loading, } A = \frac{I_s Z}{\pi D} \quad (4.6)$$

$$A = \frac{n_{\text{conductors}} * I_{\text{rms}}}{\pi D} = \frac{n_{\text{conductors}} * J * A_{\text{conduc}}}{\pi D} \quad (4.7)$$

where $n_{\text{conductors}} = Z$ = total number of conductors

J = current density in A/mm^2 ;

A_{conduc} = area of each conductor in mm^2

$$\text{Total Area of copper ; } A^T = n_{\text{conduc}} * A_{\text{conduc}} \quad (4.8)$$

$$\text{Hence } A = \frac{A^T * J}{\pi D} = \frac{N_{\text{slots}} * A_{\text{slot}}^1 * k_{\text{sf}} * J}{\pi D} \quad A/m \quad (4.9)$$

N_{slots} = number of slots ;

A_{slot}^1 = area of 1 slot ;

k_{sf} = slot fill factor ;

A = Sp. Electric Loading = Ampere Loading

4.1.1.3 Sizing Equation

Back emf - rms and peak value

The induced voltage of a stator coil with N_c -turns directly expressed from the flux-linkage Ψ waveform by Faraday's Law as shown in [1]

$$e(\xi) = \frac{d\Psi(t)}{dt} = \frac{d\xi}{dt} \cdot \frac{d\Psi(\xi)}{d\xi} = \omega_m \frac{d\Psi(\xi)}{d\xi} = \omega_m N \frac{d\Phi(\xi)}{d\xi} \quad (4.10)$$

where Φ is the flux-linkage for one turn of coil (Wb)

ξ is the rotor position compared with the stationary reference axis (rad)
 ω_m , which equals to $d\xi/dt$, is the rotor angular speed (rad/sec)

When Ψ_m is the peak flux linkage of a full pitch coil aligned with d axis

p = number of pole-pairs

B_g = air-gap flux density

N_c = number of turns of coil

k_w = coil winding factor

Then for a rectangular magnetic flux distribution, voltage developed per coil e_c is

$$e_c = \frac{d\Psi_m}{dt} = N_c \phi_m = k_w N_c B_g \frac{\pi D L \omega_m}{2p} \quad (4.11)$$

If all coils in one phase have the same voltage induced in them, in phase with each other, then the total phase mmf has a peak value, \hat{e}_{ph}

$\hat{e}_{ph} = e_c * \# \text{coils in series per phase}$

or if $N_{ph} = \# \text{ turns in series per phase}$

if $Z = \# \text{ conductors in machine}$; $a = \# \text{ parallel paths}$

$$N_{ph} = (1/3) * (Z/2a) \quad (4.12)$$

$$\text{then } \hat{e}_{ph} = k_w N_{ph} B_g \frac{\pi D L \omega_m}{2p} \quad (4.13)$$

In a square wave generator 3-phase generator, the line-line voltage is

$$\text{Wye-connected, } \hat{e}_{LL} = 2\hat{e}_{ph} \quad (4.14)$$

$$\text{Delta-connected, } \hat{e}_{LL} = \hat{e}_{ph} \quad (4.15)$$

$$\text{The EMF constant, } k_E = \frac{\hat{e}_{LL}}{\omega_m} \quad (4.16)$$

ELECTRIC LOADING :- this is defined as linear current density around the air-gap circumference.

$$A = \frac{\text{Total Ampere-Conductors}}{\text{air-gap circumference}} = \frac{2mN_{ph}I}{\pi D} \quad \text{Ampere/m} \quad (4.17)$$

SIZING EQUATION

Let us consider the active power supplied by the PM machine as shown by Lippo in [25]

$$S \cdot pf = m \frac{1}{T} \int_0^T e(t) i(t) dt \quad (4.18)$$

$$\text{or } S \cdot pf = m \frac{1}{T} \int_0^T \frac{e(t) i(t)}{E_{pk} I_{pk}} dt \cdot E_{pk} I_{pk} = m k_p E_{pk} I_{pk} \quad (4.19)$$

where:

S - Apparent Power of the P.M. Machine (KVA)

pf - power factor as seen in AC line

T - period of the voltage waveform (in seconds)

e(t), i(t) - instantaneous value of the voltage and current of the machine

E_{pk} - peak value of the machine output voltage

I_{pk} - peak value of the machine output current

m - number of phases

k_p - power waveform factor, given by (4.3)

$$k_p = \frac{1}{T} \int_0^T \frac{e(t)i(t)}{E_{pk} I_{pk}} dt \quad (4.20)$$

We will be trying to relate the active power generated to the main dimensions: the armature diameter (D) and core length/ stack length (L), in terms of magnetic loading and electric loading .

The maximum available air-gap power = mEI

$$mEI = \frac{T\omega}{P} = \frac{m\omega k_{w1} N_{ph} B_g \alpha_m \pi DL}{2p} \frac{I}{\sqrt{2}} \frac{2\pi D}{2\pi D} \quad (4.21)$$

$$\text{Re-arranging } mEI = \frac{T\omega}{P} = \omega k_{w1} \frac{2mN_{ph} I B_g \alpha_m \pi^2 D^2 L}{\pi D \sqrt{2} 4p} \quad (4.22)$$

$$\text{We know } A = \frac{\text{Total Ampere-Conductors}}{\text{air-gap circumference}} = \frac{2mN_{ph} I}{\pi D} \quad \text{Ampere/m} \quad (4.23)$$

Thus substituting the above equation in (4.22) we get

$$mEI = \frac{T\omega}{P} = \frac{\omega k_{w1}}{\sqrt{2}} A \frac{B_g \alpha_m \pi^2 D^2 L}{4p} \quad (4.24)$$

$$\text{rearranging we get } mEI = \frac{T\omega}{P} = \frac{\omega k_{w1}}{\sqrt{2}} \frac{AB_g \alpha_m \pi^2}{4p} D^2 L = KD^2 L \quad (4.25)$$

$$\text{where } K = \frac{\omega k_{w1}}{\sqrt{2}} \frac{AB_g \alpha_m \pi^2}{4p} \quad (4.26)$$

Solving for (4.25) would give the machine dimensions to start with in terms of D^2L , for a fixed mEI. To further split D^2L we use the ratio $\frac{L}{\tau} = \frac{L}{\pi D / 2p}$ (4.27)

where p stands for pole pairs. $\frac{L}{\tau}$ ratio is varied between .7 & 1.4 to get the actual machine parameters for minimum weight and maximum efficiency.

The involvement of the machine volume (a function of D^2L) in the power output of the machine. Equation (4.25) reveals that for minimum volume (and maximum power density) it will be necessary to maximize the product ($B_g A$). This is one of the objectives of this design method. The product of the magnetic and electric loading will be monitored when iterating the other variables.

It is not assumed that the machine with the minimum volume will be selected as this design solution may not satisfy other requirements. This idea will be developed when the algorithm is explained.

4.2 Methodology of Design

We use the optimization routines provided in the Matlab to arrive at the optimal machine parameters. The MATLAB function, fmincon, is employed for solving inequality constrained optimization problem. The machine parameters are first expressed in terms of some of the basic variables. Total power generated, total machine weight, total power loss etc. are then expressed in terms of these machine parameters. We then optimize for the minimum cost function which is expressed as a function of power loss and minimum weight. Thus to get the optimal design with minimum weight and minimum power loss, we have to arrive at the optimal design variables which satisfy certain inequality constraints which is factor of certain machine requirements like power generated, machine size, magnet not getting demagnetized because of the stator current etc. Chapter 5 clearly explains the optimization principle and design algorithm. The flow chart which follows clearly gives methodology of design of the generator.

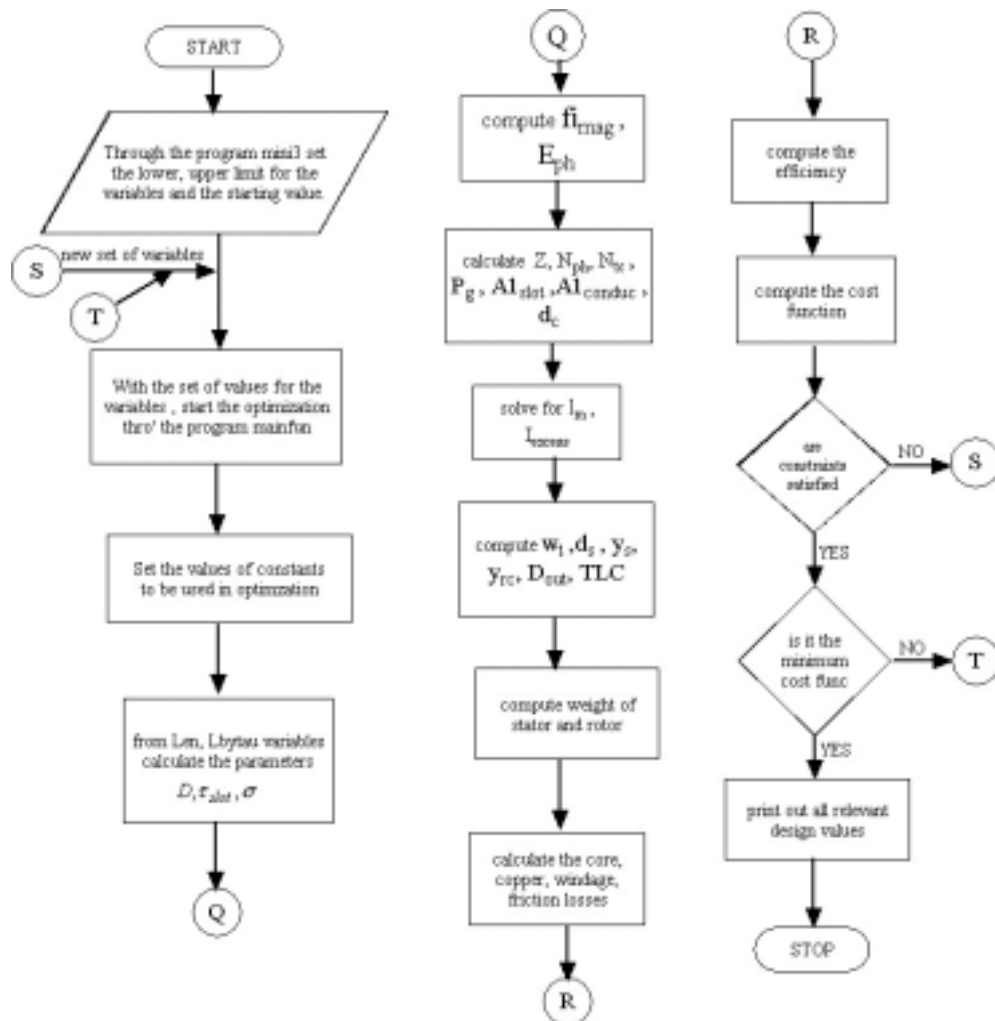


Figure: 4.2 Flowchart for optimal design methodology of PMSG

4.3 Magnetic Design

Flux is clearly the most important parameter in the design of a permanent magnet machine. This part describes the simplest methods of calculating it, to be used later for emf and torque calculations. But first the choice of magnet and the operating point of magnet.

The flux is intended to link the coils of the phase windings on the stator. The laminated steel core of the stator and rotor acts as a guide for the flux. Because stator and rotor steel absorb very little MMF at normal operating range, most of magnetic MMF is available to drive the flux across the air-gap. However, the steel does not have unlimited capacity for carrying flux. Beyond a flux density of 1.6-1.7 T , permeability of steel decreases rapidly which would increase MMF drop in steel. Core losses (eddy and hysteresis losses) also increase at high air-gap flux density.

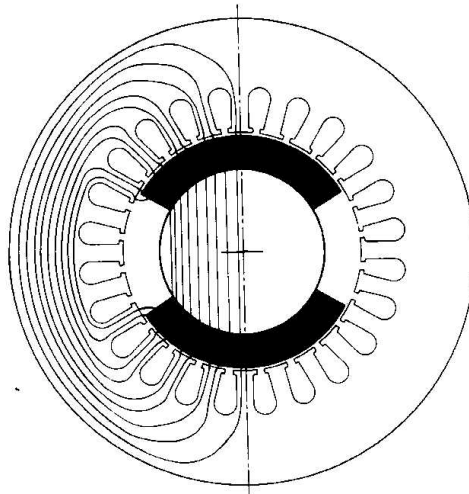


Fig : 4.3 Cross Section of a two pole generator showing the flux [1]

From the design of stator (slot and teeth arrangement) clearly there is concentration of flux at the teeth. Usually the air-gap flux density is just half the maximum flux density in steel. This is a very important consideration in the design of generator.

4.3.1 Permanent Magnet and Magnetic Circuits

Basically, the magnetic material is categorized into two types that are soft magnetic material and hard magnetic material. Soft magnetic materials are characterized by a narrow hysteresis loop. Hard magnetic materials are characterized by wide loop. The intersection of the loop with the ordinate is called the residual or remanent flux density B_r . The intersection of the abscissa and the loop is called the coercive force, H_c . Figures 4.4 and 4.5 show the typical characteristic curves for the soft and hard magnetic materials.

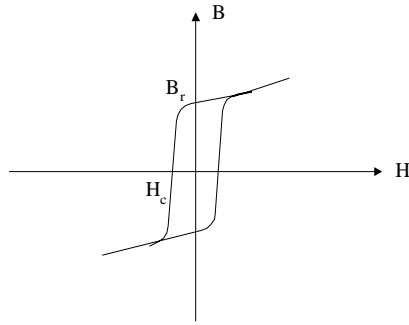


Figure 4.4 : B-H curve of soft magnetic material

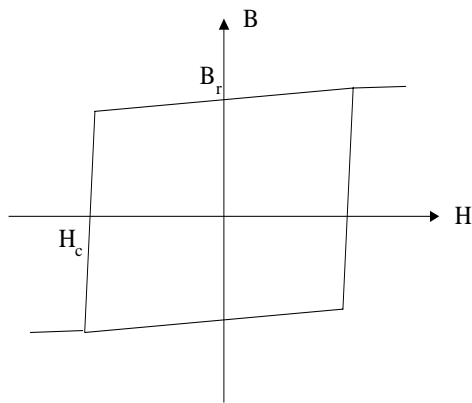


Figure 4.5 : B-H curve of hard magnetic material

Many of the magnetic materials commonly used in machines exhibit a linear normal magnetization characteristics in the second quadrant. If a linear model is employed in designing, the actual demagnetizing curve would be checked for all expected operating conditions also.

The value of H to bring the intrinsic flux density to zero is a larger (negative) value called H_{ci} , the intrinsic coercive force. When the intrinsic flux density is approximately a straight line over a wide range the magnetization vector inside the material is constant. Thus the ampere-turns available to magnetize an external magnetic circuit are constant, i.e., independent of the external reluctance or external source. The intrinsic and normal curves are plotted in Figure 4.6.

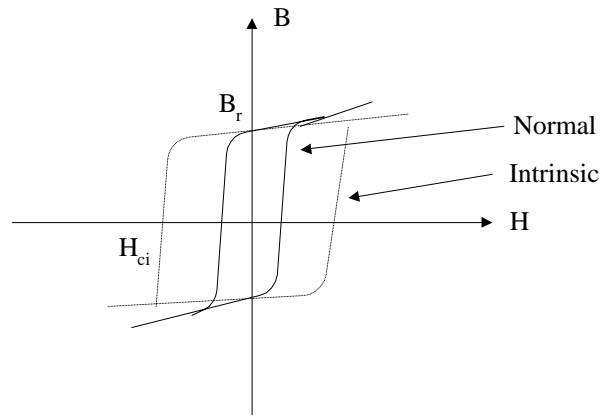


Figure 4.6 : Intrinsic and normal demagnetization curves

A typical B-H loop of a permanent magnet is given below

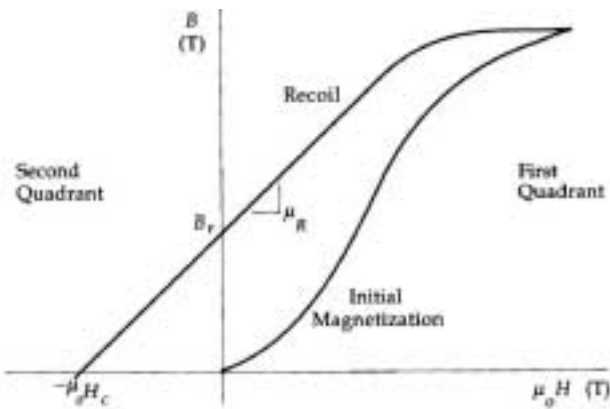


Figure 4.7 : The B-H loop of a permanent magnet [1]

The typical demagnetizing curves of the permanent magnet types can be seen in Figure 4.8. In addition, the magnetic and physical characteristics of the popular permanent magnets can be shown in Appendix B.

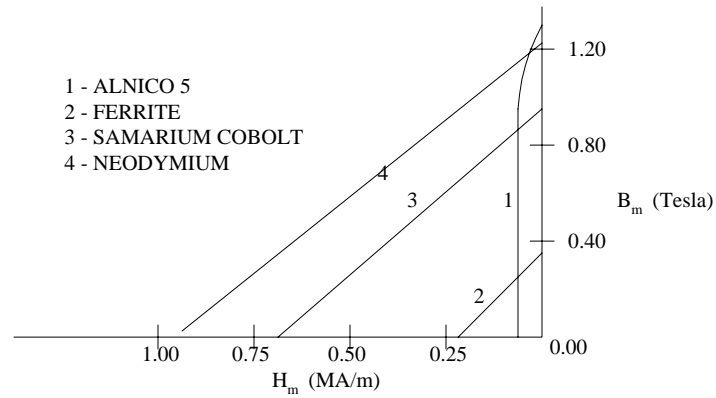


Figure 4.8 : Demagnetization curves for some PM materials [1],[2]

In magnetic circuits a permanent magnet can be represented by a Thevenin's Equivalent circuit :- mmf source in series with internal reluctance.
 Norton's Equivalent circuit:- mmf source in parallel with internal reluctance.

$$\text{Permeance}(P) = \frac{1}{\text{Reluctance}(R)} = \frac{\mu A}{l} \quad (4.28)$$

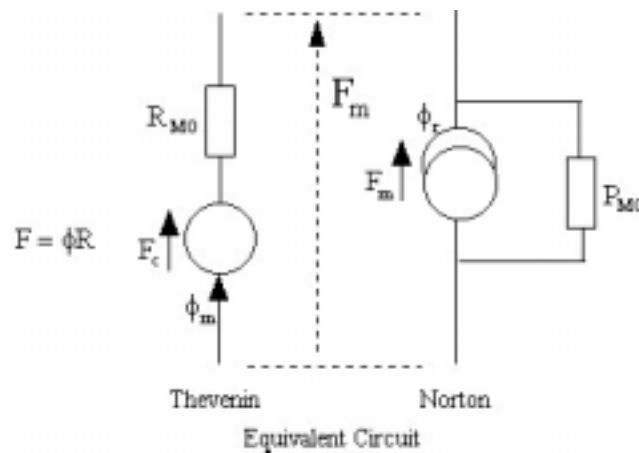


Figure 4.9 : Thevenin and Norton Equivalent Theorem [1]

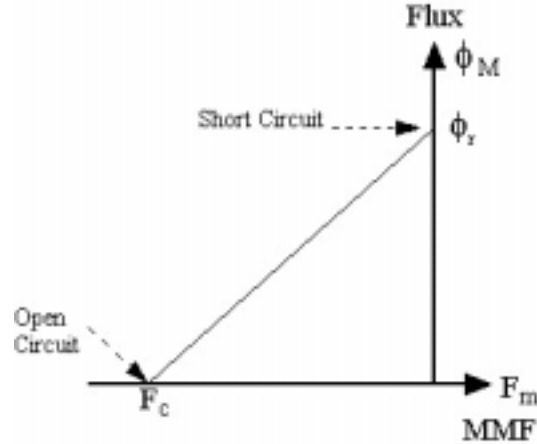


Figure 4.10: MMF/flux characteristic of Permanent Magnet in the second quadrant [1]

ϕ_r = Remnent flux, that which remains in the magnet after it has been magnetized.

F_c = Coercive force, because it is the force (MMF) required to coerce the magnet to produce zero flux. It represents resistance of magnet to demagnetize.

Magnets require the two parameters F_c and ϕ_r to characterize them properly. For a given remnent flux ϕ_r it is desirable to have the flattest possible slope since this is associated with a high value of F_c , and a high resistance to demagnetize. The operating point of a permanent magnet has to be determined around the point of $(B \cdot H)_{\max}$ in the B-H curve because the magnet volume used in the machine will be minimized at this point, thereby reducing the magnet cost. For a detailed discussion on the operating point refer [2].

4.3.1.1 Some Basic Formulae

The remanent flux ϕ_r and the coercive MMF F_c depends not only on the material properties B_r, H_c respectively, but also on the dimensions of the magnet

$$\phi_r = B_r A_m \quad F_c = H_c L_m \quad (4.29)$$

A_m = magnet pole area ; L_m = length of magnet ; B_r = remanent flux density;

H_c = coercive magnetizing force or coercivity .

Magnet flux ϕ_m , and mmf drop F_m at operating point are

$$\phi_m = B_m A_m \quad F_m = H_m L_m \quad (4.30)$$

B_r at any temperature (T 'C) can be giveb by

$$B_r(T) = B_r(20) * [1 + \alpha_{Br} * \frac{T - 20}{100}] \quad (4.31)$$

α_{Br} = reversible temperature co-efficient of B_r quoted in %/ 'C .

$B_r(20)$ = value of B_r at 20 'C.

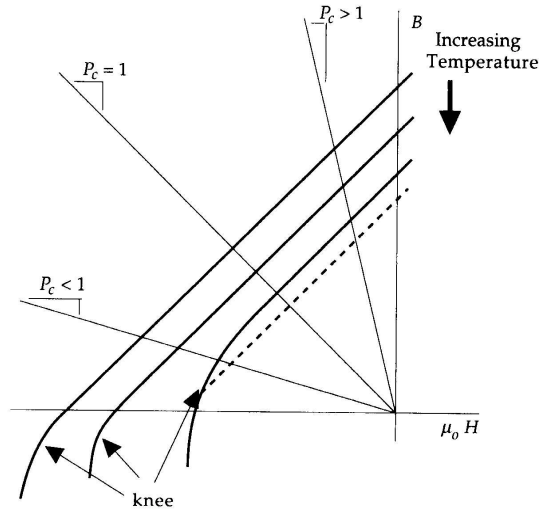


Figure 4.11 : Typical temperature characteristics of permanent magnet [1]

4.3.1.2 Linear Design of Magnetic Circuit

When the generator windings are energised, the operating point dynamically varies following minor hysteresis loops about static operating point. Refer [1] for further details.

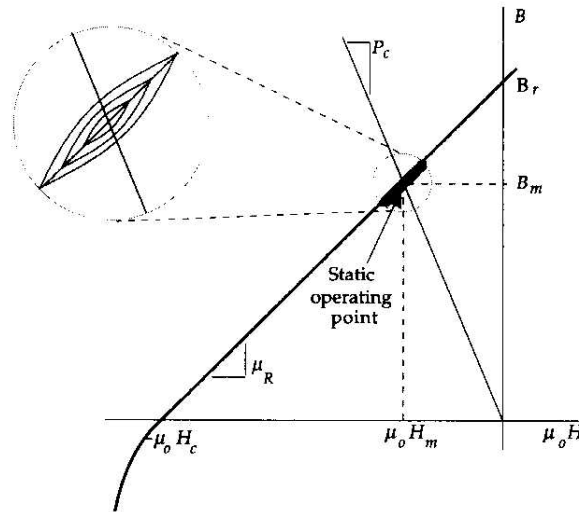


Figure 4.12 : Dynamic operation of a magnet about its operating point [1]

$$B_m = B_r + \mu_r \mu_0 H_m \quad (4.32)$$

$$\phi_m = A_m B_m = B_r A_m + \mu_r \mu_0 H_m A_m \quad (4.33)$$

$$\phi_m = \phi_r + P_m F_m$$

$$\text{where } \phi_m = B_r A_m; \quad P_m = \frac{\mu_r \mu_0 H_m A_m}{L_m}; \quad F_m = H_m L_m \quad (4.34)$$

Usually the shape of the magnet in machine is not rectangular but more often like an arc shape as shown below.

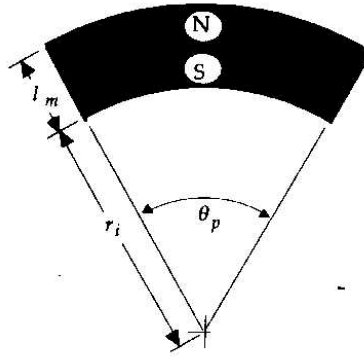


Figure 4.13 : An arc shaped magnet

We have $\theta_p = \alpha_m \frac{\pi}{p}$ (4.35)

$$P_m = \frac{\mu_0 \mu_r L \theta_p}{\ln\left(1 + \frac{l_m}{r_i}\right)}$$
(4.36)

since $l_m \ll r_i$; $P_m = \mu_0 \mu_r L \theta_p \left(\frac{1}{2} + \frac{l_m}{r_i}\right)$ (4.37)

4.3.1.3 Basic Translational P.M Generator Structure

When the machine is opened and sectionalized we see a structure as shown below

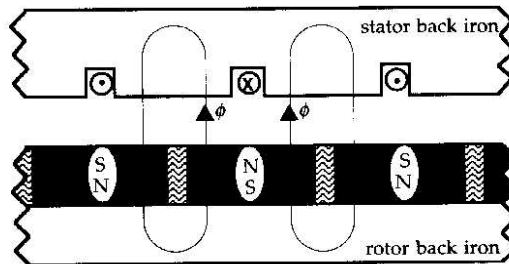


Figure 4.14a : Basic Translational structure of permanent magnet generator [3]

The magnetic equivalent circuit model for the above structure is

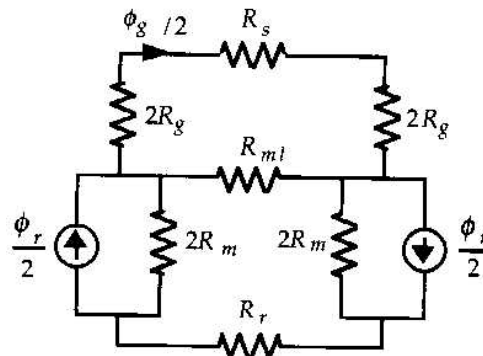


Figure 4.14b : Magnetic circuit model for the structure shown in fig 4.14a [3]

$$R_m = \text{magnet reluctance} ; R_m = \frac{1}{P_m} \quad (4.38)$$

$R_s, R_r =$ stator and rotor stack reluctance which is negligible when compared with air-gap and magnet reluctance and so is neglected here in the derivation which follows but is used as such in the actual model.

$R_{ml}, R_g =$ magnetic leakage reluctance and air-gap reluctance respectively.

Neglecting R_s, R_r and adding 2 magnet models in series and simplifying we get

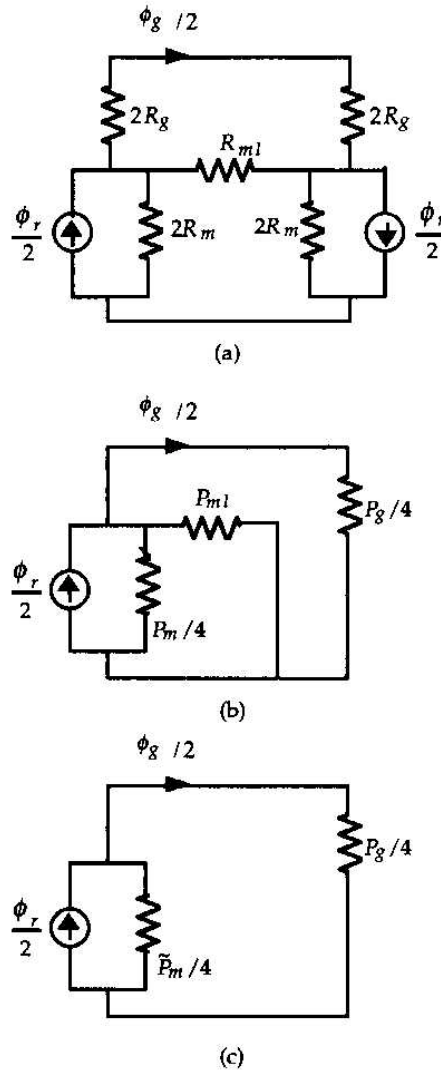


Figure 4.15 : Simplifications of the magnetic circuit in fig 4.14 [3]

$$\tilde{P}_m = P_m + 4P_{ml} \quad (4.39)$$

$$P_m = \frac{\mu_r \mu_0 \alpha_m \tau_p L}{l_m}; \quad \alpha_m = \frac{\tau_m}{\tau_p} \quad (4.40)$$

$$P_{ml} = \frac{\mu_0 L}{\pi} \ln \left(1 + \frac{\pi g}{(1 - \alpha_m) \tau_p} \right) \quad (4.41)$$

$$P_g = \frac{\mu_0 \tau_p (1 + \alpha_m) L}{2g_e}; \quad g_e = g k_c \quad (4.42)$$

where L, l_m = stack and magnet length respectively
 τ_m, τ_p, τ_s = magnet , pole and slot pitch respectively
 g = air-gap length
 g_e = air-gap length after correction
 ω_s = width of slot

$$k_c = \text{carter's coefficient} = \left[1 - \frac{\omega_s}{\tau_s} + \frac{4g'}{\pi \tau_s} \ln \left(1 + \frac{\omega_s \pi}{4g'} \right) \right]^{-1} \quad (4.43)$$

$$g' = g + \frac{l_m}{\mu_r} \quad (4.44)$$

$$\text{Flux concentration factor, } C_\phi = \frac{A_m}{A_g} = \frac{2\alpha_m}{1 + \alpha_m} \quad (4.45)$$

A_m, A_g are the cross-sectional area of magnet and air-gap respectively.

$$\text{Permeance co-efficient, } PC = \frac{l_m}{g C_\phi} \quad (4.46)$$

$$\text{And in S.I unit } PC = \frac{\mu_0}{f_{lkg}} * \frac{l_m}{g C_\phi} \quad (4.47)$$

where f_{lkg} = flux leakage co-efficient $\cong 0.9$

Air-gap Flux Density :-

From the figure 4.14 and figure 4.15 by the division of flux , the air-gap flux is related to the

$$\text{magnetic flux by } \frac{\phi_g}{2} = \frac{\frac{P_g}{4} \phi_r}{\frac{P_g}{4} + \frac{\tilde{P}_m}{4}} \quad (4.48)$$

$$\phi_g = \frac{1}{1 + \frac{\tilde{P}_m}{P_g}} \phi_r \quad (4.49)$$

$$\text{substituting the known equations considered above } \phi_g = \frac{1}{1 + \frac{2\mu_r \alpha_m k_{ml} k_{cg}}{(1 + \alpha_m) l_m}} \phi_r \quad (4.50)$$

rewriting the above equations using PC, C_ϕ , we get
$$\phi_g = \frac{1}{1 + \frac{\mu_r k_c k_{ml}}{PC}} \phi_r \quad (4.51)$$

when expressed the above equation in terms of flux densities we get the average value of flux density crossing the air-gap
$$B_g = \frac{C_\phi}{1 + \frac{\mu_r k_c k_{ml}}{PC}} B_r \quad (4.52)$$

Refer [1], [2], [3] for further details.

4.3.1.4 Non-Linear Model for Magnetic Circuit

The magnetic circuit calculations in the previous section neglects mmf absorbed by the steel parts of the magnetic circuits and is therefore valid only when flux-density levels are low. But when high energy magnets are used (as in done usually) it is necessary to take mmf drop in steel also into account.

In nonlinear calculation method we must satisfy Ampere's Law which takes into account mmf drops around the flux path, as shown clearly in [1]

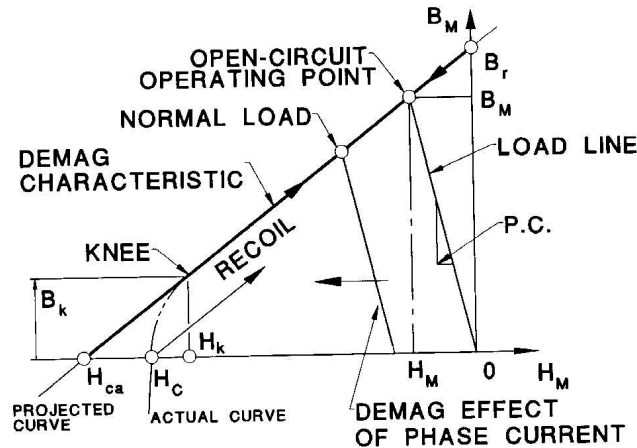


Figure 4.16 : Characteristics of hard magnet - II Quadrant part of Full Hysterisis Loop [1]

An attempt to make the operating point below B_k results in irreversible demagnetization. This shall be one of the primary conditions that we check in our iterations ie $B_{operating} > B_k$. the procedure is to add mmf drops around the magnetic circuit, taking into account the nonlinear B/H curve of steel and equate them to the apparent open circuit mmf of the magnet, F_{ca} .

$$F_{ca} = H_{ca} * L_m$$

where H_{ca} = apparent co-ercivity of magnet ; L_m = length of magnet .

$$\text{From figure 4.17 we see } \phi_m = \phi_g + \phi_1 \quad (4.53)$$

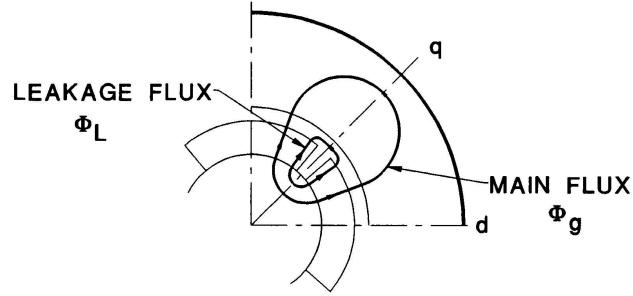


Figure 4.17 : Main flux path in surface mounted interior magnet generator [1]

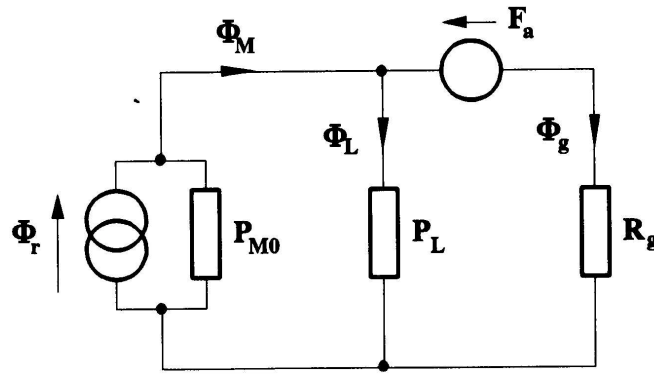


Figure 4.18 : Magnetic Equivalent circuit of one pole [1]

$$\text{Therefore flux leakage co-efficient } f_{lkg} = \frac{\phi_g}{\phi_m} = \frac{\phi_g}{\phi_g + \phi_l} \quad (4.54)$$

The individual mmf drops :-

$$1. \quad \text{Air-gap : } B_g = \frac{C_\phi}{1 + \frac{\mu_r k_c k_{ml}}{PC}} B_r \quad (4.55)$$

$$F_g = g' * \frac{B_g}{\mu_0} \quad (4.56)$$

$$2. \quad \text{Stator Yoke : } B_{sy} = B_g * \frac{A_g}{A_{sy}} \quad (4.57)$$

$$F_{sy} = H_{sy} L_{sy} = F(B_{sy}) L_{sy} \quad (4.58)$$

$$B = \mu_0 \mu_r H + B_r \quad (4.59)$$

from which H of the corresponding part is found.

$$3. \quad \text{Teeth : } B_{st}, H_{st} \text{ are the Flux density and Flux intensity at teeth.}$$

$$F_{st} = H_{st} L_{st} = F(B_{st}) L_{st} \quad (4.60)$$

4. Rotor Yoke : B_{ry}, H_{ry} are the Flux density and Flux intensity at rotor yoke.

$$F_{ry} = H_{ry}L_{ry} = F(B_{ry})L_{ry} \quad (4.61)$$

5. Magnet : $B_m = \frac{\phi_m}{A_m} = \frac{B_g A_g}{A_m f_{lkg}}$ (4.62)

Knowing B_m , we could find the value of H_m from $B_m = \mu_0 \mu_r H_m + B_r$ (4.63)

$$F_m = H_m L_m \quad (4.64)$$

$L_m, L_{sy}, L_{st}, L_{ry}$ are the length of magnetic path in magnet, stator yoke, stator teeth, rotor yoke respectively.

Adding all mmf we have $F = F_g + F_{sy} + F_{st} + F_{ry} + F_m$. The ampere's law is checked with F_{ca} . if

$F > F_{ca}$; B_g is decreased and iterated

$F < F_{ca}$; B_g is increased and iterated.

This iteration is continued until $F \leq 0.1\%$ of F_{ca} . Always check for $B_m > B_k$.

For the non-linear calculation of magnetic circuit to be performed, we determine the height of teeth, yoke width of stator and rotor ie structure of the machine is determined first for non-linear calculation of magnetic circuit to be performed.

4.3.2 Design of Iron Magnetic Path

The flux that passes through the stator/ rotor cannot be infinitely increased because of the saturation effects.

Assuming a square wave flux density, B_g we have the following term

$$\alpha_m = \frac{\text{pole arc}}{\text{pole pitch}} \quad (4.65)$$

$$\text{slot pitch, } \lambda = \frac{2\pi r_g}{N_s} \quad (4.66)$$

where N_s = number of stator slots ; $r_g = \frac{D_g}{2}$ = inner radius of stator

Considering that all flux flows through the stator teeth and nothing in slot.

$$\phi_{\text{tooth}} = B_g \lambda L k_{st} \quad (4.67)$$

k_{st} = lamination stacking factor, L = length of stack, B_g = air-gap flux density

If B_{gsat} is the maximum value of flux density, value just before saturation, allowed in teeth, then flux at stator tooth with this maximum value would be $B_{gsat} w_t L k_{st}$

Equating the above two equations we have the minimum value of tooth width

$$B_g \lambda L k_{st} = B_{gsat} w_t L k_{st}$$

$$\text{minimum value of tooth width , } w_t(\text{min}) = \frac{B_g}{B_{gsat}} \lambda \quad (4.68)$$

$$\text{In a machine with p pole-pairs , total flux per pole , } \phi_p = \frac{B_g D_i L \alpha_m \pi}{2p} \quad (4.69-a)$$

At stator yoke , the total flux at yoke will be equally divided into both sides of stator yoke

$$\phi_y = \frac{\phi_p}{2} \quad (4.69-b)$$

$$\text{at the limit of saturation , we have } \phi_y = B_{gsat} A_{yoke} = B_{gsat} y_s Lk_{st} = \frac{1}{2} \frac{B_g D_i L \alpha_m \pi}{2p}$$

$$\text{minimum value of stator yoke width } \therefore y_s(\text{min}) = \frac{D_i \alpha_m \pi}{4pk_{st}} \frac{B_g}{B_{gsat}} \quad (4.70)$$

By the flux continuity the flux of the stator yoke also travels through the rotor core

$$\therefore \phi_{rc} = B_{gsat} y_{rt} Lk_{st} = \frac{\phi_p}{2}$$

$$\text{minimum value of rotor core width is } y_{rc}(\text{min}) = \frac{(D_i - 2l_m) \alpha_m \pi}{4pk_{st}} \frac{B_g}{B_{gsat}} \quad (4.71)$$

4.4 Winding Design and Slot Design

4.4.1 Two Layer Winding

Almost all AC machines have two layered windings. This composition in the number of layers in winding decreases the length of coil that is used from a single layered winding. As a result I^2R losses also reduce because this loss is directly proportional to the length of winding. Also machine is more compact because since the diameter of stator reduces.

But the two layered winding increases the slot leakage because of the increased depth of slot. But the advantages more than compensate for the increase in leakage loss.

In our design of 4-pole /12 slot machine , with two layered winding have

Number of coils/ phase = $2 * p$; $p = \text{pole pair}$.

Therefor we have in our machine $N_{cp} = 2 * 2 = 4$, since $p=2$.

For the ideal current and voltage sharing amongst the coils we have

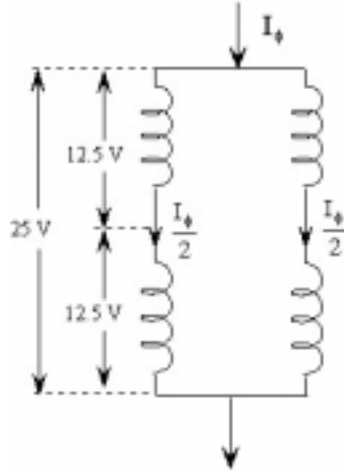


Figure 4.19 : Phase Winding depicting the voltage and current sharing between them

25 V/ phase was the requirement (refer chapter on Machine Requirements). The above composition for the circuit /phase reduces the losses to least.

More detailed account of why this winding design was chosen is clearly enumerated in the thesis presented by Mongkol Konghirun .

4.4.2 Conditions for good 2 layered winding

$$N_s = 2mpq = \text{integer} \quad (4.72)$$

where N_s = number of stator slots

m = number of phases

p = number of pole-pairs

q = number of slots/pole/phase

Also $2pq$ must be an integer. If the winding is made by having 'a' parallel paths then

$$\frac{2p}{a} = \text{integer}$$

Skewing is used to reduce the cogging torque of the machine.

4.4.3 Winding Factor

$$k_w, \text{ the winding factor in the machine is } k_w^n = k_d^n * k_p^n * k_s^n \quad (4.73)$$

where k_w^n = winding factor of n^{th} harmonic .

k_d^n = distribution factor of n^{th} harmonic

k_p^n = short pitching of n^{th} harmonic

k_s^n =skewing factor of n^{th} harmonic

Distribution Factor : if the conductors of winding are distributed in N_s stator slots, the angle γ between any 2 consecutive slots would be , $\gamma = \frac{2\pi}{2pqm}$ (4.74)

$$k_d^n = \frac{\text{Sin}\left(\frac{nq\gamma}{2}\right)}{q\text{Sin}\left(\frac{n\gamma}{2}\right)} \quad (4.75)$$

in our machine the number of slots/pole/phase, $q = 1$

$$\therefore k_d^n = \frac{\text{Sin}\left(\frac{n\gamma}{2}\right)}{\text{Sin}\left(\frac{n\gamma}{2}\right)} = 1 \quad (4.76)$$

Short Pitching Factor : if the coil was short pitched by an angle α then

$$k_p^n = \text{Sin}\left(\frac{n\alpha}{2}\right) = \text{Cos}\left(\frac{n\beta}{2}\right) \quad (4.77)$$

but in our machine the coils are full pitched and so $k_p^n = 1$

Skewing Factor : usually to avoid some noise in the machine when it is running we skew the stator slots by an angle. This not only reduces the noise but also smoothens the emf generated by the machine. Usually slots are skewed by a slot pitch, σ .

$$\therefore k_s^n = \frac{\text{Sin}(n\sigma/2)}{n\sigma/2} \quad (4.78)$$

where σ = skewing angle = slot pitch .

Number of coils/phase

$$\text{Stator voltage per phase, } E_s = 4.44 f\phi_m T_s k_{ws} \quad (4.79)$$

$$\text{where } k_{ws} = \text{winding factor and } \phi_m = B_{av} L \tau = B_{av} L \frac{D\pi}{2p} \quad (4.80)$$

$$\text{Turns/phase, } T_s = \frac{E_s}{4.44 f k_{ws} \phi_m} \text{ where } E_s \text{ is 25 V for our machine.} \quad (4.81)$$

Turns/coil, $N_c = T_s/2$.

Diameter of conductor

$$\text{Stator current/phase, } I_s = \frac{Q}{3E_s} \quad (4.82)$$

In our design we have current sharing between the coils in 1 phase. Therefore, maximum current in coil/phase = $I_s/2$.

$$\text{Therefore area of stator conductor} = \frac{I_s / 2}{\delta} \quad (4.83)$$

where δ = current density in A/mm².

$$\text{If } d_s = \text{slot depth ; } w_s = \text{slot width , area of each slot is } A_s = d_s w_s \quad (4.84)$$

$$\text{Therefore the copper area in each slot } A_{cu} = A_{eff} = A_s k_{sf} \quad (4.85)$$

$$\text{where } k_{sf} = \text{slot filling factor . The copper area in one slot is } A_{eff} = \frac{2N_c * \pi d_c^2}{4} \quad (4.86)$$

$$\text{which implies that diameter of the conductor is } d_c = \sqrt{\frac{4A_{eff}}{2N_c \pi}} \quad (4.87)$$

If the value of d_c is too big compared to usual cases then we split the conductors into parallel paths. This must fulfill the condition $\frac{2p}{a} = \text{integer}$.

$$\text{Diameter of the conductor in one of the 'a' parallel path , } d_c' = \frac{d_c}{\sqrt{a}} \quad (4.88)$$

4.5 Losses in the Machine

4.5.1 Copper Losses

Winding Resistance :- Resistance of several conductor sizes at 20'C and 100'C are available. Interpolation is to be used for estimation of resistance of conductor at other temperatures.

$$\text{D.C. Resistance , } R = \frac{\rho_r l_c}{A_c} \quad (4.89)$$

where ρ_r = conductor resistivity at 20'C $\left(\Omega \cdot \text{m or } \frac{\Omega \cdot \text{m}}{\text{m}^2} \right)$
 l_c = conductor length (m)
 A_c = cross sectional area of conductor (m²)

$$\rho_r \text{ at any other temperature is ; } \rho_r (T_2) = \rho_r (T_1) [1 + \beta (T_2 - T_1)] \quad (4.90)$$

$$\rho_r (T_1) = \rho_r (20'C) = 1.7241 * 10^{-8} \Omega \cdot \text{m and } \beta = 4.3 * 10^{-3} \text{C}^{-1}$$

A.C. Resistance of a conductor differs with frequency. In our thesis of the 4 pole machine frequency varies between 60-600 Hz corresponding to the speed of 1800-18000 rpm. This frequency not being high enables us to use D.C. Resistance given in winding data with acceptable error.

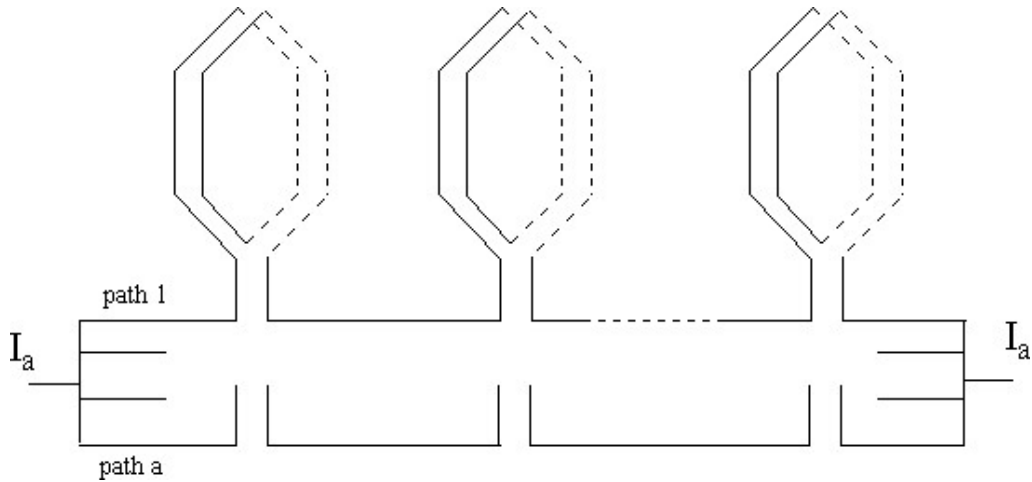


Figure 4.20: Phase 'a' winding having 2p groups of coil

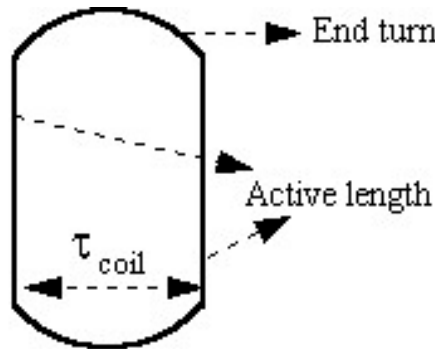


Figure 4.21 : Structure of one coil

A single coil has 2 conductors and 2 end turns .

$$\text{Therefore the length of coil , } L_c = 2L + 2\left(\frac{\pi\tau_{\text{coil}}}{2}\right) \quad (4.91)$$

$$= 2L + 2\left(\frac{\pi N_s \pi D_i}{2 \cdot 2p N_s}\right)$$

$$L_c = 2L + 2\left(\frac{\pi \pi D_i}{2 \cdot 2p}\right) \quad (4.92)$$

For skewed winding the length of active conductor increases to $\frac{L}{\cos(\sigma)}$

where σ is the angle of skew which is equal to the slot pitch.

$$\text{Therefore the length of conductor in each coil now becomes , } L_c = \frac{2L}{\cos(\sigma)} + 2\left(\frac{\pi \pi D_i}{2 \cdot 2p}\right) \quad (4.93)$$

Windings have the linking conductors to connect the group of coils. If there are 2p groups of coils in a 2 layered winding.

$$\text{Length of linking conductors, } l_{lc} = 2p * \tau_{stator} = 2p * \frac{\pi D_i}{2p} = \pi D_i \quad (4.94)$$

$$\text{Therefore length of the conductor for a parallel path/ phase, } L_{pp} = N_{coil} * L_c + l_{lc} \quad (4.95)$$

$$\text{Resistance of a coil/phase, } R_c = \frac{\rho_r L_{pp}}{\pi/4 d_c^2} \quad (4.96)$$

In our machine we have a parallel path in each phase having 2 coils in series, thereby giving the resistance per phase to be , $R_a = 2R_c \parallel 2R_c = R_c$ (4.97)

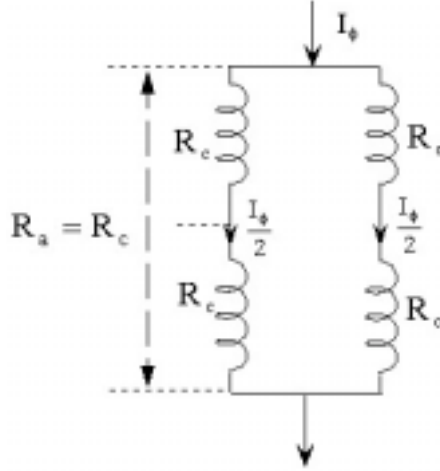


Figure 4.22 : Resistance of coils per phase

$$\text{The copper losses of the machine, } P_{cu} = m * R_a * I_{\phi_{rms}}^2 \quad (4.98)$$

4.5.2 Core losses

Generally, the core losses consist of two components of power losses, hysteresis and eddy-current losses. The cyclical magnetic flux variation is related to the B-H curve of the iron/steel. The enclosed area of B-H curve is the energy hysteresis loss per cycle due to hysteresis characteristics of the iron/steel. The eddy-current loss is also produced by the time-varying magnetic flux in the iron/steel, which induce current to flow in the stator steel at the same frequency as the variation in the magnetic field of permanent magnet. The eddy-current loss can be reduced by using thin lamination steels. The core losses formula presented in [13] will mainly be used in this thesis because the core losses coefficients are already extracted for Si-Steel. This core losses formula can be expressed as follow.

$$P_{core} = K_c f^\alpha B_p^\beta \quad \text{Watts/kg} \quad (4.99)$$

where

B_p is the peak sinusoidal flux density (T)

f is the frequency (Hz)

K_c is the core losses coefficient

α and β are the constants

The constants shown in equation (4.99) and other properties for Si-Steel can be summarized in Table 4.1. Referring to equation (4.99) and three constants (i.e., K_c , α , and β) for Si-Steel, the core losses of Si-Steel can be plotted as a function of peak flux densities, B_p , and frequencies, f in Figure 4.23 [2].

Material	B_{sat} (T)	μ_r	ρ_r ($\Omega.m$)	ρ_d (kg/m^3)	K_c	α	β
Si-Steel	2.0	10000	0.01	7650	0.5×10^{-3}	1.7	1.9

Table 4.1 : Property data for Si-Steel [17]

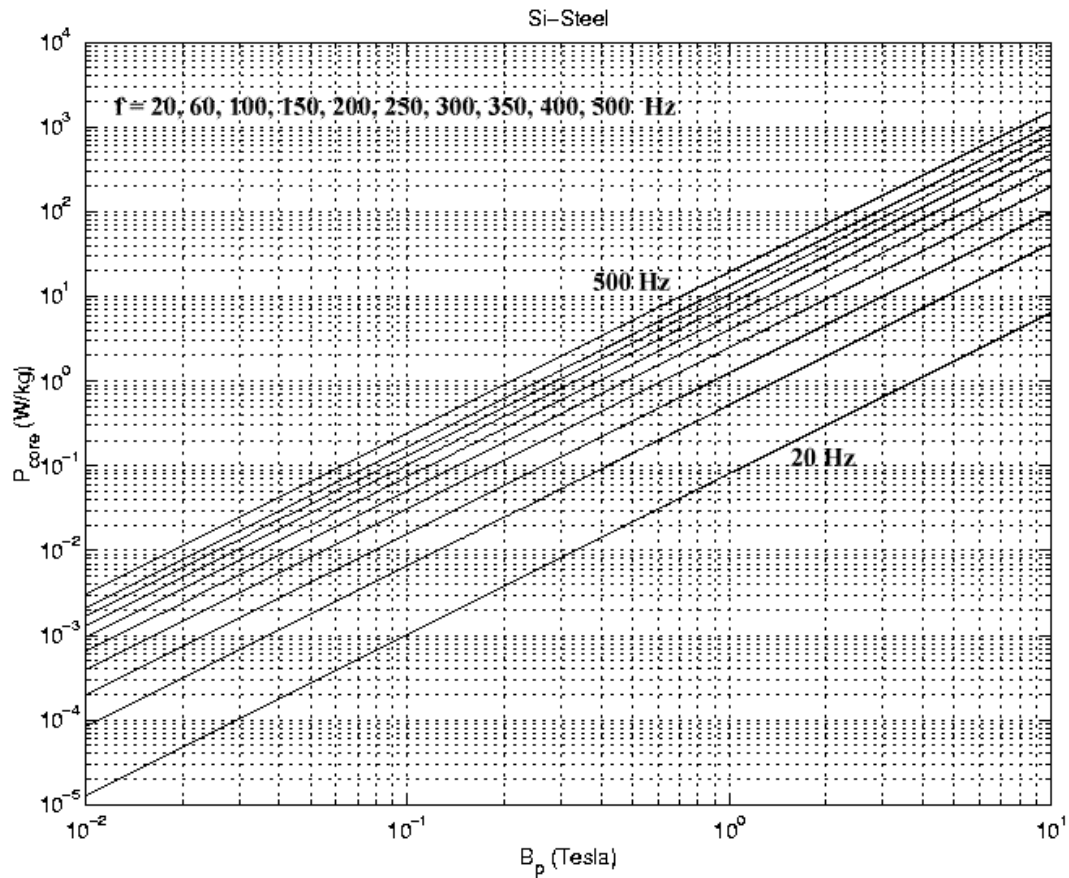


Figure 4.23: The core losses vs peak flux density at different frequencies for Si-Steel [17]

The core losses formula sometimes is expressed separately for hysteresis and eddy-current losses. Ref. [1] shows such core losses formula as follow.

$$P_{core} = C_h f B_p^{a+b} + C_e f^2 B_p^2 \quad \text{Watts/kg} \quad (4.100)$$

where

Ch is the hysteresis losses coefficient

Ce is the eddy-current losses coefficient

a and b are the constants depending on the soft magnetic material

f is the frequency (Hz)

Bp is the peak of the sinusoidal flux density (T)

Refer [2] for the detailed derivation for the values of Ch, a, b

$$Ch = 0.0025, \quad a = 1.8317, \quad b = -0.0035 \quad (4.101)$$

$$P_{core} = 0.0025 \times f B_p^{1.8317 - 0.0035 \times B_p} + 7.9365 \times 10^{-5} \times f^2 B_p^2 \quad \text{Watts/kg} \quad (4.102)$$

Mongkol Konghirun showed (through plot 4.24) the difference in core losses between the two is negligible at high frequencies ie. 200 Hz.

In reality, the flux density is not equal all stator because magnetic flux of permanent magnet flows through the different cross-sectional area in the stator, i.e., stator teeth and stator yoke. Consequently, we need to compute the core losses at teeth and yoke individually.

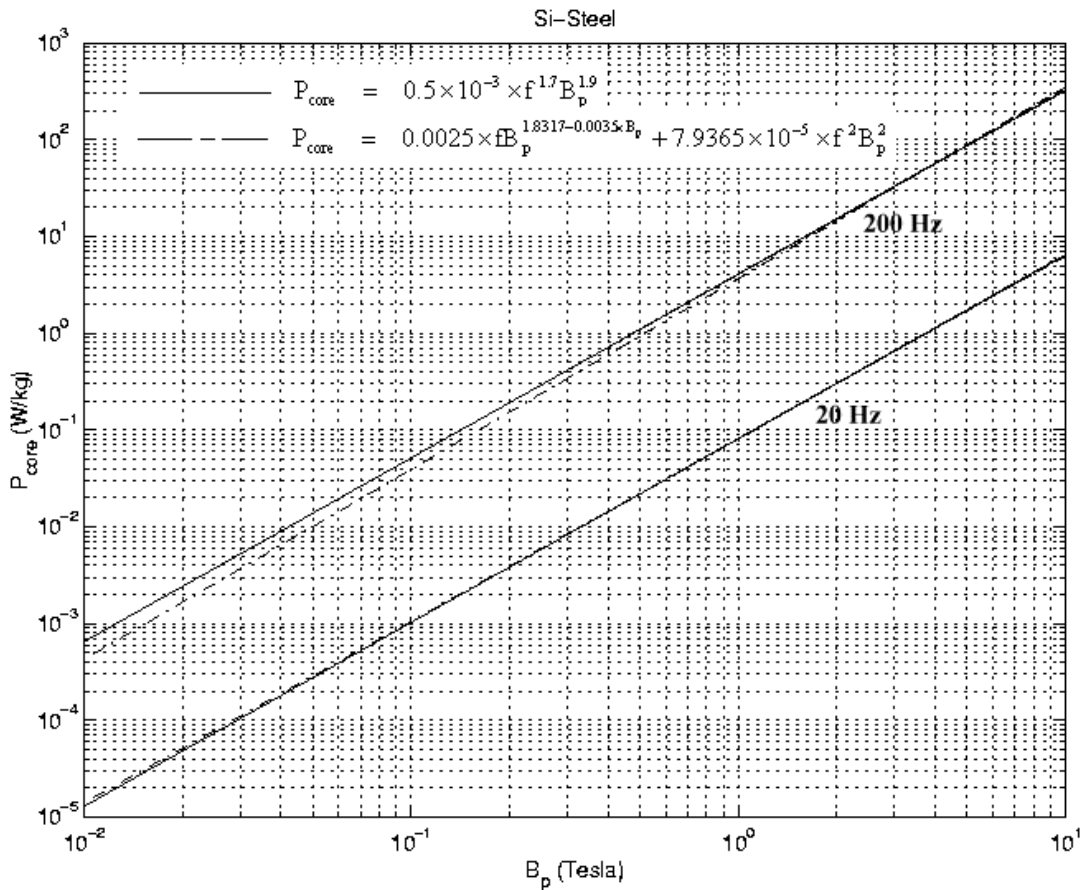


Figure 4.24: Core losses computed from equations (4.99) and (4.102) for $f = 20$ and 200 Hz.

The total volume of stator teeth and stator yoke should also be calculated by using material density, shown in Table 4.1, in order to find the weight of stator teeth and stator yoke. Then, the core losses in Watts can be found separately at stator teeth and stator yoke

$$V_{teeth} = k_v w_t d_s * Len * N_{slot} \quad (4.103)$$

$$V_{yoke} = 2\pi k_v \left(r_g + d_s + \frac{y_s}{2} \right) y_s Len \quad (4.104)$$

where k_v = core volume factor used to take into account the insulation used
 $k_v = 0.94$.

When the material density is employed, the steel weight of stator teeth and stator yoke, and core losses equation in Watts can be found as follows.

$$W_{teeth} = \rho_d V_{teeth} = \rho_d k_v w_t d_s * Len * N_{slot} \quad \text{kg} \quad (4.105)$$

$$W_{yoke} = \rho_d V_{yoke} = 2\pi k_v \rho_d \left(r_g + d_s + \frac{y_s}{2} \right) y_s Len \quad \text{kg} \quad (4.106)$$

$$P_{core} = W_{teeth} [P_{core}, \text{W/kg}]_{tooth} + W_{yoke} [P_{core}, \text{W/kg}]_{yoke} \quad \text{Watts} \quad (4.107)$$

4.5.3 Rotational losses

The rotational losses or mechanical losses, P_{rot} or P_{mech} , consist mainly of friction losses, P_{fric} , and windage losses, P_{wind} . The friction losses in bearings of small machines can be given in [3] as follow

$$P_{fric} \cong k_{fb} W_r n_m \times 10^{-3} \quad \text{Watts} \quad (4.108)$$

where

k_{fb} is a constant in a range of 1-3

W_r is weight of rotor (kg)

n_m is the speed of machine (rpm)

In reality, rotor mainly consists of back rotor iron, and permanent magnet. Therefore, the weight of rotor, W_r , can be found as follow.

$$W_r = \rho_{d,steel} k_v \pi (r_g - l_g - l_m)^2 Len + \rho_{d,magnet} 2\pi \left(r_g - l_g - \frac{l_m}{2} \right) l_m Len \quad \text{kg} \quad (4.109)$$

where $\rho_{d,magnet} = 7,600 \text{ kg/m}^3$ (for MQ3-F 36H and MQ3-F 42) [13]

$= 7,500 \text{ kg/m}^3$ (for HS-40 DH and HS-36 EH) [14]

$$P_{wind} \cong 2 D_r^3 Len * n_m^3 \times 10^{-6} \quad \text{Watts} \quad (4.110)$$

where

D_r is the outer diameter of rotor which equals to $2(r_g - l_g)$ (m)

As a result, the rotational losses can be approximate as follow.

$$P_{rot} = P_{fric} + P_{wind} \cong k_{fb} W_r n_m \times 10^{-3} + 2 D_r^3 Len * n_m^3 \times 10^{-6} \quad \text{Watts} \quad (4.111)$$

4.6 Thermal Analysis

Heat transfer is an important mechanism describing the temperature distribution in any kind of electrical machines. The precise analysis of temperature distribution would be established by Finite Element Analysis (FEA). The partial differential equations describing heat transfer behavior are more complex, more nonlinear, more difficult than those for electromagnetic behavior. As a result, the simplified thermal equivalent circuit of an electrical machine is mostly employed rather than FEA scheme [1] whereas exact methods are followed for electromagnetic design. The electromagnetic design determines the geometry of laminations and design of windings etc. which determines if the generator supplies the required power or not. They also determine the exact voltages and currents that will be experienced by the power semi-conductors in the controller. All these affect the manufacturing cost critically. By contrast as long as the temperature does not rise above a critical value, it has only marginal influence on the power supplied by the generator.

The two major aspects of thermal problem are : Heat Removal and Temperature Distribution within the motor.

Basically, there are three ways to remove heat from an electrical machine; heat can be dissipated by conduction, convection, and radiation.

The most important aspect of the temperature distribution is finding the hottest temperature in the motor and its position given the distribution losses and known rate of heat removal.

The main reasons for limiting the temperature rise of windings and frame of generator are : [1]

- ❖ To preserve the life of insulation and bearings.
- ❖ To prevent excessive heating of surroundings.
- ❖ To prevent injury caused by touching of hot surfaces.

Heat Removal

Heat is removed from a generator by conduction, convection, radiation. The fundamental equations of these three mechanisms can be briefly explained as following sections [1], [20].

4.6.1 Conduction

Equation (4.112) describes the fundamental law of conduction for a specific material as seen in Figure 4.25.

$$q = kA \frac{t_1 - t_2}{\Delta x} \text{ Watts} \quad (4.112)$$

where q is heat flow (Watts)

k is thermal conductivity of material (W/m-°C)

t_1 is temperature of material surface which heat flow into (°C)

t_2 is temperature of material surface which heat flow out (°C)

Δx is thickness of material (m)

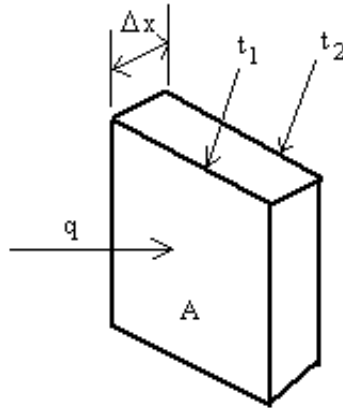


Figure 4.25 : Conduction for a specific material

4.6.2 Convection

Convection is simply expressed by introduction of Newton's Law of cooling.

$$\frac{q}{A} = h(t_s - t_f) \quad \text{Watts/m}^2 \quad (4.113)$$

where h is heat transfer coefficient or unit thermal conductance ($\text{W/m}^2\text{-}^\circ\text{C}$)

t_s is temperature of material surface which cooling fluid flows through ($^\circ\text{C}$)

t_f is temperature of cooling fluid ($^\circ\text{C}$)

4.6.3 Radiation

Stefan-Boltzmann Law gives a fundamental equation of radiation as follow.

$$\frac{q}{A} = \epsilon\sigma(t_s^4 - t_r^4) \quad \text{Watts/m}^2 \quad (4.114)$$

where σ is Stefan-Boltzmann constant, $5.67 \times 10^{-8} \text{ W/m}^2/\text{K}^4$

ϵ is emissivity of emitting material surface

t_s is temperature of radiating material surface (K)

t_r is temperature of radiating surrounding (K)

4.6.4 Simplified thermal equivalent circuit

The thermal equivalent circuit is analogous to the electrical circuit and magnetic circuits. Table 4.2 summarizes analogous variables for thermal, electrical, and magnetic circuits.

Thermal circuit	Electrical circuit	Magnetic circuit
Temperature, t	Voltage, v	mmf, \mathcal{F}
Heat flow, q	Current, i	Magnetic flux, Φ
Thermal resistance, R	Resistance, R	Reluctance, \mathfrak{R}

Table 4.2: Analogous variables for thermal, electrical, and magnetic circuits [1]

The typical temperature distribution due to thermal contact resistance can be shown in Figure 6.11. Referring to Figure 6.11, heat is transferred from material A to material B by conduction for contacting spots and by convection (perhaps radiation) for non-contacting spots due to rugged surfaces of both materials. As a result, the thermal contact resistance is defined as follow

$$R = \frac{t_A - t_B}{q} \quad \text{°C/Watts} \tag{4.115}$$

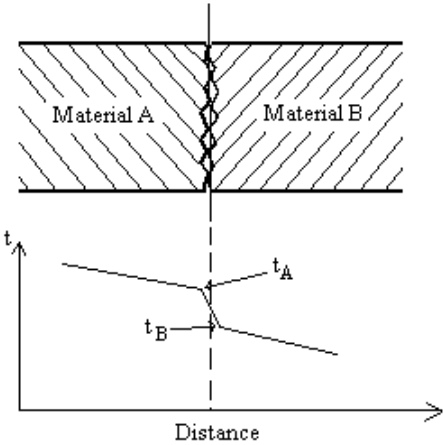


Figure 4.26 : Typical temperature distribution due to thermal contact resistance [1]

For metallic surfaces held tightly together, the thermal contact resistance is about 1.4 °C/Watts [1]. In an electrical machine, heat is generated by total power losses (i.e., winding copper losses, core losses, rotational losses) and dissipated throughout the machine. For simplicity, the thermal contact resistance (between magnet and back rotor iron) and radiation are not used in our thermal equivalent circuit seen in Figure 4.27

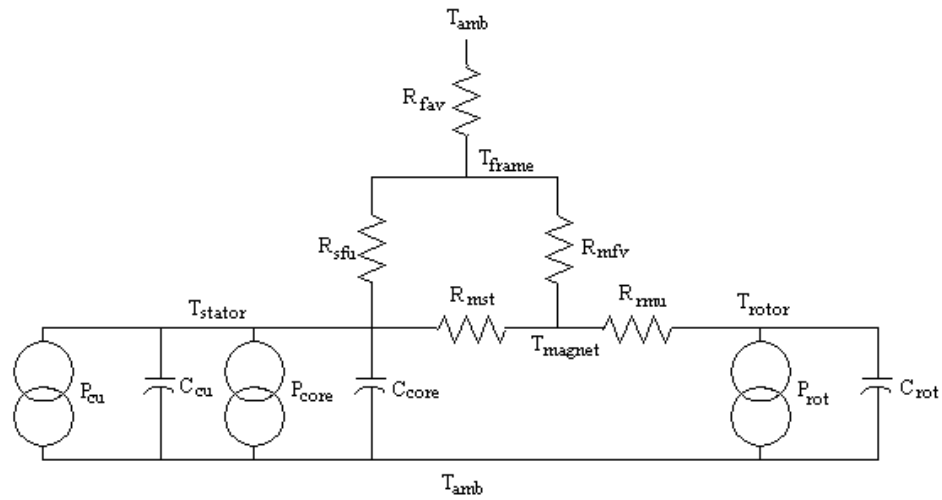


Figure 4.27 : Thermal equivalent circuit for an electrical machine [1], [2]

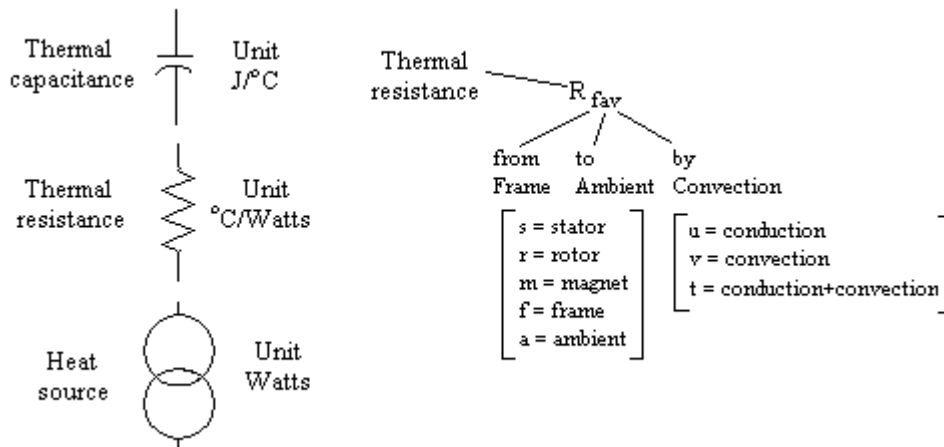


Figure 4.28 : Explanation of subscripts and units in thermal circuit [2]

Referring to equations (4.112) and (4.113), the thermal resistance for conduction and convection can be expressed as follows.

$$\text{Conduction: } R = \frac{\Delta x}{kA} \text{ } ^\circ\text{C/Watts} \quad (4.116)$$

$$\text{Convection: } R = \frac{1}{hA} \text{ } ^\circ\text{C/Watts} \quad (4.117)$$

In Figure 4.27, the subscripts of thermal resistance can be described in Figure 4.28. Winding copper losses, core losses, and rotational losses (P_{cu} , P_{core} , and P_{rot}) are given in Watts and temperatures at stator, rotor, magnet, frame, and ambient (T_{stator} , T_{rotor} , T_{magnet} , T_{frame} , and T_{amb}) are given in $^\circ\text{C}$.

4.6.5 Temperature rise computation

The temperature rise can be computed from this simplified thermal equivalent circuit by using the following equation.

$$T - T_{amb} = R \times P_d \left(1 - e^{-t/\tau} \right) \quad (4.118)$$

when $\tau = RC$ (so called thermal time constant) and an initial condition of temperature equals to ambient temperature.

Referring to equation (4.118), the steady state ($t = \infty$ sec) temperature rise can be simply expressed as follow.

$$T - T_{amb} = R \times P_d \left(1 - e^{-\infty/\tau} \right) = R \times P_d \quad (4.125)$$

Consequently, the thermal equivalent circuit seen in Figure 4.27 can be modified for the steady-state thermal equivalent circuit in Figure 4.29. The transformation from $\Delta - Y$ loop of thermal resistance (i.e., R_{rst} , R_{sfu} , R_{mfv}) in Figure 4.29 is applied as seen in Figure 4.30. In Figure 4.30, q_1 and q_2 represent the heat flow in the system. As a result, the temperature rises of magnet and frame can be calculated from the thermal equivalent circuit in Figure 4.30 in a similar fashion as electrical circuit analysis.

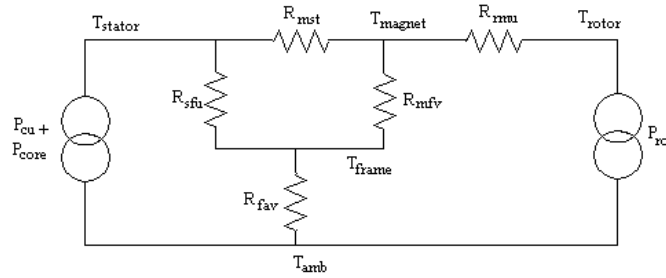


Figure 4.29 : Steady-state thermal equivalent circuit for an electrical machine

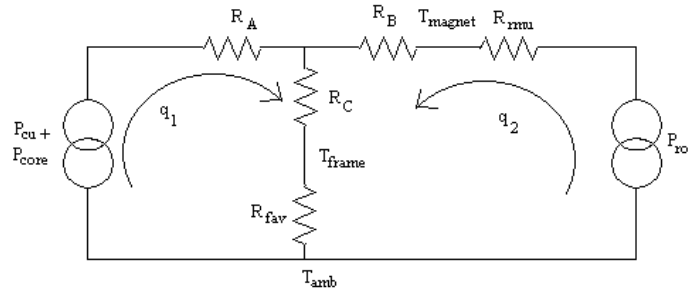


Figure 4.30 : Steady-state thermal equivalent circuit for an electrical machine after $\Delta - Y$ transformation is applied

In Figure 4.30, R_A , R_B , and R_C can be computed by using $\Delta - Y$ transformation as follows.

$$R_A = \frac{R_{mst} R_{sfu}}{R_{mst} + R_{sfu} + R_{mfv}} \quad (4.120)$$

$$R_B = \frac{R_{mfv} R_{mst}}{R_{mst} + R_{sfu} + R_{mfv}} \quad (4.121)$$

$$R_C = \frac{R_{sfu} R_{mfv}}{R_{mst} + R_{sfu} + R_{mfv}} \quad (4.122)$$

Due to analog to electrical circuit analysis, the temperature rises of permanent magnet and stator frame can be computed as follows.

$$q_1 = P_{cu} + P_{core} \quad \text{Watts} \quad (4.123)$$

$$q_2 = P_{rot} \quad \text{Watts} \quad (4.124)$$

$$T_{magnet} - T_{amb} = q_2 R_B + (q_1 + q_2) (R_c + R_{fav}) \quad ^\circ\text{C} \quad (4.125a)$$

$$T_{frame} - T_{amb} = (q_1 + q_2) R_{fav} \quad ^\circ\text{C} \quad (4.125b)$$

The thermal resistance that appears in equivalent thermal circuit in Figures 4.30 can be computed by using equations (4.116) and (4.117) as follows.

$$R_{sfu} = \frac{y_t}{k_{si-steel} \left[2\pi \left(r_g + d_s + \frac{y_t}{2} \right) L \right]} \quad ^\circ\text{C/Watts} \quad (4.126)$$

$$R_{rmu} = \frac{l_m}{k_{NdFeB} \left[2\pi \left(r_g - l_g - \frac{l_m}{2} \right) L \right]} \quad ^\circ\text{C/Watts} \quad (4.127)$$

$$R_{msu} = \frac{l_g}{k_{air} \left[2\pi \left(r_g - \frac{l_g}{2} \right) L \right]} \quad ^\circ\text{C/Watts} \quad (4.128)$$

$$R_{mfv} = \frac{1}{h_{air} \left[2\pi (r_g - l_g) L \right]} \quad ^\circ\text{C/Watts} \quad (4.129)$$

$$R_{fav} = \frac{1}{h_{air} \left[2\pi (r_g + d_s + y_t) L \right]} \quad ^\circ\text{C/Watts} \quad (4.130)$$

$$R_{msv} = \frac{1}{h_{air} \left[2\pi (r_g - l_g) L \right]} \quad ^\circ\text{C/Watts} \quad (4.131)$$

$$R_{mst} = \frac{R_{msu} R_{msv}}{R_{msu} + R_{msv}} \quad ^\circ\text{C/Watts} \quad (4.132)$$

where

$$k_{si-steel} = 31 \text{ W/m-}^\circ\text{C} \quad \text{at } 20^\circ\text{C} \quad (\text{for 2\% silicon}) \quad [18]$$

$$k_{NdFeB} = 7 \text{ W/m-}^\circ\text{C} \quad (\text{for MQ3-F 36H and MQ3-F 42}) \quad [13]$$

$$= 7.7 \text{ kcal/m-hr-}^\circ\text{C} = 8.957 \text{ W/m-}^\circ\text{C} \quad (\text{for HS-40 DH and HS-36 EH}) \quad [14]$$

$$k_{air} = 25.64 \times 10^3 \text{ W/m-}^\circ\text{C} \quad \text{at } 20^\circ\text{C} \quad (\text{for dry air at atmospheric pressure}) \quad [18]$$

$$h_{air} = 5\text{--}50 \text{ W/m}^2\text{-}^\circ\text{C} \quad (\text{for free convection in air}) \quad [18]$$

Note that $1 \text{ cal/s-m-}^\circ\text{C} = 4.1876 \text{ W/m-}^\circ\text{C}$

Reference

- [1] J.R. Hendershot Jr. and T.J.E. Miller, 'Design of brushless Permanent Magnet Motors', *Magna Physics Publishing and Clarendon Press, Oxford, 1994.*
- [2] Mongkol Konhirun, 'Optimal Design of Permanent Magnet Synchronous Generator', *a Master's Thesis in the Dept. of Electrical Engineering, The Ohio State University, 1999.*
- [3] D.C. Hanselman, 'Brushless Permanent-Magnet Motor Design', *McGraw-Hill, 1994.*
- [8] J.F Gieras and M. Wing, 'Permanent Magnet Motor Technology- Design and Applications', *Marcell Dekker Inc., 1997.*
- [9] 'Optimization Toolbox manual of Matlab (version 5.3.1)', *chapter- Introduction to Algorithms.*
- [11] S.S. Rao, 'Optimization : Theory and Applications', *John Wiley & Sons, 1984.*
- [12] W.G. Hurley, W.H. Wolfle and J.G. Breslin, 'Optimized Transformer Design: inclusive of high frequency effects', *IEEE Transactions on Power Electronics, vol.13, no.4, pp. 651-659, July 1998.*
- [13] Y. Hayashi and T.J.E. Miller, ' A new approach to calculating core losses in the SRM' *IEEE Transactions on Industry Applications, vol. 31, no.5, pp. 1039-1046, September/October 1995.*
- [14] Y. Lee, H. Lee and S. Hahn, 'Temperature analysis of induction motor with distributed heat sources by finite element method', *IEEE Transactions on Magnetics, vol.32, no.2, pp. 1718-1721, March 1997.*
- [15] Huang S., Luo J, Leonardi F., Lipo T.A. , 'A General Approach to Sizing and Power Density Equations for Comparison of Electrical Machines', *IEEE Transactions on Industry Applications, vol. 34 NO 1, January/February 1998.*
- [18] Permanent Magnet Catalogue, *Magnaquench International Inc.*
- [19] Hitachi Rare-Earth Magnet, *Hitachi Metal America, Ltd.*
- [20] A.J. Chapman, Heat Transfer, *Macmillan, 1984.*

CHAPTER 5

Optimization Of Machine Parameters And Finite Element Analysis

5.1 Introduction

In this chapter we discuss in detail on the principle of optimization of machine parameters to arrive at optimized machine dimensions for generating the power required at minimum power loss and minimum weight. The machine parameters are solved by the use of a Matlab function, *fmincon*, an inequality constrained multi-objective optimization function. *fmincon* uses medium scale Sequential Quadratic Programming (SQP), Quasi-Newton, Line-search algorithms. Refer the chapter 'Introduction to Algorithms' of the Toolbox manual of Matlab details on algorithms.

An insight on how the cost function (power loss and weight of the machine) and the various constraints are derived from the machine parameters is also provided here.

5.2 Introduction to Optimization Theory

The constraints are inequality functions because of the limitation to machine parameters and machine dimension in general due to limitations in the geometry. Hence we always start our optimization with some preferable machine structure and specification. This gives direction to the optimization procedure to limit the values of machine parameters within a certain range. The preferable machine structure can be summarized as follows.

- 3-phase, 4-pole, 12-slot structure
- Machine speed in the range of 1800-18000 rpm.
- Square wave output voltages with peak of 25Volt/ coil in a phase.
- Maximum output current of 65Amp/ coil.
- Number of coils per phase is to be limited to 4 which can be in parallel, series, or a combination of parallel and series connections.
- Uniformly distributed full pitched stator windings (i.e., coil span = pole pitch)
- Conductor size of AWG 10-21
- Nd-Fe-B permanent magnet from Magnequench Int. and Hitachi Metals which can withstand a maximum temperature of 185°C.

5.3 Objective Functions of Power Losses and Machine Weight

We have to express the objective function (cost function) in terms of the machine parameters. The cost function is then optimized for minimum power loss and machine weight.

The variables that are put through the optimization procedure so as to achieve optimized machine parameters are

- Length of the machine i.e. stack length of the stator, rotor – L_{en} in cm.

- Ratio of length of the stack to the slot pitch, L_{bytau} . This gives the ratio of length to the stator inner diameter of the machine – L_{bytau} .
- Current density at the stator coils – J in A/mm^2 .
- Curvature of the permanent magnet – α_{mag} in degrees.
- Specific electric loading of the machine – A in Ampere/m.
- Specific magnetic loading or average air-gap flux density – B_g in T.
- Permeance co-efficient of the magnet – PC .

The following is the list of machine design parameters

- ❖ Power generated, P_g (power delivered + power loss)
- ❖ Voltage generated per phase at the coils, E_{ph} (supply voltage +voltage loss)
- ❖ Number of slots in the machine, N_{slots} .
- ❖ Inner diameter of the stator, D
- ❖ Slot pitch, τ_{slot}
- ❖ Angle of skew for the stator slot, σ
- ❖ Flux per pole, ϕ_{mag} .
- ❖ Total number of conductors, Z .
- ❖ Number of turns/phase/parallel path, N_{ph} .
- ❖ Number of coils, Number of turns per coil, N_{tc} .
- ❖ Length of the magnet, l_m
- ❖ Width of the tooth, w_t
- ❖ Depth of teeth, d_s
- ❖ Stator yoke depth, y_s
- ❖ Rotor core depth, y_{rc}
- ❖ Outer diameter of the stator, D_{out}
- ❖ Area of 1 conductor and diameter of 1 conductor

In our Matlab program the various machine parameters are all expressed in terms in terms of these variables. The power loss and machine weight are also functions of these parameters. Hence by optimizing these variables we arrive at an optimum machine design for the generator delivering the power of 3000W at 42V.

5.3.1 Weight of the Machine

5.3.1.1 Weight of Stator teeth and yoke

When the material density is employed, the steel weight of stator teeth and stator yoke, can be found as follows.

$$V_{\text{teeth}} = k_v w_t d_s * Len * N_{\text{slot}} \quad (5.1)$$

$$V_{\text{yoke}} = 2\pi k_v \left(r_g + d_s + \frac{y_s}{2} \right) y_s Len \quad (5.2)$$

where k_v = core volume factor used to take into account the insulation used
 $k_v = 0.95$.

$$W_{teeth} = \rho_d V_{teeth} = \rho_d k_v w_t d_s L_{en} N_s \quad \text{kg} \quad (5.3)$$

$$W_{yoke} = \rho_d V_{yoke} = 2\pi k_v \rho_d \left(r_g + d_s + \frac{y_s}{2} \right) y_s L_{en} \quad \text{kg} \quad (5.4)$$

5.3.1.2 Weight of Coils

When the material density is employed, the weight of coils can be found to be

$$V_{coils} = A_{1conduc} * 6 * L_{pp} \quad (5.5)$$

$$W_{coils} = V_{coils} * \rho_{d,copper} \quad (5.6)$$

where L_{pp} = length of the conductor for a parallel path/ phase

$A_{1conduc}$ = area of cross section of 1 conductor

$\rho_{d,copper}$ = density of copper = 8900 kg/m^3

5.3.1.3 Rotor weight

Rotor mainly consists of back rotor iron, and permanent magnet. Therefore, the weight of rotor, W_r , can be found as follow.

$$W_{rotor} = \rho_{d,steel} k_v \pi (r_g - l_g - l_m)^2 L_{en} + \rho_{d,magnet} 2\pi \left(r_g - l_g - \frac{l_m}{2} \right) l_m L_{en} \quad \text{kg} \quad (5.7)$$

where

$$\begin{aligned} \rho_{d,magnet} &= 7,600 \text{ kg/m}^3 \text{ (for MQ3-F 36H and MQ3-F 42) [13]} \\ &= 7,500 \text{ kg/m}^3 \text{ (for HS-40 DH and HS-36 EH) [14]} \end{aligned}$$

5.3.1.4 Total machine weight

As a result, total machine weight can be computed as

$$W_{tot} = W_{teeth} + W_{yoke} + W_{coils} + W_{rotor} \quad \text{kg} \quad (5.8)$$

The total machine weight shown in equation (5.8) is also the objective function, $f(\mathbf{x})$, which will be minimized.

5.3.2 Power losses equation

5.3.2.1 Winding copper losses

Referring to the chapter 4, section 4.6.1 on Winding resistance we have

$$\text{The length of conductor in each coil now becomes, } L_c = \frac{2L}{\text{Cos}(\sigma)} + 2 \left(\frac{\pi \pi D_i}{2 \ 2p} \right) \quad (5.9)$$

$$\text{Length of linking conductors, } l_{lc} = 2p * \tau_{stator} = 2p * \frac{\pi D_i}{2p} = \pi D_i \quad (5.10)$$

$$\text{Therefore length of the coil for a parallel path/ phase, } L_{pp} = N_{coil} * L_c + l_{lc} \quad (5.11)$$

$$\text{Resistance of a coil/phase, } R_c = \frac{\rho_r L_{pp}}{\pi/4 d_c^2} \quad (5.12)$$

In our machine we have a parallel path in each phase having 2 coils in series, thereby giving the resistance per phase to be , $R_a = 2R_c \parallel 2R_c = R_c$ (5.13)

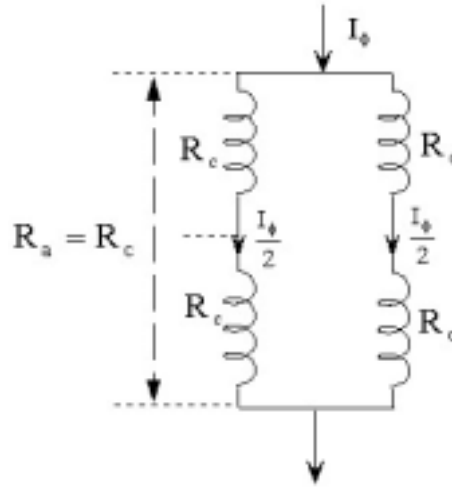


Figure 5.1 : Resistance of coils per phase

The copper losses of the machine, $P_{cu} = m * R_a * I_{\phi rms}^2$ (5.14)

5.3.2.2 Core losses

Referring to Chapter 4, section on core losses we have the core loss formula

$$P_{core} = K_c f^\alpha B_p^\beta \quad \text{Watts/kg} \quad (5.15)$$

where

B_p is the peak sinusoidal flux density (T)

f is the frequency (Hz)

K_c is the core losses coefficient

α and β are the constants

The constants shown in equation (5.15) and other properties for Si-Steel can be summarized in Table 5.1.

Material	M sat (T)	B (T)	μ_r	ρ_r ($\Omega.m$)	ρ_d (kg/m^3)	ρ_c	K	α	β
i-Steel	S .0	2	1 0000	.01	7 650	0 .5 $\times 10^{-3}$	0 .7	1	1 .9

Table 5.1 : Property data for Si-Steel [17]

In reality, the flux density is not equal all stator because magnetic flux of permanent magnet flows through the different cross-sectional area in the stator, i.e., stator teeth and stator yoke. Consequently, the core losses are needed to compute for both stator teeth and stator yoke

due to different flux density. Due to square wave flux density, the harmonic contents of flux density at stator tooth and yoke are to be computed.

$$W_{\text{teeth}} = \rho_d V_{\text{teeth}} = \rho_d k_v t_t d_s L N_s \quad \text{kg} \quad (5.16)$$

$$W_{\text{yoke}} = \rho_d V_{\text{yoke}} = 2\pi k_v \rho_d \left(r_g + d_s + \frac{y_t}{2} \right) y_t L \quad \text{kg} \quad (5.17)$$

$$P_{\text{core}} = W_{\text{teeth}} [P_{\text{core,W/kg}}]_{\text{tooth}} + W_{\text{yoke}} [P_{\text{core,W/kg}}]_{\text{yoke}} \quad \text{Watts} \quad (5.18)$$

$$P_{\text{core}} = K_c \left[k_v \rho_{d,\text{steel}} t_t d_s L N_s \left(\frac{8B_g r_g}{t_t N_s} \right)^\beta f^\alpha \left(1 + 3^{(\alpha-\beta)} + 5^{(\alpha-\beta)} + \dots \right) + \right. \\ \left. K_c \left[2\pi k_v \rho_{d,\text{steel}} \left(r_g + d_s + \frac{y_s}{2} \right) y_s L \left(\frac{4B_g r_g}{p y_s} \right)^\beta f^\alpha \left(1 + 3^{(\alpha-\beta)} + 5^{(\alpha-\beta)} + \dots \right) \right] \right] \quad \text{Watts} \quad (5.19)$$

5.3.2.3 Rotational losses

The rotational losses or mechanical losses, P_{rot} or P_{mech} , consist mainly of friction losses, P_{fric} , and windage losses, P_{wind} . There are many empirical equations for calculating the rotational losses giving various degrees of accuracy. The friction losses in bearings of small machines can be given in [3] as follow.

$$P_{\text{fric}} \cong k_{fb} W_r n_m \times 10^{-3} \quad \text{Watts} \quad (5.20)$$

where

k_{fb} is a constant in a range of 1-3

W_r is weight of rotor (kg)

n_m is the speed of machine (rpm)

$$W_{\text{rotor}} = \rho_{d,\text{steel}} k_v \pi (r_g - l_g - l_m)^2 L n_m + \rho_{d,\text{magnet}} 2\pi \left(r_g - l_g - \frac{l_m}{2} \right) l_m L n_m \quad \text{kg} \quad (5.21)$$

where $\rho_{d,\text{magnet}} = 7,600 \text{ kg/m}^3$ (for MQ3-F 36H and MQ3-F 42) [13]
 $= 7,500 \text{ kg/m}^3$ (for HS-40 DH and HS-36 EH) [14]

If the speed does not exceed 6000 rpm, the windage losses can be estimated as follow [2].

$$P_{\text{wind}} \cong 2D_r^3 L n_m^3 \times 10^{-6} \quad \text{Watts} \quad (5.22)$$

where

D_r is the outer diameter of rotor which equals to $2(r_g - l_g)$ (m)

As a result, the rotational losses can be approximate as follow.

$$P_{\text{rot}} = P_{\text{fric}} + P_{\text{wind}} \cong k_{fb} W_r n_m \times 10^{-3} + 2D_r^3 L n_m^3 \times 10^{-6} \quad \text{Watts} \quad (5.23)$$

5.3.2.4 Total power losses

The total power losses shown in equation (5.42) is the objective function, $f(\mathbf{x})$, which will be minimized.

$$TP_{\text{loss}} = P_{\text{cu}} + P_{\text{core}} + P_{\text{rot}} \quad \text{Watts} \quad (5.24)$$

5.3.3 Inequality Constraints

In PMSG designing, due to saturation effect the minimum values of w_t , y_s , and y_{rc} are taken into account. Temperature rise on permanent magnet is checked to ensure that the magnet is not demagnetized. From magnet manufacturer's data sheet [18,19], the highest temperatures that permanent magnets can normally operate are 180°C for Magnequench Int. and 200 °C for Hitachi Metals. With the highest possible operating temperature 80 °C, at the air surrounding the machine, we limit the maximum temperature at the surface of the magnet to be 135°C.

We limit the maximum current at the stator coils ie. phase current to be less than the maximum current which the magnet can withstand without demagnetizing. This maximum current which the magnet can withstand is

$$I_{\text{max}} = \frac{(477.46e3) * I_m}{2 * N_{ph}} \quad (5.25)$$

From the machine requirement we know the I_{phase} .

This inequality constraint is given as

$$I_{\text{phase}} < I_{\text{max}} \quad \text{or} \quad I_{\text{phase}} - I_{\text{max}} < 0 \quad (5.26)$$

The second constraint is to limit the outer diameter of stator to 14 cms. This limits the weight of the machine and maximizes the power density. This could be given as

Fixed value, $D_o = 14\text{cms}$.

The outer diameter of stator as calculated from the program is

$$D_{\text{out}} = D + 2(y_s + d_s). \quad (5.27)$$

This inequality constraint is given as $D_{\text{out}} - D_o < 0$.

$$(5.28)$$

The third constraint is make sure we deliver a power of 3000 Watt to the system. For this we have to generate a total of 3000+ power loss.

This inequality constraint is given as $TP_{\text{sup } p} > 3000$ or $3000 - TP_{\text{sup } p} < 0$.

$$(5.29)$$

Overall the inequality constraint is stated as ,

$$c = \left[I_{\text{phase}} - I_{\text{max}} \quad D_{\text{out}} - D_o \quad 3000 - TP_{\text{sup } p} \right]. \quad (5.30)$$

5.3.4 Cost Function

The cost function to optimize for minimum weight , minimum power loss could be stated as

$$\text{CostFunction} = \gamma_1 * \text{Total Power Loss} + \gamma_2 * \text{Total Machine Weight}$$

where γ_1, γ_2 are some constant value less than 1. In our case we have the value of $\gamma_1 = \gamma_2 = 0.5$.

5.4 Flowchart of Optimized PMSG Design

Figure 5.5 shows the flowchart for optimal design of PMSG. The variables to be optimized with its range, machine parameters to be determined and some of the constants used in the optimizing procedure are given below

The variables

$$x = \begin{bmatrix} x_1 \\ x_2 \\ x_3 \\ x_4 \\ x_5 \\ x_6 \\ x_7 \end{bmatrix}_{7 \times 1} = \begin{bmatrix} Len \\ L_{bytau} \\ J \\ alphamag \\ A \\ B_g \\ PC \end{bmatrix}_{7 \times 1} \quad (5.31)$$

VARIABLE	LOWER LIMIT	UPPER LIMIT
Length of machine (Len)	7 cm	10 cm
Lbytau	0.7	1.4
Current Density (J)	8 A/mm ²	10 A/mm ²
Extensity of magnet (alphamag)	0.6	0.9
Sp. Electric Loading (A)	30,000 A/m	60,000 A/m
Sp.Magnetic Loading (B_g)	0.9 T	1.2 T
Permeance Co-efficient (PC)	5	7

Table : 5.2 Table showing the upper and lower limits for variables that are optimized

Machine Design Parameters

- Power generated, P_g (power delivered + power loss)
- Voltage generated per phase at the coils, E_{ph} (supply voltage +voltage loss)
- Number of slots in the machine, N_{slots} .
- Inner diameter of the stator, D
- Slot pitch, τ_{slot}
- Angle of skew for the stator slot, σ
- Flux per pole, ϕ_{mag} .
- Total number of conductors, Z .
- Number of turns/phase/parallel path, N_{ph} .
- Number of coils, Number of turns per coil, N_{tc} .
- Length of the magnet, l_m
- Width of the tooth, w_t
- Depth of teeth, d_s
- Stator yoke depth, y_s
- Rotor core depth, y_{rc}
- Outer diameter of the stator, D_{out}

- Area of 1 conductor and diameter of 1 conductor

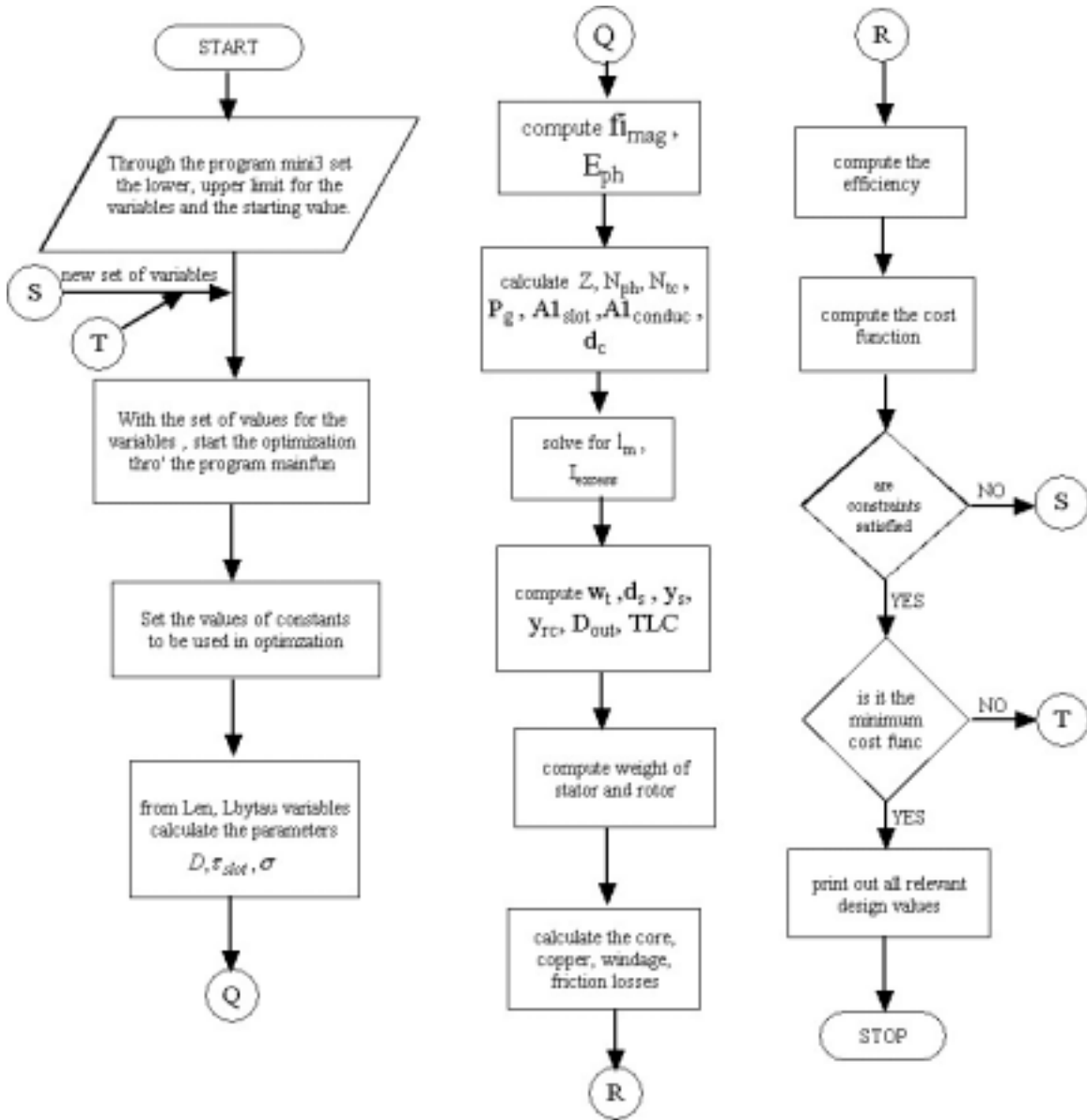


Figure 5.2: Flowchart for optimal design of PMSG

5.5 Results from the Matlab Optimization Routine

In a multi-objective optimization it is very difficult to state that there is unique parameter set as solution, which satisfies all objective requirements. We present some of the optimized machine design, which satisfy the inequality constraint and minimum cost function. The different solutions are possible only when we change either upper limit or lower limit or initial condition of the variables.

When we perform the Finite Element Analysis, some of the optimized machine design might not satisfy thermal conditions giving rise to hot spots within the structure which will render the design unsuitable for construction. We may then be forced to change the initial conditions of the variable to give us a different optimized machine design to make the temperature distribution within the machine acceptable. Usually an increase in the size of the machine (ie. increase in outer diameter of rotor) will help in reducing the hot spots within the machine.

We here present the values of parameters of various design all of which satisfy the inequality constraints and done to obtain different thermal distribution within the machine by changing the value of variables.

5.5.1 Optimized Values of Parameters Of Machine Design

We will be presenting five optimal geometry for varying initial conditions and upper and lower limits of variables. We would be presenting the graph which traces the path traversed by some of the variables and design parameters of Machine- 2. Also through a *Finite Element Software (Flux 2D)* we would be performing the

- ❖ *Electric Analysis : to study the current and voltage waveform pattern in the coils.*
- ❖ *Magnetic Analysis : to study the flux and flux density distribution within the machine and also to make sure the machine does not saturate.*
- ❖ *Thermal Analysis : to study the temperature distribution in the machine and also to make sure the geometry does not have any hot spots.*

on Machine- 2 which offers the most optimal values for geometry satisfying the inequality constraints and objective function of minimum power loss and minimum weight. A detailed Matlab output file for the Machines 1 through 5 will be available in the Appendix –A.

The following table shows the optimized value of variables for machine 1 and machine 2

VARIABLE	MACHINE 1	MACHINE 2
Length of machine (Len) in cm	7.916	7
Lbytau	1.4	1.39
Current Density (J) in A/mm ²	9.21	8
Extrengity of magnet (alphamag)	0.9	0.9
Sp. Electric Loading (A) in A/m	36,908	38,164
Sp.Magnetic Loading (B_g) in T	0.875	1.2
Permeance Co-efficient (PC)	7	7

Table 5.3 Optimized value for variables of Machine 1 and 2.

	MACHINE - 1	MACHINE - 2
Voltage generated per phase at the coils, E_{ph} (supply voltage +voltage loss) in Volts	66	65.2
Current/phase in A	53.16	53.16
Number of slots in the machine, N_{slots} .	12	12
Outer diameter of the rotor, D mm	72	63.84
Length of stator stack, Len mm	79.2	70
Total number of conductors, Z	314	287
Number of turns/phase/parallel path, N_{ph}	26	24
Number of coils, Number of turns per coil, N_{tc}	13	12
Length of the magnet, l_m in mm	5.99	5.99
Maximum current the magnet can sustain, I_{max}	54.95	62.12
Safety limit we maintain ie I_{excess}	1.79	8.96
Width of the tooth, w_t in mm	9.71	11.8
Depth of teeth, d_s in mm	19.4	16.9
Stator yoke depth, y_s in mm	14.56	17.7
Rotor core depth, y_{rc} in mm	12.14	14.38
Outer diameter of the stator, D_{out} in mm	140	133
Area of 1 conductor in m^2 and diameter of 1 conductor in mm	2.903e-6 1.92	3.45e-6 2.1
Total Length of conductor, TLC in m	57.59	45.26
Resistance of coil/phase in ohm	0.057	0.0376
Weight of stator in Kg	7.23	6.98
Weight of rotor in Kg	2.73	1.88
<i>Total Weight of machine in Kg</i>	9.965	8.87
Power generated, P_g Watt (power delivered + power loss)	3729	3674.7
Total copper loss in Watts	483.3	319.1
Total core loss in Watts	235.3	313.5
<i>Total power loss in Watts</i>	728.7	639.5
<i>Efficiency of the machine</i>	80.45	82.6

Table 5.4 Optimized Geometry of Machine 1 and 2

Further we would perform various cases for thermal analysis of Machine 3, 4, 5 using the same Finite Element Software. The effect of change in the inner diameter of stator on the

temperature distribution within the machine is studied through Machine 3, 4, 5. Also various cases for temperature distribution is studied ie for free and forced air- flow through the machine.

VARIABLE	MACHINE - 3	MACHINE - 4	MACHINE - 5
Length of machine (Len) in mm	70	70	71.2
Lbytau	1.34	1.2	1.27
Current Density (J) in A/mm ²	8	8	8.3
Extrency of magnet (alphamag)	0.9	0.78	0.9
Sp. Electric Loading (A) in A/m	35103	33149	35000
Sp.Magnetic Loading (B_g) in T	1.2	1.2	1.05
Permeance Co-efficient (PC)	7	7	7

Table 5.5 Optimized value of variables of machine 3, 4, 5

	Machine 3	Machine 4	Machine 5
Voltage generated per phase at the coils, E_{ph} (supply voltage +voltage loss) in Volts	65.17	66.69	66.7
Current/phase in A	53.16	53.16	53.16
Number of slots in the machine, N_{slots} .	12	12	12
Inner diameter of the stator, D mm	66.5	74.27	71.31
Length of stator stack (Len) mm	70	70	71.2
Total number of conductors, Z	276	292	296
Number of turns/phase/parallel path, N_{ph}	22	24	24
Number of coils, Number of turns per coil, N_{tc}	11	12	12
Length of the magnet, l_m in mm	5.99	5.99	5.99
Maximum current the magnet can sustain, I_{max}	64.95	59.53	59.53
Safety limit we maintain ie I_{excess}	11.78	6.37	6.37
Width of the tooth, w_t in mm	12.29	13.7	11.53
Depth of teeth, d_s in mm	15.54	14.67	17.04
Stator yoke depth, y_s in mm	18.4	17.8	17.2
Rotor core depth, y_{rc} in mm	15.12	14.95	14.4
Outer diameter of the stator, D_{out} in mm	134.5	139.2	140
Area of 1 conductor in m^2 and diameter of 1 conductor in mm	3.46e-6 2.1	3.36e-6 2.06	3.28e-6 2.04
Total Length of conductor, TLC in m	44.25	51.07	50.37
Resistance of coil/phase in ohm	0.0367	0.0437	0.0441
Weight of stator in Kg	7.09	7.38	7.3
Weight of rotor in Kg	2.05	2.47	2.4
<i>Total Weight of machine in Kg</i>	9.13	9.85	9.71
<i>Power generated, P_g Watt (power delivered + power loss)</i>	3669	3741	3742.9
Total copper loss in Watts	311.5	370.6	374.5
Total core loss in Watts	349.9	361.15	359.4
<i>Total power loss in Watts</i>	669.04	741	742.9
<i>Efficiency of the machine</i>	81.76	80.19	80.15

Table 5.6 Optimized geometry of Machine 3, 4, 5

5.6 FINITE ELEMENT ANALYSIS

In this section we analyze the machine designed using a *Finite Element Package* , *Flux 2D*. With the *Finite Element Software (Flux 2D)* we would be performing the

- ❖ *Electric Analysis* : to study the current and voltage waveform pattern in the coils.
- ❖ *Magnetic Analysis* : to study the flux and flux density distribution within the machine and also to make sure the machine does not saturate.
- ❖ *Thermal Analysis* : to study the temperature distribution in the machine and also to make sure the geometry does not have any hot spots.

Electric, Magnetic, Thermal analysis are done on Machine- 2 to verify the geometry obtained through the analytical (Matlab) model.

We also perform the thermal analysis on machines 3, 4, 5 mainly to study the variation in the temperature distribution within the structure with change in the inner diameter of stator. Temperature gradient from the outer stator surface to the center of the shaft are studied for various cases ie. for free and forced air- flow through the machine.

5.6.1 Transient Magnetic Analysis -FEA Of Machine –2

Some general steps and features of Flux2D, pertaining to the electric, magnetic and thermal analysis, are described as the model is entered and solved. The results from the 2D analysis are also included in this chapter. We have referred to [5], [6] for some of our analysis.

5.6.1.1 Machine Parameters

The PM machine consists of the following parts:

- (1) A twelve slot stator yoke
- (2) A solid body rotor on a shaft
- (3) Rare earth permanent magnets eg :MQ3-F 36H. The isotropic high energy permanent magnets are surface mounted and, for simulation purposes, are assumed to have radial magnetization.

Component	Parameter	Value
Rotor	Stack Length (mm)	70
	Inner diameter (mm)	11.56
	Outer diameter (mm)	25.94
	Core thickness (mm)	14.38
Magnet	Thickness (mm)	5.9
	Ratio of magnet curvature to pole pitch	0.9
	Axial length	70
Stator	Axial length (mm)	70
	Inner diameter (mm)	64.8
	Outer diameter (mm)	133
	Number of slots	12

	Tooth width (mm)	11.8
	Yoke thickness (mm)	17.7
	Depth of tooth (mm)	16.9
	Slot opening (mm)	1.3
	Slot opening depth (mm)	0.98
	Shoe bevel angle	40°

Table 5.7: Permanent Magnet Machine Parameters.

5.6.1.2 Stator and Rotor

The values in table 6.1 are referred to as base model parameters when referring to the model in Flux2D. The following figure shows cross section of a quadrant of the base machine model.

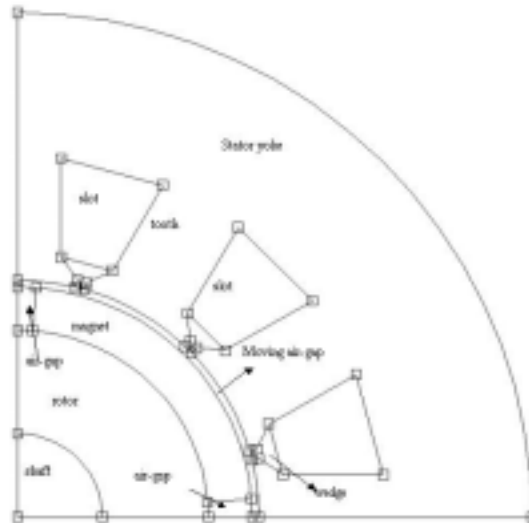


Figure : 5.3 Cross Section of a quadrant of the base model of the Machine –2

For greater flexibility in design variations, the equations used to parameterize the rotor are segregated from those used to parameterize the stator. Thus, stator and rotor parameters can be varied without affecting the rest of the geometry.

5.6.1.3 The Moving Air Gap

The moving air gap is a feature of Flux2D that allows a rotating machine to be analyzed at various rotor positions without having to manually recreate a new geometry and mesh for each rotor position. When used, the moving air gap is required to have one layer of mesh within it [9].

Two concentric circles, placed within the air gap, are used to define the moving air gap region. This allows the moving air gap region to have one layer of mesh while the entire air gap region can be finely meshed. The moving air gap width (the distance from one concentric circle to the other) is fixed at an arbitrary value. The concentric circles are parameterized to keep the

moving air gap centered between the rotor outer radius and the stator inner radius. Thus, as parameter values are varied, the moving air gap remains fixed at the center of the actual air gap and has a width allowing for one layer of mesh.

5.6.1.4 *The Mesh*

The two main concerns taken into account when creating the mesh for the machine are memory size and computation time. The finer the mesh, the more accurate the results, but more memory is used and it takes longer to compute and process the results.

When set to auto-mesh generator mode, the Flux 2D would give us sparsely meshed structure which had some fault in the structure. The fault was removed by manually increasing the density of the mesh nodes at rotating air-gap, rotor inner diameter and along the tooth. The following figure shows the final mesh nodes, which was used as such to mesh the structure.

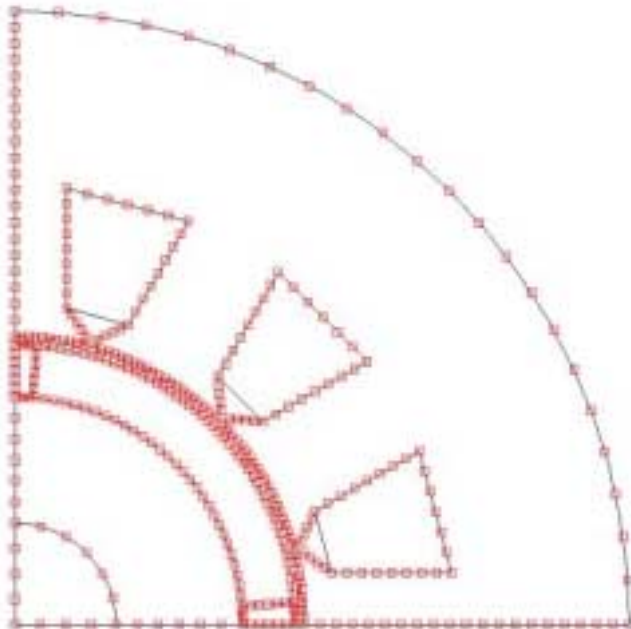


Fig : 5.4a Final Mesh nodes used to mesh the structure without any faulty region

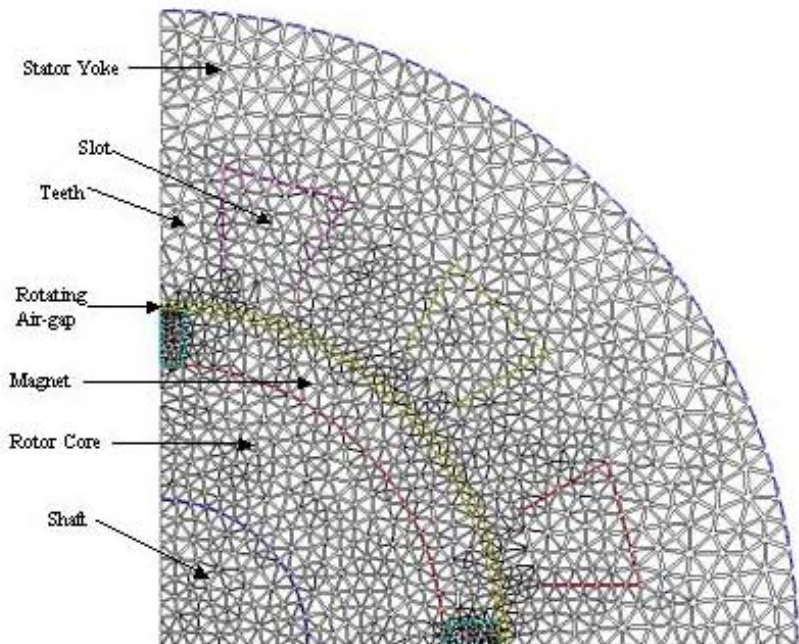


Fig : 5.4b Final Mesh structure of the quadrant of machine

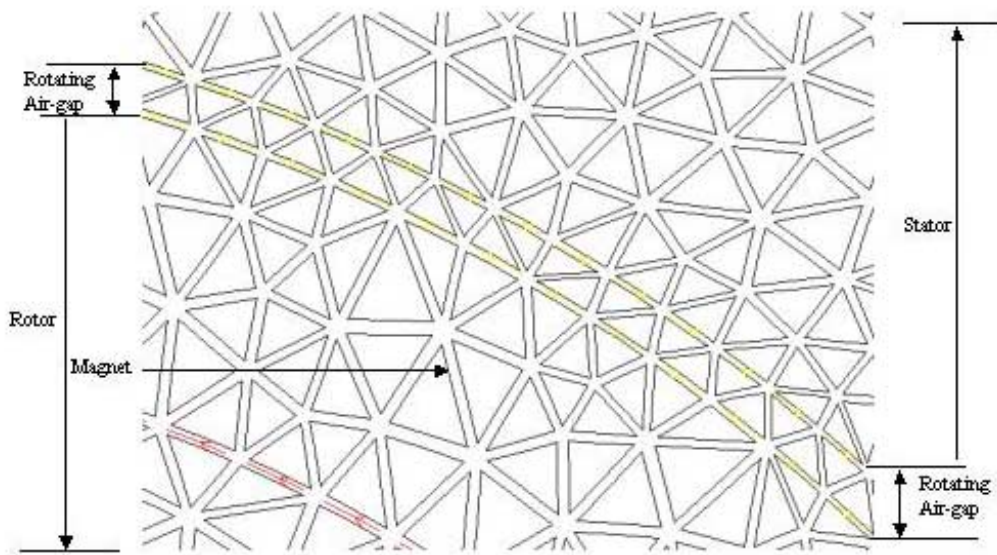


Fig : 5.4c Enlarged view of the single layer mesh of rotating air-gap

5.6.1.5 The Back EMF Computation

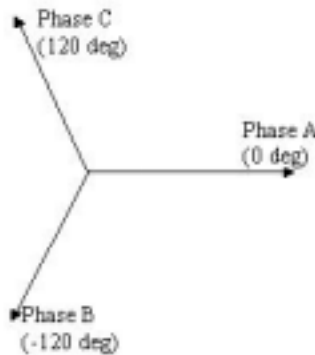
Flux 2D computes the back emf of the stator winding by connecting the stator winding power supply to an open circuit load and rotating the rotor over one complete cycle. The Line - Line and phase voltages with harmonics fully taken into account are readily available through the external circuit model.

The stator winding connections for the model (1/4 of the generator or 1 pole) are 3 phase –Wye connected.

The External Circuit Model

(A) Convention

For a 3 phase-Wye connected windings, the phase diagram is shown below



(B) External Circuit connections

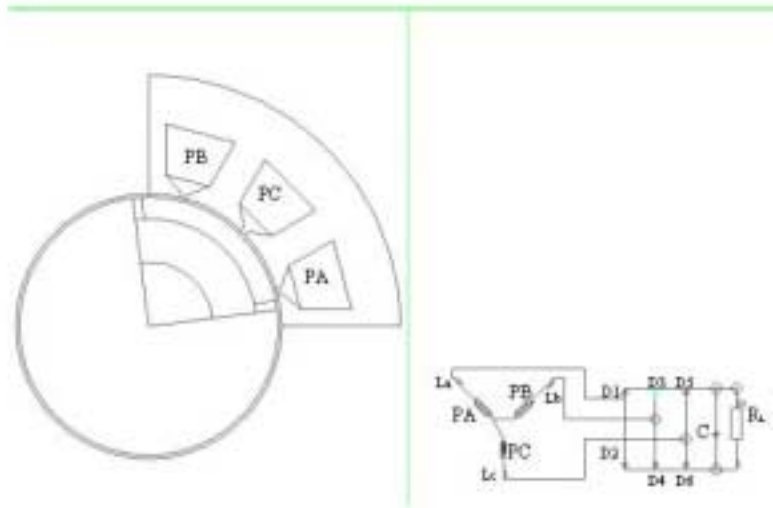


Figure 5.5 Back EMF external circuit connection

The components

PA, PB, PC are phase A, B, C coils respectively.

La, Lb, Lc are coil self inductances

RL is the Load Resistances

D1 through D6 forms the diode bridge rectifier

We use the “hot point” convention to draw the circuit model (for detailed information refer External Circuit Connection User’s Guide).

5.6.1.6 The Material Base and The Physical Property for Machine – 2

The material base contains the properties of the permanent magnets, the rotor back iron, and the stator yoke. For transient magnetic analysis we would be interested in the B-H property of the magnet, steel.

We would assign the property of vacuum to shaft, slots, wedges and air. The moving air-gap is assigned the property of vacuum but moving with a constant speed of 1800 rpm.

Properties like the thermal conductivity, convective exchange coefficient, radiative exchange coefficient, specific heat are to be used for thermal analysis. We will state the value of these properties when we deal with the thermal analysis.

(A) Permanent Magnets

To enter a permanent magnet into the material base of Flux2D, all that is required is the remanence and relative permeability [9] for *electrical and magnetic analysis*.

We have a permanent magnet modeled as

- remanent flux density $B_r = 1.2$ Tesla
- relative permeability = 1.07

(B) The Rotor Back Iron and the Stator Yoke

The rotor back iron and stator yoke are made of steel having a non-linear magnetization (BH) curve.

A plot of the Delphi model BH curve was obtained, with Matlab, to assist with using the scalar spline function in Flux2D. Figure 6.3 displays the BH curve with the tangent line used for obtaining the saturation magnetization. From the Matlab plot, the values for the maximum field intensity, H_{\max} , maximum flux density, B_{\max} , and saturation magnetization, J_s were obtained.

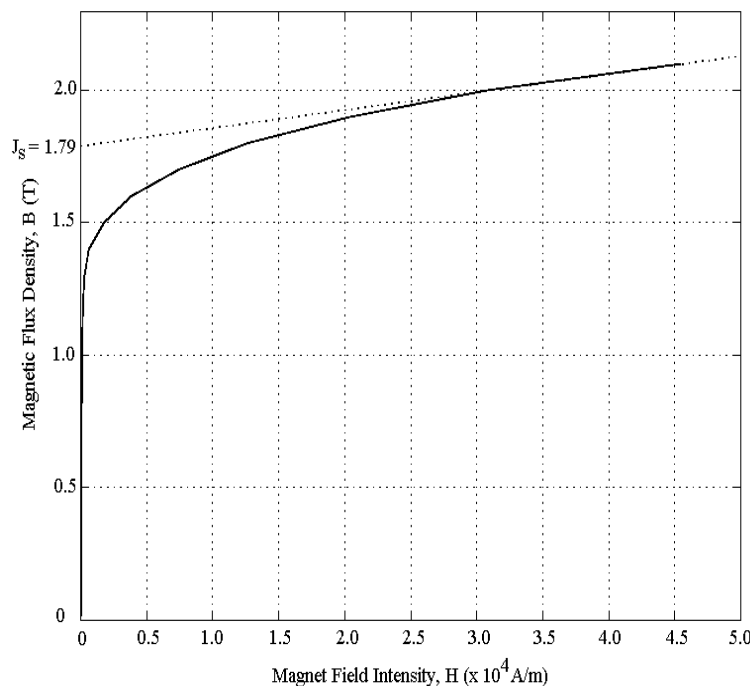


Figure 5.6 BH Curve for Delphi Model Rotor and Stator Back Iron.

The saturation magnetization is obtained from a tangent line on the BH curve (refer to figure 5.5). The equation used to determine the saturation magnetization is (from the equation for a line):

$$J_s = B - \frac{\Delta B}{\Delta H} H \quad (5.32)$$

where J_s is the saturation magnetization in Tesla, B is the flux density in Tesla, H is the field intensity in amperes per meter, and $\frac{\Delta B}{\Delta H}$ is the slope of the tangent line. Using the values of point 21 and 22 from table 6.2, the saturation magnetization is approximately equal to 1.79 Tesla.

5.6.1.7 The Boundary Conditions

The boundary conditions are set on the nodes. They allow us to set the limits to the study domain by setting the value of the variable, to take into account physical symmetries, to impose the value of the variable inside the study domain. In the transient magnetics the variable is the vector potential (field). More information could be obtained from the *Flux 2D USER'S GUIDE*.

A Dirichlet boundary condition allows us to set the value of the variable to the boundaries of the study domain and the internal shell and pinpoint regions. We assign Dirichlet's boundary condition with a vector potential equal to zero is set at the stator outer radius and the center of the shaft. The first condition assumes no magnetic flux leaks radially out of the machine.

Anticyclic Boundary Condition allows us to make a link between 2 boundaries. The value of the variable is unknown on these boundaries, but it is of opposite sign on the homologous nodes (inverse variable form).

The moving air gap feature of Flux2D allows for a symmetrical part of the machine (for example, one quarter or half) to be analyzed, if desired [9]. Using this capability of the moving air-gap region allows us to save a lot of memory and computation time. We use the anti-cyclic boundary condition in the stator and rotor side boundaries. This makes the condition at one side-boundary exactly opposite to the other side-boundary.

5.7 Analyzing the Results of Transient Magnetic of Machine – 2

Flux 2D allows us to analyze the results of a computation in different ways :

- Plots of color shades, isovalues, vectors
- Time and space varying curves, spectra
- Computing the quantities at a point, for a region and electric quantities. \

5.7.1 Magnetic Flux Density Distribution

The following figure shows the flux density distribution of the magnet at the 2nd time instant (1 time step= 0.000667 seconds). We could clearly see that the machine is not saturated (ie $B < 1.79$ T) at any point. In fact the steel available at the market currently has the saturation flux density of 2 T.

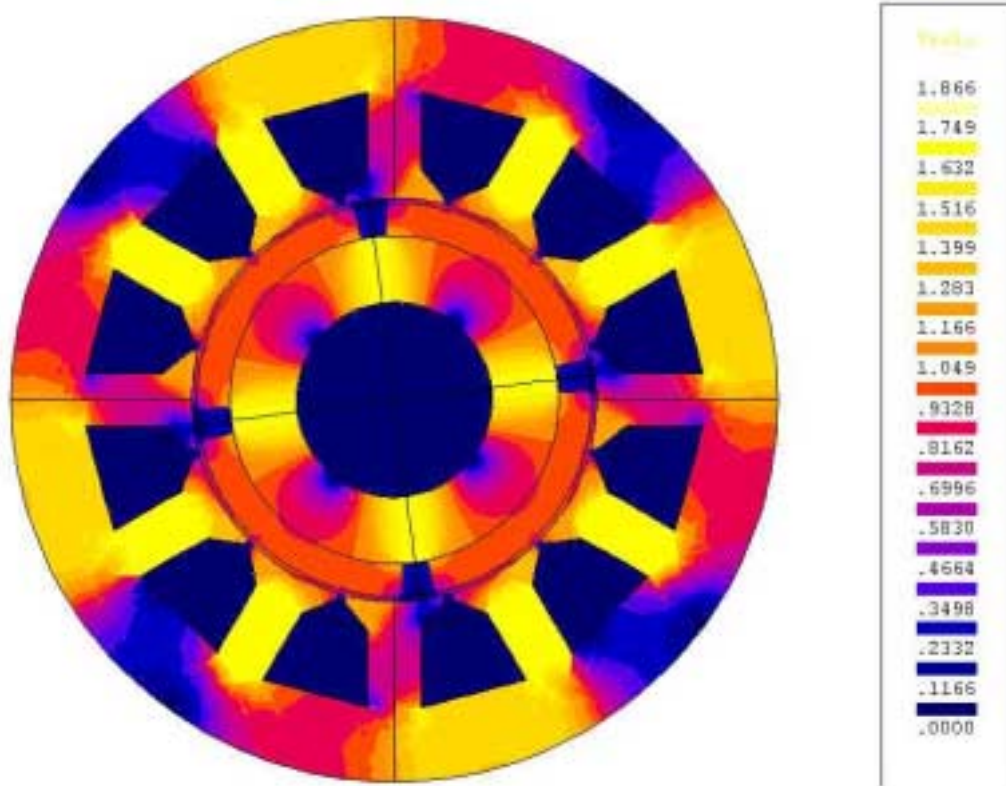


Figure 5.7a The Flux Density distribution at the 2nd time instant

We also clearly see that the flux density distribution pattern repeats itself for every pole which validates our initial assumption. The distribution at some other time instant would confirm that the machine does not saturate at any time instant.

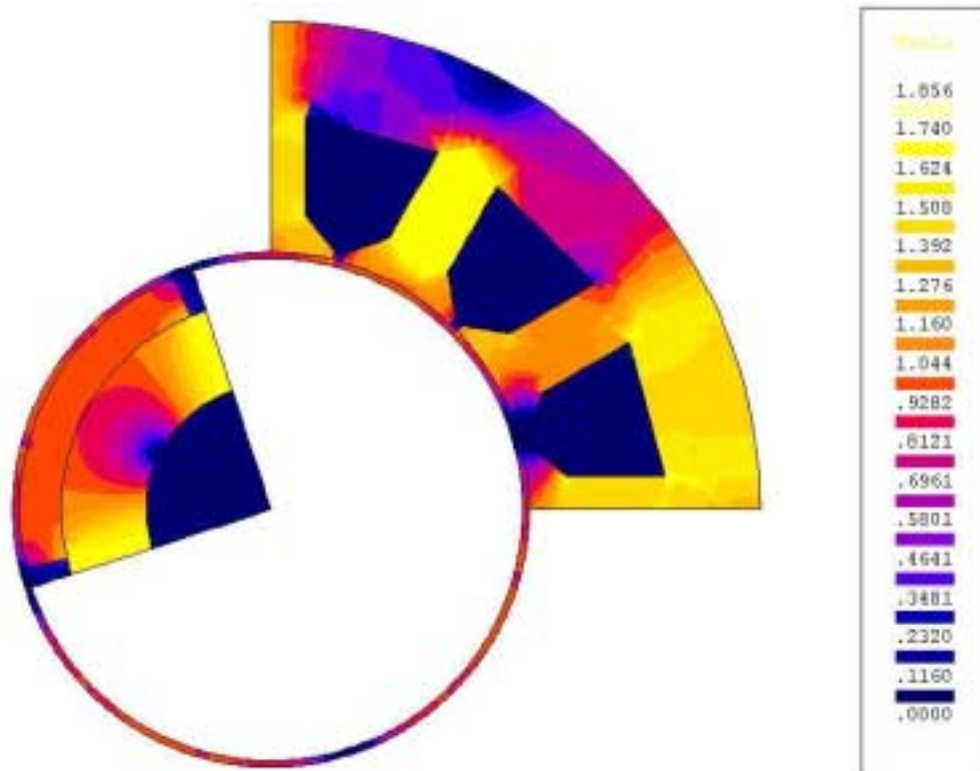


Figure 5.7b The Flux Density distribution at the 15th time instant

The flux density variation at the individual points over an entire cycle are required to compute the core loss at that point. We could select some points in the machine stator yoke, stator teeth, air-gap and rotor core to study the flux density variation over the region in general.

The flux density variation at various points are given below

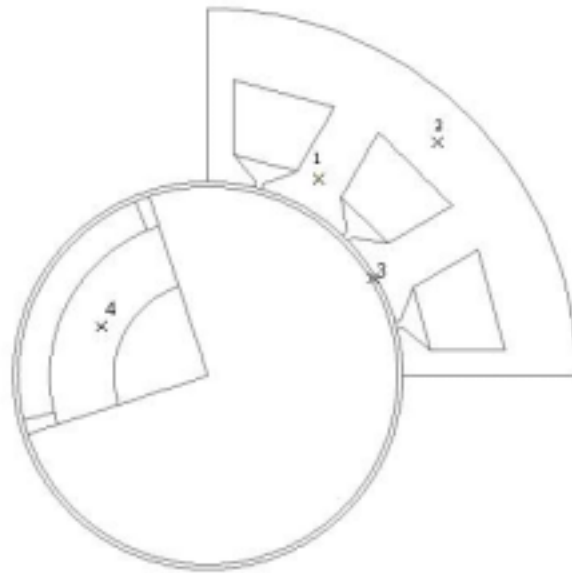


Figure 5.8 The structure showing 4 points where flux density variation many cycles are studied

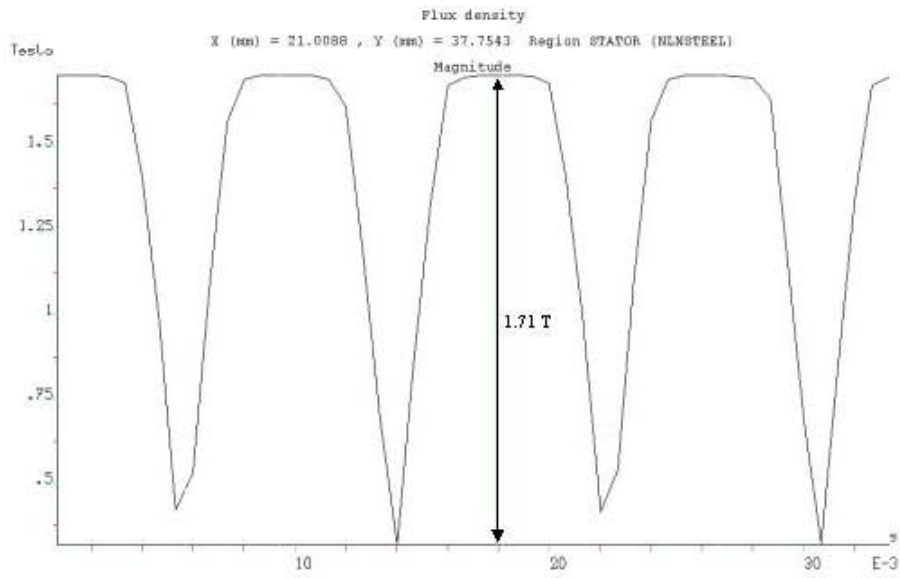


Figure 5.9 The flux density variation at point -1 over many cycles

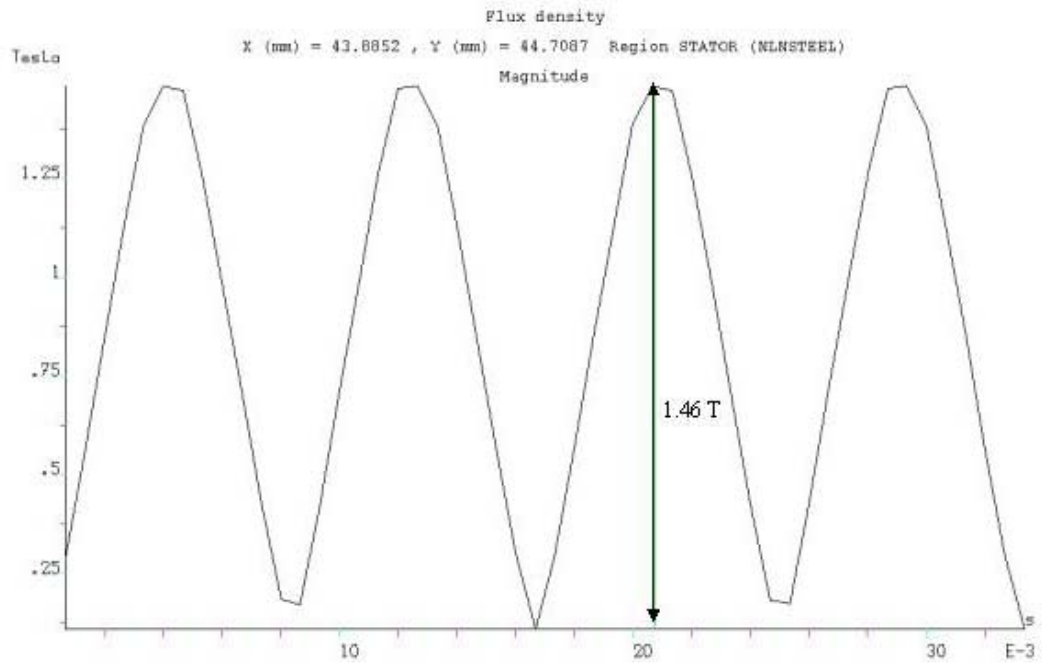


Figure 5.10 The flux density variation at point -2 over many cycles

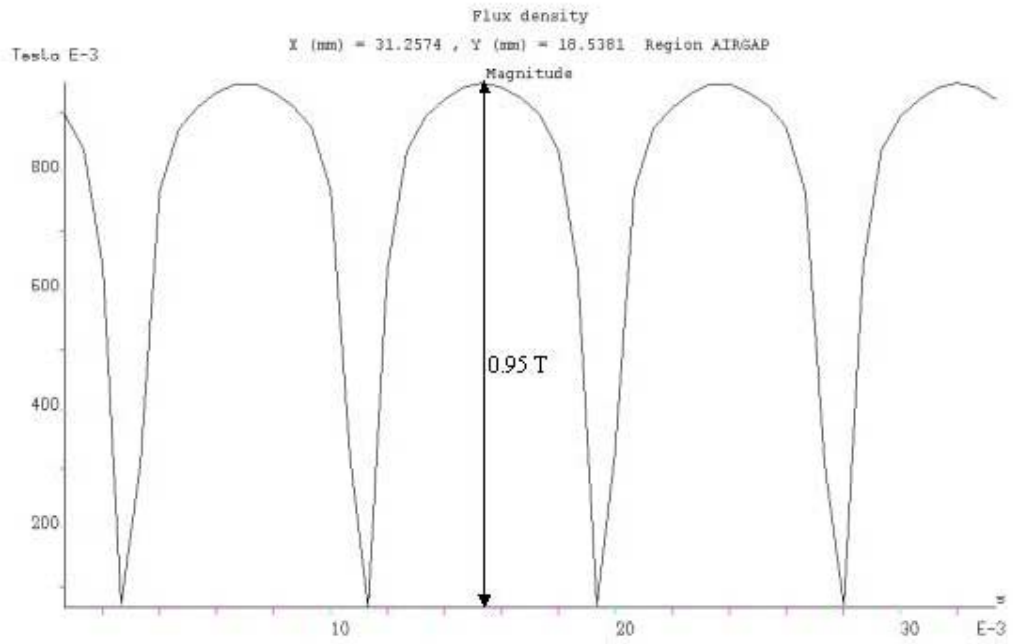


Figure 5.11 The flux density variation at point - 3 over many cycles

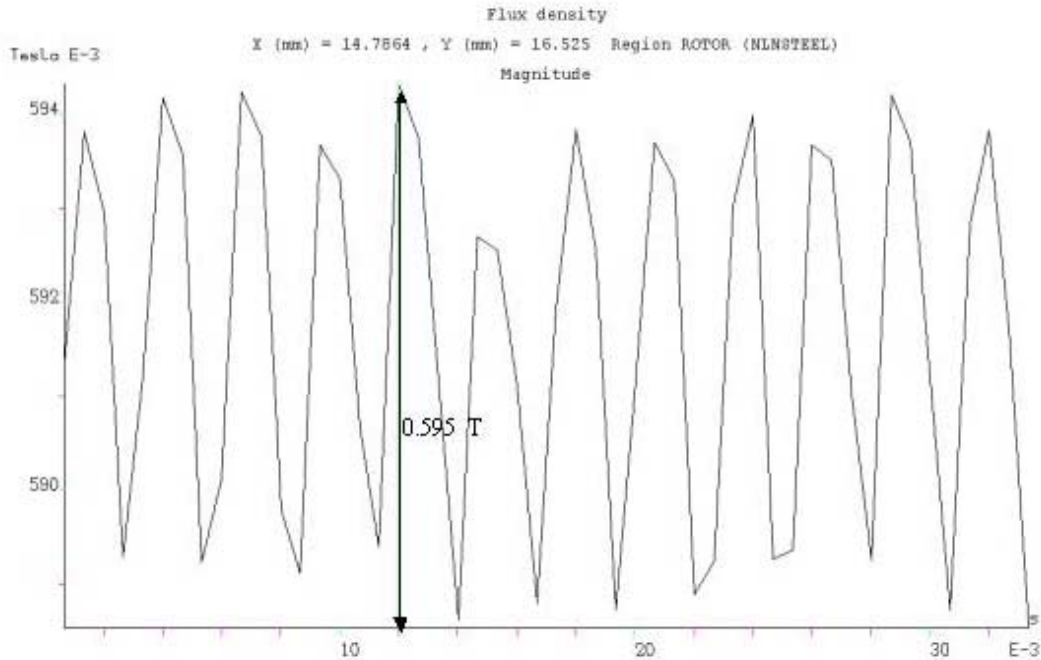


Figure 5.12 The flux density variation at point – 4 over many cycles

The change in the flux density in the yoke, teeth sections are measured to use them in the core loss calculation. In our case the average change in flux density at teeth, yoke sections are 1.5 T and 1.1 T respectively. This value is substituted in

$$P_{core} = 0.5 * 10^{-3} * f^{1.7} B_p^{1.9}$$

to obtain the core loss per kg at tooth and yoke sections individually.

5.7.2 Back EMF Computation

The current and voltage requirement are derived in section 4.5 of chapter 4. The following figure states the current and voltage (splitting) requirement

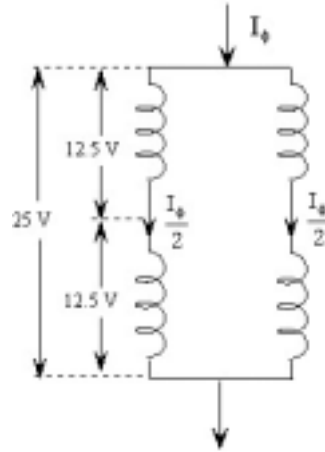


Figure 5.13 : Phase Winding depicting the voltage and current sharing between them

In the structure analyzed we have taken just a quadrant of the machine into account. Two coil sides/phase ie. one coil/phase are allocated in each slot. Comparing it with the figure above , we see a quadrant of the machine can have only one coil/phase ie. we should be able to see a square wave voltage with a peak amplitude of 12.5 V being developed per coil.

From the figure 5.14 we find that the voltage developed in the coil/phase satisfies the requirement.

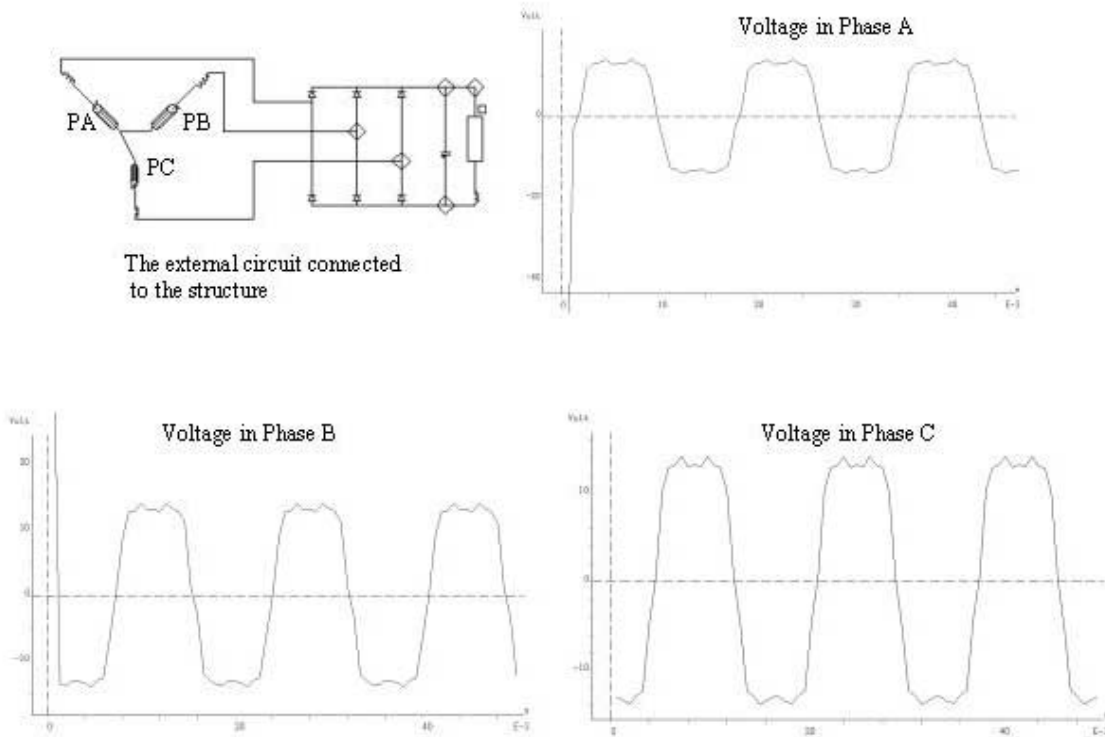


Figure 5.14: The figure showing the external circuit connected to the structure and the voltages generated in the coil of phase A, B, C

5.7.3 Thermal Analysis of the Machine –2

Through the Thermal Analysis we try to

1. Validate the geometric and electrical design of the Machine –2, ie. it is devoid of any hot spot.
2. Establish the effect of free and forced air-cooling on the temperature gradient in the machine.
3. Establish the effect of increasing the outer diameter of the rotor on the temperature gradient in the machine.

The core and copper losses heat the materials involved increasing the temperature of the material. We need to study the temperature distribution within the structure and make sure that there are no hot spots in the machine which will result in the breakdown of the insulation shorting the coils. This might cause permanent damage to the machine and render it useless. Hence thermal analysis of the structure is an important aspect in the design of electric machines.

Generally we calculate the core loss and copper loss through the Matlab program. In thermal analysis the stator yoke, teeth and copper coils are the source of heat, and we assign those values calculated from the matlab program to the stator yoke and copper coils. We then perform the steady state thermal analysis to find the temperature gradient between the stator outer surface and center of the shaft.

In our machine

- a) Each slot is a source of $1/12^{\text{th}}$ of the total copper loss. The slots are now assigned the property of copper. In the Transient Magnetics they were assigned property of vacuum.
- b) The quadrant of the stator is a source of $1/4^{\text{th}}$ of the total core loss.

Some of the physical properties of the materials which must be added in order to perform the Thermal analysis are the

Isotropic Property name	Unit	Command in Flux 2D
Specific heat	J/m ³ /degree	[B_ROcp]
Thermal conductivity	W/m/degree	[9_iso_K]
Convective exchange coefficient	W/m ² /degree	[C_Conv_R]
Radiative exchange coefficient	W/m ² /degree ⁴	[D_Rad_R]

Table 5.8 Necessary physical property of materials in Thermal Analysis

Material	Thermal conductivity	Convective exchange coefficient	Radiative exchange coefficient
Non linear steel	$V=V_0(1+a.t)$		

	$V_0=47 \text{ W/m}^2\text{C}$ $a=-0.25e-3$	50	0.5
Magnet	10	50	0.5
Air	10	Varied	
Copper	40	50	
Shaft	40	50	
Insulator	1	10	0.1
Conval	1	Varied	0.8

Table 5.9 Physical property of materials used

Material	Region
Air	Rotating air-gap, region between 2 magnets along circumferential direction
Steel	Rotor and stator
Magnet	Magnet
Insulator	Wedge
Shaft	Shaft
Copper	Slots
Conval	Stator outer surface

Table 5.10 Materials assigned to the corresponding region

The tables 6.3, 6.4, 6.5 lists the material involved, their physical properties and the regions associated with the material .

From magnet manufacturer's data [18,19], the highest temperatures that permanent magnets can normally operate are 180 °C for Magnequench Int. and 200 °C for Hitachi Metals. The insulator used in the machine can withstand 200 °C .

In our case a hot spot in the machine could be stated as that spot which has a temperature more than 180 °C when the machine is subject to a steady state Thermal Analysis.

Objective 1 : to validate the geometry of machine -2 and also establish the effect of free and forced air-cooling

We achieve the objective by considering the following 3 cases

	Convective co-efficient of air	Convective co-efficient of conval	Ambient temperature at the stator outer surface
Case-1	50	60	50 °C
Case-2	70	100	50 °C
Case-3	70	100	80 °C

Table 5.11 Cases considered to achieve the objective

In all the 3 cases the quadrant of stator (yoke and teeth) was a source for 90 Watts and each slot a source for 26 Watts of energy which are to be dissipated as heat.

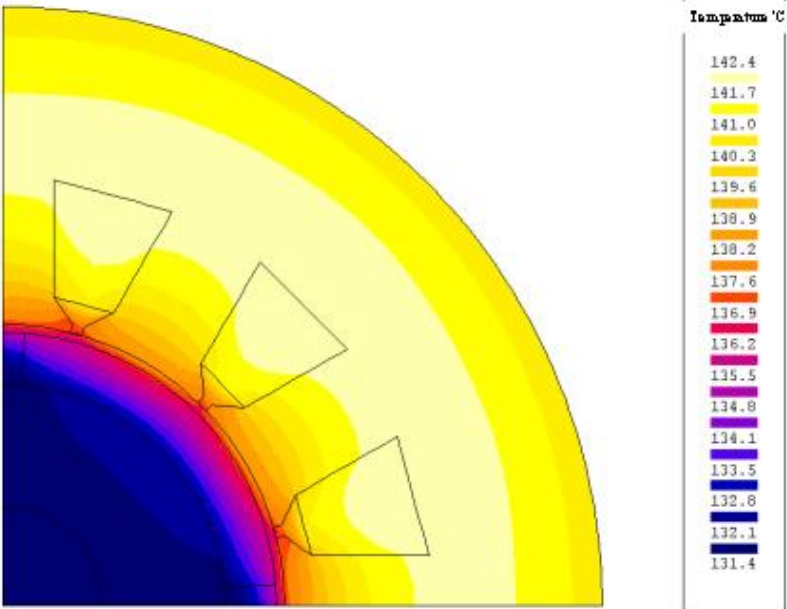


Figure 5.15 : Temperature Gradient of machine -2 for case-1

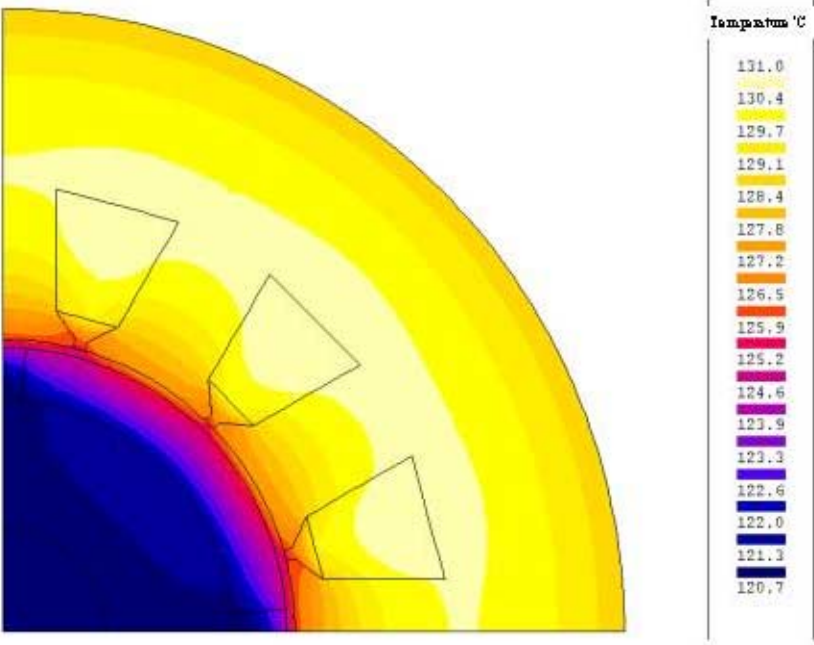


Figure 5.16 Temperature Gradient of machine -2 for case-2

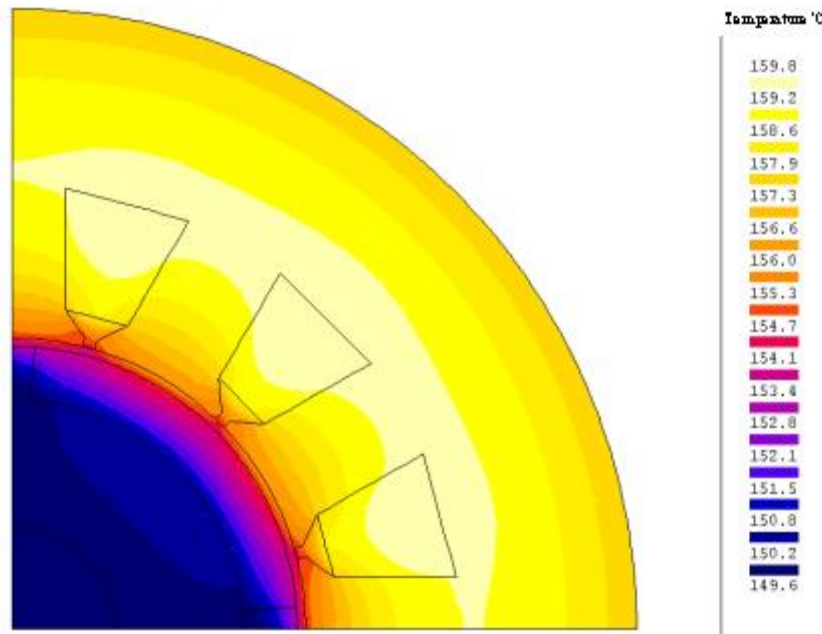


Figure 5.17 : Temperature Gradient of machine –2 for case-3

The figures 5.15-5.17 clearly indicate that

- The machine does not have any hot spot for the cases considered.
- We see that when we cool the machine by forcing air to flow through, the steady state temperature of all the surfaces reduces. Also there is marked difference in the steady state temperature between case-1 and case-2.
- As the ambient temperature at the stator outer surface increases we are forced to cool the machine forcing the air to flow through ie. forced-air cooling. If the ambient temperature was 80 °C self cooling mechanism as in case-1 might have resulted in hot spots.

Objective 2: Establish the effect of increasing the outer diameter of the rotor on the temperature gradient in the machine.

We achieve the objective by applying the following 2 cases on the Machine-4 and Machine-5 (The geometric parameters of these machines were stated in the previous chapter).

	Convective co-efficient of air	Convective co-efficient of conval	Ambient temperature at the stator outer surface
Case-A	50	60	50 °C
Case-B	70	100	50 °C

Table 5.12 Cases considered to achieve the objective

In both cases the quadrant of stator (yoke and teeth) was a source for 90 Watts and each slot a source for 30 Watts which is to be dissipated as heat. The outer diameter of rotor in machine-5 is less than machine-4. The following figures show the thermal distribution in the machines considered.

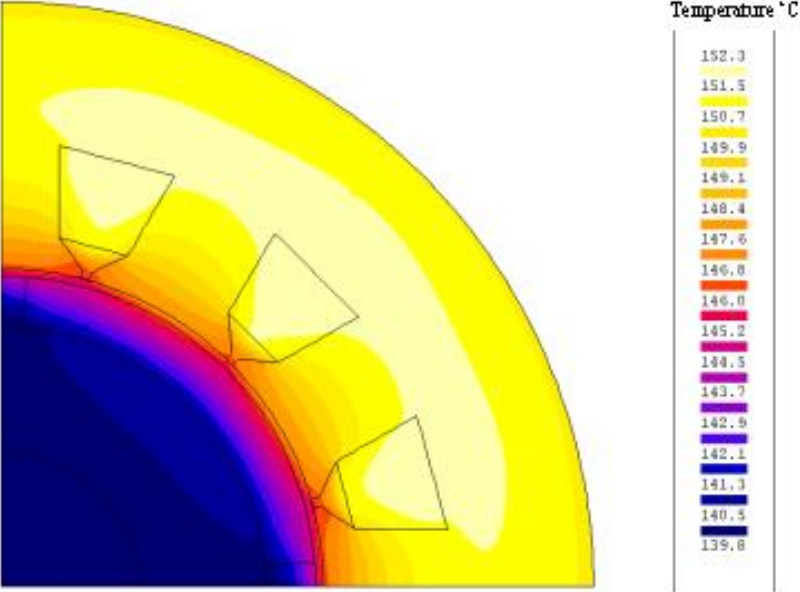


Figure 5.18 : Temperature Gradient of machine –5 case-A

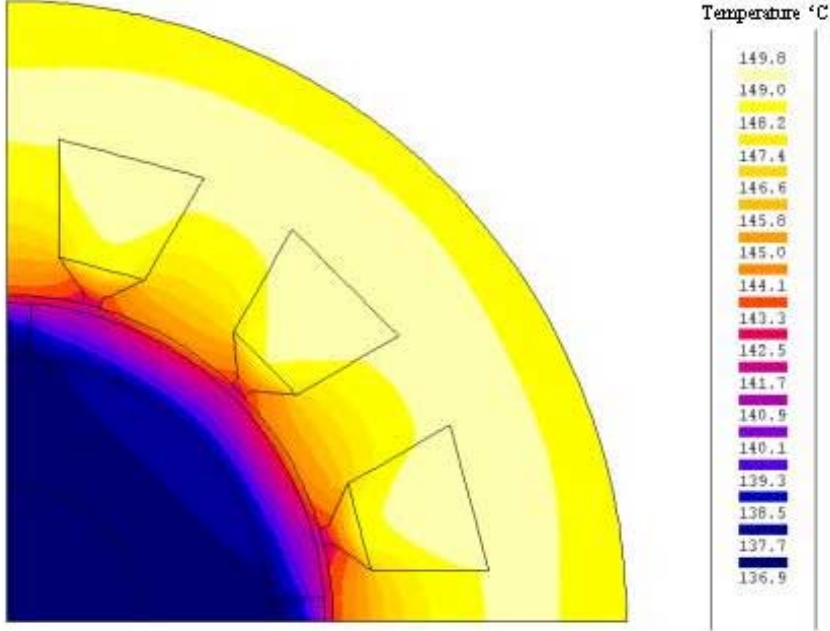


Figure 5.19 : Temperature Gradient of machine –4 for case-A

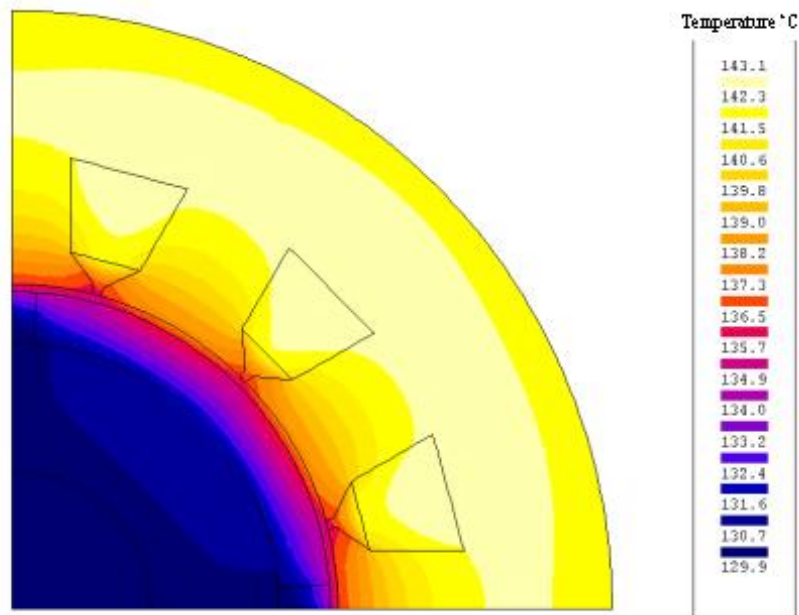


Figure 5.20 : Temperature Gradient of machine -5 for case-B

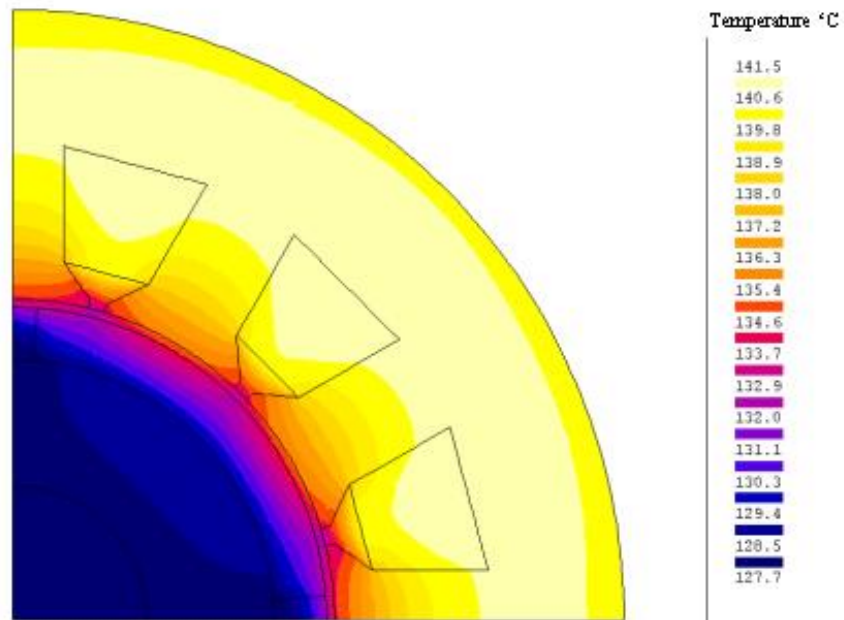


Figure 5.21 : Temperature Gradient of machine -4 for case-B

The outer diameter of machine 4 is greater than that of machine-5. Also we could observe that the stator yoke and rotor core size of machine 4 to be greater than machine 5. These factors play a role in the thermal distribution within the machine. We see for similar conditions and same iron and copper losses machine 4 is better cooled than machine 5, thus proving the validating our assumption.

Reference

- [5] Magsoft Corporation, 'Finite Element Analysis Software Reference Manuals', *Magsoft Corporation, Troy, NY, April 1995.*
- [6] Coy Brian Studer, 'Study Of Cogging Torque In Permanent Magnet Machines', a Master's Thesis in the Dept. of Electrical Engineering, The Ohio State University, 1998.
- [7] S.J. Salon, 'Finite Element Analysis of Electrical Machines', *Kluwer Academic Publisher, 1995.*
- [10] Ansoft Corporation, 'Finite Element Analysis Software Reference Manuals', Ansoft Corporation, Pittsburgh, PA, September 1996.
- [18] Permanent Magnet Catalogue, *Magnaquench International Inc.*
- [19] Hitachi Rare-Earth Magnet, *Hitachi Metal America, Ltd.*

CHAPTER – 6

Conclusion And Future Implementation

6.1 Conclusion

The optimal design of permanent magnet synchronous generator in the single-excitation PMSG system was mainly addressed in this thesis. The optimal machine geometry for minimum power losses and minimum power weight was provided. The studied structure of PMSG is 3-phase, 4-pole, and 12-slot machine with uniformly distributed stator windings. The waveform of output ac voltage is square wave because of the full pitch coil. The parallel coils for each phase was designed because the high current capability of loads. The Nd-Fe-B permanent magnet is selected because of its properties of high both H_c and $(B \times H)_{\max}$, causing greatly withstanding the permanent magnet demagnetization even in the worst case of short circuit condition.

The machine parameters are solved by the use of a Matlab function, *fmincon*, an inequality constrained multi-objective optimization function. *fmincon* uses medium scale Sequential Quadratic Programming (SQP), Quasi-Newton, Line-search algorithms. We had briefly discussed these algorithms. An insight on how the cost function (power loss and weight of the machine) and the various constraints are derived from the machine parameters was also provided.

We also had presented the fundamentals and mathematical formulations of developed modeling approach for permanent magnet machines (chapter-3). The simplicity and analytic properties of the magnetic circuit analysis make it most commonly used magnetic field approximation method. Also in this method geometry of the machine is related to the field distribution giving substantial design insight which helped in the design of the 42 V/3000W PMSG.

The model was based on developing equivalent reluctance model from the dimensions and material properties of the machine. Sectoral model of the machine were developed. A linear reluctance matrix was used to relate the flux and magnetomotive force throughout the different sectors of the machine. The saturation effects were evaluated according to the iron section properties and dimensions and then used to adjust the flux distribution.

We had initially presented the basics of reluctance modeling for some basic shapes which are rectangular where the direct substitution of formulae is possible. But in actual case the machine structure is complex with lots of curvature ie magnet, stator, rotor etc are all curved. Hence some stress was laid on how to calculate reluctance of each part and then model stator, rotor etc. individually and then how to interface them and arrive at the complex reluctance model for the entire machine. A case study of the machine when projected on to 2-Dimension was studied first and then the permanent magnet motor was modeled. FEA was extensively used to validate the model developed.

6.2 Future Implementation

- A method to compute precisely the core losses in the machine could be developed.

- Dual excitation mode (excitation due to both permanent magnets and coils in the rotor) could be used to increase the efficiency and also smoothen the waveforms.
- An accurate detailed thermal model for the machine could be developed.
- A precise calculation of the operating point (in a magnet) at a particular temperature.
- Study of the Cogging Torque for the current machine structure could be done.
- An analysis of various other machine structures (4 poles, 24 slots etc.) for the same power requirements could be done.

APPENDIX

APPENDIX- A1

Matlab Results of Optimization for Machine –2

Length of the machine

```
Len=X(1);
```

```
Lbytau=X(2);
```

J=current density in the conductors

```
J=X(3)*1e6;
```

alphamag= spread of the magnet with respect to the pole pitch

```
alphamag=X(4);
```

A is the specific electric loading of the machine

```
A=X(5);
```

Bg is the average magnetic flux density in the airgap

```
Bg=X(6);
```

PC is the permeance coefficient of the magnet (machine)

```
PC=X(7);
```

```
x =
```

```
    1.0e+04 *  
    Columns 1 through 4  
    0.000700000000000    0.00013959047807    0.000800000000000  
0.000090000000000  
    Columns 5 through 7  
    3.81632386290087    0.000120000000000    0.000700000000000
```

```
feval =    3.417795474203693e+02
```

```
flag =    1
```

```
out =
```

```
    iterations: 37  
    funcCount: 582  
    stepsize: 1  
    algorithm: 'medium-scale: SQP, Quasi-Newton, line-  
search'  
    firstorderopt: []  
    cgiterations: []
```

values of various parameters as calculated from the minimisation routine

inner diameter of the machine

D = 0.06384874481834

volatge developed by the winding for each pahse

Eph = 65.28256172065117

number of windings per phase/parallel path

Nph = 23

Approximated to Nph = 24

number of turns per coil

Ntc = 11.500000000000000

Approximated to Ntc = 12.

number of conductors in the machine

Z = 287

power developed at the coils of the machine

Pg = 3.674694430076336e+03

length of the magnet

lm = 0.005985000000000

maximum current allowed in the coil

Imax = 62.12169782608696

Imax -Ispphase ie safety limit for current is maintained

Iexces = 8.96169782608696

width of tooth

wt = 0.01179922045072

depth of yoke

ys = 0.01769883067608

rotor core depth

yrc = 0.01438075443518

depth of teeth

ds = 0.01689518376805

outer diameter of stator

Dout = 0.13303677370660

area of 1 conductor in square meter

Alconduc = 3.454918478260869e-06
diameter of 1 conductor

dc = 0.00209736473470
total length of the conductor

TLC = 45.25291881123754
wt of conductors in the machine

Wcoils = 1.39147179402603
weight of the various parts of stator in kgs

Wteeth = 1.51897521750072

Wyoke = 4.07211332648428

Wstator = 6.98256033801104
wieght of various parts of rotor in kgs

Wcore = 1.24570089984790

Wmag = 0.63640352655220

Wrotor = 1.88210442640010
Total weight of machine

TWmac = 8.86466476441114
losses at various parts of machine in watts

Rphase = 0.03763524982402

Rcoil = 0.03763524982402
total copper loss in the conductors

Pcu = 3.190700221652125e+02
core loss at teeth/kg

Pcoreteeth = 1.138676931090131e+02
core loss at yoke/kg

Pcoreyoke = 43.14077055253947
total core loss in the machine

TPcore = 3.486363105883650e+02

TPcoreyoke = 1.756741066817968e+02

TPcoreteeth = 1.729622039065682e+02
total power loss in the machine

TPLoss = 6.746944300763274e+02
efficiency of machine considering all losses

effi2 = 81.63944124022547
efficiency of the machine considering just copper and core loss

effi = 81.82960936047935
total power supplied by the machine for use ie Pgenerated-
Plosses

TPsupp = 3.000000000000009e+03

ans = 3.417795474203693e+02

APPENDIX- A2

Matlab Results of Optimization for Machine –3

```
format long;
global mmm; global data; mmm=1;
options=optimset('TolX',1e-8,'TolFun',1e-8,'TolCon',1e-8);
[x, feval, flag, out]=fmincon('mainfun', [7 1.3 9 .9 35000 0.8
5],
                                [], [], [], [], [7 1.1 8 .6 30000 .8 5],
                                [10 1.4 10 .9 60000 1.2 7],
'constrfun',options)
exploitation(x)
```

Length of the machine
Len=X(1);

Lbytau=X(2);

J=current density in the conductors
J=X(3)*1e6;

alphamag= spread of the magnet with respect to the pole pitch
alphamag=X(4);

A is the specific electric loading of the machine
A=X(5);

Bg is the average magnetic flux density in the airgap
Bg=X(6);

PC is the permeance coefficient of the magnet (machine)
PC=X(7);

```
x =
  1.0e+04 *
  Columns 1 through 4
  0.00070000164421    0.00013398094825    0.0008000000000000
  0.0000900000000000

  Columns 5 through 7
  3.51033086685561    0.000120000000000    0.0007000000000000
```

```

feval =      3.390891511783781e+02
flag =      1
out =
    iterations: 32
    funcCount: 456
    stepsize: 1
    algorithm: 'medium-scale: SQP, Quasi-Newton, line-
search'
    firstorderopt: []
    cgiterations: []

values of various parameters as calculated from the minimisation
routine
inner diameter of the machine

D =      0.06652212769085
    volatge developed by the winding for each pahse

Eph =      65.17225869521738
number of windings per phase/parallel path

Nph =      22
number of turns per coil

Ntc =      11
number of conductors in the machine

Z =      275
power developed at the coils of the machine

Pg =      3.669041433884511e+03
length of the magnet

lm =      0.00598500000000
maximum current allowed in the coil

Imax =      64.94541136363637
Imax -Isphase ie safety limit for current is maintained

Iexces =      11.78541136363637
width of tooth

wt =      0.01229326045028
depth of yoke

```

ys = 0.01843989067542
rotor core depth

ycr = 0.01512181443452
depth of teeth

ds = 0.01554052727514
outer diameter of stator

Dout = 0.13448296359196
rea of 1 conductor in square meter

Alconduc = 3.460937499999999e-06
diameter of 1 conductor

dc = 0.00209919091244
total length of the conductor

TLC = 44.25888241699752
wt of conductors in the machine

Wcoils = 1.36327731019919
weight of the various parts of stator in kgs

Wteeth = 1.45568801334966

Wyoke = 4.26856267419451

Wstator = 7.08752799774336
wieght of various parts of rotor in kgs

Wcore = 1.38253444458064

Wmag = 0.66680602992405

Wrotor = 2.04934047450469
Total weight of machine

TWmac = 9.13686847224804
losses at various parts of machine in watts

Rphase = 0.03674453010054

Rcoil = 0.03674453010054
total copper loss in the conductors

Pcu = 3.115185388286824e+02

core loss at teeth/kg

Pcoreteeth = 1.138676931090131e+02

core loss at yoke/kg

Pcoreyoke = 43.14077055253947

total core loss in the machine

TPcore = 3.499049188831279e+02

TPcoreyoke = 1.841490829165595e+02

TPcoreteeth = 1.657558359665685e+02

total power loss in the machine

TPLoss = 6.690414338845081e+02

efficiency of machine considering all losses

effi2 = 81.76522544265256

efficiency of the machine considering just copper and core loss

effi = 81.97285395571170

total power supplied by the machine for use ie Pgenerated-
Plosses

TPsupp = 3.000000000000003e+03

ans = 3.390891511783781e+02

APPENDIX- A3

Matlab Results of Optimization for Machine –4

```
[x, feval, flag, out]=fmincon('mainfun', [7 1.1 9 .9 35000 0.8  
5],  
[], [], [], [], [7 1 8 .6 30000 .8 5],  
[10 1.2 10 .9 60000 1.2 7],  
'constrfun',options)  
exploitation(x)
```

Length of the machine
Len=X(1);

Lbytau=X(2);

J=current density in the conductors
J=X(3)*1e6;

alphamag= spread of the magnet with respect to the pole pitch
alphamag=X(4);

A is the specific electric loading of the machine
A=X(5);

Bg is the average magnetic flux density in the airgap
Bg=X(6);

PC is the permeance coefficient of the magnet (machine)
PC=X(7);

```
x =  
1.0e+04 *  
  
Columns 1 through 4  
0.000700000000000 0.000120000000000 0.000800000000000  
0.00007795216328  
  
Columns 5 through 7  
3.31490605521945 0.000120000000000 0.000700000000000
```

```
feval = 3.754025823274875e+02
```

```

flag =      1

out =

      iterations: 19
      funcCount: 258
      stepsize: 1
      algorithm: 'medium-scale: SQP, Quasi-Newton, line-
search'
      firstorderopt: []
      cgiterations: []

values of various parameters as calculated from the minimisation
routine
inner diameter of the machine

D =      0.07427230677622
  volatge developed by the winding for each pahse

Eph =      66.69119376931368
number of windings per phase/parallel path

Nph =      24
number of turns per coil

Ntc =      12
number of conductors in the machine

Z =      291
power developed at the coils of the machine

Pg =      3.740950767739435e+03
length of the magnet

lm =      0.00598500000000
maximum current allowed in the coil

Imax =      59.53329375000001
Imax -Isphase ie safety limit for current is maintained

Iexces =      6.37329375000001
width of tooth

wt =      0.01372549019608
depth of yoke

ys =      0.01783219421351

```

rotor core depth

yrct = 0.01495829175914
depth of teeth

ds = 0.01467536534863
outer diameter of stator

Dout = 0.13928742590049
area of 1 conductor in square meter

Alconduc = 3.357109375000000e-06
diameter of 1 conductor

dc = 0.00206746327954
total length of the conductor

TLC = 51.06814114387997
wt of conductors in the machine

Wcoils = 1.52582788504169
weight of the various parts of stator in kgs

Wteeth = 1.53479805053946

Wyoke = 4.32040133811613

Wstator = 7.38102727369729
weight of various parts of rotor in kgs

Wcore = 1.81949194712692

Wmag = 0.65387769471584

Wrotor = 2.47336964184276
Total weight of machine

TWmac = 9.85439691554004
losses at various parts of machine in watts

Rphase = 0.04370896978002

Rcoil = 0.04370896978002
total copper loss in the conductors

Pcu = 3.705627575674770e+02
core loss at teeth/kg

Pcoreteeth = 1.138676931090131e+02
core loss at yoke/kg

Pcoreyoke = 43.14077055253947
total core loss in the machine

TPcore = 3.611493562256917e+02

TPcoreyoke = 1.863854428225526e+02

TPcoreteeth = 1.747639134031390e+02
total power loss in the machine

TPLoss = 7.409507677394349e+02
efficiency of machine considering all losses

effi2 = 80.19351727028545
efficiency of the machine considering just copper and core loss

effi = 80.44047732188349
total power supplied by the machine for use ie Pgenerated-
Plosses

TPsupp = 3.000000000000000e+03

ans = 3.754025823274875e+02

APPENDIX- A4

Matlab Programs used in the Optimization

The program that initiates optimization

```
format long;
global mmm; global data; mmm=1;
options=optimset('TolX',1e-8,'TolFun',1e-8,'TolCon',1e-8);

[x, feval, flag, out]=fmincon('mainfun', [7 1.4 9 .9 35000 1 5],
                             [], [], [], [], [7 1.2 8 .6 30000 .8
5],
                             [10 1.4 10 .9 60000 1.2 7],
                             'constrfun',options)
exploitation(x)
```

APPENDIX- A5

Matlab Programs used in the Optimization

The program that uses the cost function for minimization

```
function [costfunc]= mainfun(X) ;
global mmm; global data;

Len=X(1)*1e-2;
Lbytau=X(2);
J=X(3)*1e6;
alphamag=X(4);
A=X(5);
Bg=X(6);
%Do=X(7)*1e-2;
PC=X(7);

Do=14e-2;
P=4;           %#poles
p=2;          %#pole pairs
Nslot= 12;    %#slots in the machine
ksf=0.4;     %slot fimaglling factor
kw=0.95;     %kw= winding factor = 0.95
kst=0.9;     %Kst=stacking factor
a=2;         %#parallel path for current
m=3;         %#phases
Bav=Bg;      % connotation difference
flkg=0.9;    % flux leakage factor
lgg= 0.95*1e-3;
mm           % corrected airgap length in
Nspeed=1800; % Nspeed = speed og the machine
=1800 rpm
Kst=0.9;     %Kst=stacking factor
roacu=8900;  % density of copper
road=9650;   % density of steel
roamag=9600; % density og magnet
Kv=0.94;     % Kv=core volume factor
Kc=.5e-1;
alpha=1.7;
beta=1.9;    % all constants for cal core loss
Kfb=2;       % 1<Kfb<3 constant for frictional
loss we choose mean of 2
```

```

Ispphase=53.16;           % rms value of current/phase
Iz=Ispphase/a;           % rms current in each parallel path
Bgsat=1.7;               % 1.6T

f=p*Nspeed/60;
omega=2*pi*f;

% from Len, Lbytau variables we get the value of D
D=(2*p*Len)/(pi*Lbytau); % this gives inner diameter
D;

%tau =slot pitch
tauslot=pi*D/Nslot;
sigma=2*pi/Nslot;        % bcos skew is by an angle
slot pitch
tauslot;
sigma;

% fimag= flux per pole
fimag=(Bav*pi*D*Len*alphamag)/(2*p);
%from the Bav=(2p*fimag)/(alphamag*piDLen)

% Z=total# of conductors
Z=floor((A*pi*D)/Iz) ;   % Iz is known
Z;

Eph=fimag*Z*(Nspeed/60)*P/a;
Eph;

Nph=floor(Z/(m*2*a));    % #turns/phase/parallel
path
Nph;

Ntc=Nph/2;               % 1 phase has 2 coils in a
parallel path
Ntc;

% check
% Ntc=# turns/coil=Ts=Nph bcos we have 2 coils in parallel/phase
Es=25 ;% 25 V

Ts=2*Es/(4.44*f*fimag*kw);
Ntccheck=floor(Ts);
Ntccheck;
%Ntc=Ntccheck;          % here we calculate based on the
checked value

```

```

%Nph=2*Ntc;
%Z=24*Ntc;
Z;
Nph;
Ntc;

Pg=omega*kw*Bg*A*alphanag*pi*pi*D*D*Len/(4*sqrt(2)*p);
Pg;

% Alslot=area of 1 slot
Alslot=(A*pi*D)/(Nslot*ksf*J); % A,J is a variable here

%magnet design
%flkg=0.9; % flux leakage factor
%lgg= 0.95; % corrected airgap length in mm

lm=PC*flkg*lgg; % length of magnet
lm;

% demag charac
Imax=-(-477.46e3)*lm/(2*Nph); % maximum current allowed without
demag
Imax;
Iexces=(-Imax+Isphase);
Iexces;

% if Isphase < Imax then lm, allowed else fimagnnd another lm

% DESIGN OF STATOR

% TOOTH WIDTH
wt=tauslot*Bg/Bgsat; % Bgsat is known
wt;

%yoke depth
ys=(pi*D*alphanag*Bg)/(4*p*Kst*Bgsat); %Kst=stacking factor
% alphanag is the vaiable, rest calculated
ys;

%rotor core depth
yrc=(pi*(D-2*lm)*alphanag*Bg)/(4*p*Kst*Bgsat);
yrc ;

%depth of teeth
% 2 formulae can be used for this.. choose 1 which gives u
minimum ds..

```

```

ds=A1slot/wt; % this is from belief that Ateeth=Aslot
gives minimum wt.
ds;

% other is from outer diameter of stator Do..
%ds=((Do-2*ys)-D)/2; % here Do is a variable, rest
calculated
%ds
%ds=ds1;
Dout=D+2*(ys+ds);
Dout;

% Diameter of the conductor
Alconduc=(Z*Iz)/(Ntc*24*J); % area of 1 conductor is got here,
J=variable

dc=sqrt(4*Alconduc/pi); % dc=diameter of 1 conductor
dc;

% weights and losses r found here....

%sigma= skew angle

Llcoil=(2*Len/cos(sigma))+(2*(pi*pi*D)/(4*p)); % length of
lturn with end turns
Llcoil;

Llc=pi*D; % linking cond length of 2 coils

Lpp=2*Ntc*Llcoil+Llc; %Tleng of conduc/para path/phase
Lpp;

TLC=3*2*Lpp; %T leng of conduc in mac.. 3 phases
and 2 para path/phase
TLC;

Vcoils=Alconduc*TLC; % volume of conductors
% weight of conductors
%roacu=9000; % density of copper
Wcoils=roacu*Vcoils; % wt of conductors in the machine
Wcoils;

% T.WEIGHT OF THE MACHINE
%Kv=0.94; % Kv=core volume factor
Vteeth=Kv*wt*ds*Len*Nslot; % volume of teeth

Vyoke=2*pi*Kv*((D/2)+ds+(ys/2))*ys*Len; %volume of yoke

```

```

%road=9650; % density of steel
Wteeth=road*Vteeth; % wt of teeth
Wyoke=road*Vyoke; % wt of yoke
Wteeth;
Wyoke;

Wstator=Wcoils+Wteeth+Wyoke; % weight of the stator
Wstator;

%weight of rotor

Wcore=road*Kv*pi*((D/2)-lgg-lm)2*Len; % wt of rotor core
%roamag=9600; % density of magnet
Wmag=roamag*2*pi*((D/2)-lgg-(lm/2))*lm*Len*alphamag; % wt of
magnets,..
%here alphamag is variable

Wrotor=Wcore+Wmag; % wt of rotor
Wrotor;

TWmac=Wstator+Wrotor; % wt of the whole machine
TWmac;

%LOSSES

roar=1.724*1e-8;
Rcoil=roar*Lpp/Alconduc; % roar =roa of cu at particular temp
and resis=roa*len/area
Rphase=Rcoil; % bcos here we have R of phase=
2*Rcoil parallel with 2*Rcoil

Pcu=m*Rphase*(Isphase)2; % m pahses and I2*R is used
Pcu;

% core losses
%Kc=.5e-1;
%alpha=1.7;
%beta=1.9; % all constants for cal core loss
Bteeth=1.5;
Byoke=0.9;

%Pcore=Kc*(falpha)*(Bavbeta); %W/kg of core
%Pcore;

Pcoreyoke=Kc*(falpha)*(Byokebeta); %W/kg of cor
Pcoreyoke;

```

```

Pcoreteeth=Kc*(f^alpha)*(Bteeth^beta); %W/kg of cor
Pcoreteeth;

TPcore=(Wteeth*Pcoreteeth)+(Wyoke*Pcoreyoke); % Watts of loss
at the core
TPcore;

%Kfb=2; % 1<Kfb<3 constant for frictional loss we choose mean
of 2
Pfric=Kfb*Wrotor*Nspeed*1e-3; %watts frictional loss
Pfric;

Pwind=2*(D)^3*Len*(Nspeed)^3*1e-6; % Watts
Pwind;

TPLoss=Pcu+TPcore+Pfric+Pwind; %Watts
TPLoss;

effi=(Pg-TPLoss)/Pg*100;
effi;
TPsupp=Pg-TPLoss;
TPsupp;

% costfunction which is to be minimised
%gama1= factor for TPLoss & gama2=factor for TWmac these
can be varied
gama1=0.5;
gama2=0.5;

costfunc=gama1*TPLoss+gama2*TWmac; %
data(1:14,mmm)=[X'; D; costfunc;Pg;Pcu;TPcore;effi;TPsupp];
mmm=mmm+1;

```

APPENDIX- A6

Matlab Programs used in the Optimization

The program for evaluating the constraints

```
function [c, ceq]= constrfun(X) ;
ceq=[];

%here=0;
%disp('here');

Len=X(1)*1e-2;
Lbytau=X(2);
J=X(3)*1e6;
alphamag=X(4);
A=X(5);
Bg=X(6);
%Do=X(7)*1e-2;
PC=X(7);

Do=14e-2;
P=4;           %#poles
p=2;          %#pole pairs
Nslot= 12;    %#slots in the machine
ksf=0.4;      %slot fimaglling factor
kw=0.95;     %kw= winding factor = 0.95
kst=0.9;     %Kst=stacking factor
a=2;         %#parallel path for current
m=3;         %#phases
Bav=Bg;      % connotation difference
flkg=0.9;    % flux leakage factor
lgg= 0.95*1e-3; % corrected airgap length in
mm
Nspeed=1800; % Nspeed = speed og the machine
=1800 rpm
Kst=0.9;     %Kst=stacking factor
roacu=8900;  % density of copper
road=9650;   % density of steel
roamag=9600; % density og magnet
Kv=0.94;     % Kv=core volume factor
Kc=.5e-1;
alpha=1.7;
beta=1.9;    % all constants for cal core loss
```

```

Kfb=2; % 1<Kfb<3 constant for frictional
loss we choose mean of 2

Isphase=53.16; % rms value of current/phase
Iz=Isphase/a; % rms current in each parallel path
Bgsat=1.7; % 1.6T

f=p*Nspeed/60;
omega=2*pi*f;

% from Len, Lbytau variables we get the value of D
D=(2*p*Len)/(pi*Lbytau); % this gives inner diameter
D;

%tau =slot pitch
tauslot=pi*D/Nslot;
sigma=2*pi/Nslot; % bcos skew is by an angle
slot pitch
tauslot;
sigma;

% fimag= flux per pole
fimag=(Bav*pi*D*Len*alphamag)/(2*p);
%from the Bav=(2p*fimag)/(alphamag*piDLen)

% Z=total# of conductors
Z=floor((A*pi*D)/Iz) ; % Iz is known
Z;

Eph=fimag*Z*(Nspeed/60)*P/a;
Eph;

Nph=floor(Z/(m*2*a)); % #turns/phase/parallel
path
Nph;

Ntc=Nph/2; % 1 phase has 2 coils in a
parallel path
Ntc;

% check
% Ntc=# turns/coil=Ts=Nph bcos we have 2 coils in parallel/phase
Es=25 ;% 25 V

Ts=2*Es/(4.44*f*fimag*kw);
Ntccheck=floor(Ts);
Ntccheck;

```

```

%Ntc=Ntccheck; % here we calculate based on the
checked value
%Nph=2*Ntc;
%Z=24*Ntc;
Z;
Nph;
Ntc;

Pg=omega*kw*Bg*A*alphanag*pi*pi*D*D*Len/(4*sqrt(2)*p);
Pg;

% Alslot=area of 1 slot
Alslot=(A*pi*D)/(Nslot*ksf*J); % A,J is a variable here

%magnet design
%flkg=0.9; % flux leakage factor
%lgg= 0.95; % corrected airgap length in mm

lm=PC*flkg*lgg; % length of magnet
lm;

% demag charac
Imax=-(-477.46e3)*lm/(2*Nph); % maximum current allowed without
demag
Imax;
Iexces=(-Imax+Isphase);
Iexces;

% if Isphase < Imax then lm, allowed else fimagnd another lm

% DESIGN OF STATOR

% TOOTH WIDTH
wt=tauslot*Bg/Bgsat; % Bgsat is known
wt;

%yoke depth
ys=(pi*D*alphanag*Bg)/(4*p*Kst*Bgsat); %Kst=stacking factor
% alphanag is the vaiable, rest calculated
ys;

%rotor core depth
yrc=(pi*(D-2*lm)*alphanag*Bg)/(4*p*Kst*Bgsat);
yrc ;

%depth of teeth

```

```

% 2 formulae can be used for this.. choose 1 which gives u
minimum ds..
ds=A1slot/wt;           % this is from belief that Ateeth=Aslot
gives minimum wt.
ds;

% other is from outer diameter of stator Do..
%ds=((Do-2*ys)-D)/2;    % here Do is a variable, rest
calculated
%ds
%ds=ds1;
Dout=D+2*(ys+ds);
Dout;

% Diameter of the conductor
Alconduc=(Z*Iz)/(Ntc*24*J); % area of 1 conductor is got here,
J=variable

dc=sqrt(4*Alconduc/pi); % dc=diameter of 1 conductor
dc;

% weights and losses r found here....
%sigma= skew angle

Llcoil=(2*Len/cos(sigma))+(2*(pi*pi*D)/(4*p)); % length of
lturn with end turns
Llcoil;

Llc=pi*D;           % linking cond length of 2 coils

Lpp=2*Ntc*Llcoil+Llc; %Tleng of conduc/para path/phase
Lpp;

TLC=3*2*Lpp;       %T leng of conduc in mac.. 3 phases
and 2 para path/phase
TLC;

Vcoils=Alconduc*TLC; % volume of conductors
% weight of conductors
%roacu=9000;        % density of copper
Wcoils=roacu*Vcoils; % wt of conductors in the machine
Wcoils;

% T.WEIGHT OF THE MACHINE
%Kv=0.94;          % Kv=core volume factor
Vteeth=Kv*wt*ds*Len*Nslot; % volume of teeth

```

```

Vyoke=2*pi*Kv*((D/2)+ds+(ys/2))*ys*Len;      %volume of yoke

%road=9650;                                % density of steel
Wteeth=road*Vteeth;                          % wt of teeth
Wyoke=road*Vyoke;                             % wt of yoke
Wteeth;
Wyoke;

Wstator=Wcoils+Wteeth+Wyoke; % weight of the stator
Wstator;

%weight of rotor

Wcore=road*Kv*pi*((D/2)-lgg-lm)^2*Len; % wt of rotor core
%roamag=9600;                               % density of magnet
Wmag=roamag*2*pi*((D/2)-lgg-(lm/2))*lm*Len*alphamag; % wt of
magnets,.. here alphamag is variable

Wrotor=Wcore+Wmag;                           % wt of rotor
Wrotor;

TWmac=Wstator+Wrotor;                         % wt of the whole machine
TWmac;

%LOSSES

roar=1.724*1e-8;
Rcoil=roar*Lpp/Alconduc; % roar =roa of cu at particular temp
and resis=roa*len/area
Rphase=Rcoil; % bcos here we have R of phase=
2*Rcoil parallel with 2*Rcoil

Pcu=m*Rphase*(Isphase)^2; % m pahses and I^2*R is used
Pcu;

% core losses
%Kc=.5e-1;
%alpha=1.7;
%beta=1.9; % all constants for cal core loss
Bteeth=1.5;
Byoke=0.9;

%Pcore=Kc*(f^alpha)*(Bav^beta); %W/kg of core
%Pcore;

%TPcore=(Wteeth+Wyoke)*Pcore; % Watts of loss at the core
%TPcore;

```

```

Pcoreyoke=Kc*(f^alpha)*(Byoke^beta); %W/kg of cor
Pcoreyoke;

Pcoreteeth=Kc*(f^alpha)*(Bteeth^beta); %W/kg of cor
Pcoreteeth;

TPcore=(Wteeth*Pcoreteeth)+(Wyoke*Pcoreyoke); % Watts of loss
at the core
TPcore;

%Kfb=2; % 1<Kfb<3 constant for frictional loss we choose mean
of 2
Pfric=Kfb*Wrotor*Nspeed*1e-3; %watts frictional loss
Pfric;

Pwind=2*(D)^3*Len*(Nspeed)^3*1e-6; % Watts
Pwind;

TPLoss=Pcu+TPcore+Pfric+Pwind; %Watts
TPLoss;

effi=(Pg-TPLoss)/Pg*100;
effi;
TPsupp=Pg-TPLoss;
TPsupp;

c=[Iexces -Do+Dout 3000-TPsupp alphamag-0.9];

```

APPENDIX- A7

Matlab Programs used in the Optimization

The program for printing the optimized machine parameters

```
function [costfunc]= exploitation(X) ;

Len=X(1)*1e-2;
Lbytau=X(2);
J=X(3)*1e6;
alphamag=X(4);
A=X(5);
Bg=X(6);
%Do=X(7)*1e-2;
PC=X(7);

Do=14e-2;
P=4;                                %#poles
p=2;                                  %#pole pairs
Nslot= 12;                            %#slots in the machine
ksf=0.4;                              %slot fimaglling factor
kw=0.95;                              %kw= winding factor = 0.95
kst=0.9;                              %Kst=stacking factor
a=2;                                   %#parallel path for current
m=3;                                   %#phases
Bav=Bg;                               % connotation difference
flkg=0.9;                             % flux leakage factor
lgg= 0.95*1e-3;                       % corrected airgap length in
mm
Nspeed=1800;                          % Nspeed = speed og the machine
=1800 rpm
Kst=0.9;                              %Kst=stacking factor
roacu=8900;                           % density of copper
road=9650;                             % density of steel
roamag=9600;                           % density og magnet
Kv=0.94;                               % Kv=core volume factor
Kc=.5e-1;
alpha=1.7;
beta=1.9;                              % all constants for cal core loss
Kfb=2;                                 % 1<Kfb<3 constant for frictional
loss we choose mean of 2

Ispphase=53.16;                       % rms value of current/phase
Iz=Ispphase/a;                        % rms current in each parallel path
```

```

Bgsat=1.7; % 1.6T

f=p*Nspeed/60;
omega=2*pi*f;

disp('values of various parameters as calculated from the
minimisation routine');
disp('');

% from Len, Lbytau variables we get the value of D
D=(2*p*Len)/(pi*Lbytau); % this gives inner diameter
disp('inner diameter of the machine');
D

%tau =slot pitch
tauslot=pi*D/Nslot;
sigma=2*pi/Nslot; % bcos skew is by an angle
slot pitch
tauslot;
sigma;

% fimag= flux per pole
fimag=(Bav*pi*D*Len*alphamag)/(2*p);
%from the Bav=(2p*fimag)/(alphamag*piDLen)

% Z=total# of conductors
Z=floor((A*pi*D)/Iz) ; % Iz is known
Z;

Eph=fimag*Z*(Nspeed/60)*P/a;
Eph;
disp('');
disp(' volatge developed by the winding for each pahse');
Eph
disp('');
Nph=floor(Z/(m*2*a)); % #turns/phase/parallel
path
Nph;
disp('number of windings per phase/parallel path');
Nph
disp('');
Ntc=Nph/2; %1 phase has 2 coils in a
parallel path
disp('number of turns per coil');
Ntc
disp('');

```

```

% check
% Ntc=# turns/coil=Ts=Nph bcos we have 2 coils in parallel/phase
Es=25 ;% 25 V

Ts=2*Es/(4.44*f*fimag*kw);
Ntccheck=floor(Ts);
Ntccheck;
%Ntc=Ntccheck;           % here we calculate based on the
checked value
%Nph=2*Ntc;
%Z=24*Ntc;
disp('number of conductors in the machine');
Z
disp('');
Nph;
Ntc;

Pg=omega*kw*Bg*A*alphanag*pi*pi*D*D*Len/(4*sqrt(2)*p);
Pg;
disp('power developed at the coils of the machine');
Pg
disp('');

% Alslot=area of 1 slot
Alslot=(A*pi*D)/(Nslot*ksf*J); % A,J is a variable here

%magnet design
%flkg=0.9;                % flux leakage factor
%lgg= 0.95;              % corrected airgap length in mm

lm=PC*flkg*lgg;          % length of magnet
disp('length of the magnet');
lm
disp('');

% demag charac
Imax=-(-477.46e3)*lm/(2*Nph); % maximum current allowed without
demag
disp('maximum current allowed in the coil');
Imax
disp('');

%%Iexces=(Imax-Isphase);
%% is the right one;

Iexces=(Imax-Isphase);
disp('Imax -Isphase ie safety limit for current is maintained');

```

```

Iexces
disp('');
% if Isphase < Imax then lm, allowed else fimagnd another lm

% DESIGN OF STATOR

% TOOTH WIDTH
wt=tauslot*Bg/Bgsat;           % Bgsat is known
wt;
disp('width of tooth');
wt
disp('');

%yoke depth
ys=(pi*D*alphamag*Bg)/(4*p*Kst*Bgsat); %Kst=stacking factor
% alphamag is the vaiable, rest calculated
ys;
disp('depth of yoke');
ys
disp('');

%rotor core depth
yrc=(pi*(D-2*lm)*alphamag*Bg)/(4*p*Kst*Bgsat);
yrc ;
disp('rotor core depth');
yrc
disp('');

%depth of teeth
% 2 formulae can be used for this.. choose 1 which gives u
minimum ds..
ds=Aslot/wt;                 % this is from belief that Ateeth=Aslot
gives minimum wt.
ds;
disp('depth of teeth');
ds
disp('');

% other is from outer diameter of stator Do..
%ds=((Do-2*ys)-D)/2;         % here Do is a variable, rest
calculated
%ds
%ds=ds1;
Dout=D+2*(ys+ds);
Dout;
disp('outer diameter of stator');
Dout

```

```

disp('');

% Diameter of the conductor
Alconduc=(Z*Iz)/(Ntc*24*J); % area of 1 conductor is got here,
J=variable
disp('area of 1 conductor in square meter');
Alconduc
disp('');

dc=sqrt(4*Alconduc/pi); % dc=diameter of 1 conductor
dc;
disp('diameter of 1 conductor');
dc
disp('');

% weights and losses r found here....

%sigma= skew angle

Llcoil=(2*Len/cos(sigma))+(2*(pi*pi*D)/(4*p)); % length of
lturn with end turns
Llcoil;

Llc=pi*D; % linking cond length of 2 coils

Lpp=2*Ntc*Llcoil+Llc; %Tleng of conduc/para path/phase
Lpp;

TLC=3*2*Lpp; %T leng of conduc in mac.. 3 phases
and 2 para path/phase
disp('total length of the conductor');
TLC
disp('');

Vcoils=Alconduc*TLC; % volume of conductors
% weight of conductors
%roacu=9000; % density of copper
Wcoils=roacu*Vcoils; % wt of conductors in the machine
disp('wt of conductors in the machine');
Wcoils
disp('');

% T.WEIGHT OF THE MACHINE
%Kv=0.94; % Kv=core volume factor
Vteeth=Kv*wt*ds*Len*Nslot; % volume of teeth

```

```

Vyoke=2*pi*Kv*((D/2)+ds+(ys/2))*ys*Len;      %volume of yoke

%road=9650;                                  % density of steel
Wteeth=road*Vteeth;                          % wt of teeth
Wyoke=road*Vyoke;                            % wt of yoke
disp('weight of the various parts of stator in kgs');
Wteeth
Wyoke

Wstator=Wcoils+Wteeth+Wyoke; % weight of the stator
Wstator
disp('');
%weight of rotor
disp('wieght of various parts of rotor in kgs');
Wcore=road*Kv*pi*((D/2)-lgg-lm)^2*Len; % wt of rotor core
%roamag=9600;                               % density of magnet
Wmag=roamag*2*pi*((D/2)-lgg-(lm/2))*lm*Len*alphanmag; % wt of
magnets,.. here alphanmag is variable
Wcore
Wmag
Wrotor=Wcore+Wmag;                          % wt of rotor
Wrotor

TWmac=Wstator+Wrotor;                      % wt of the whole machine
disp('');
disp('Total weight of machine');
TWmac
disp('');
%LOSSES
disp('');
disp('losses at various parts of machine in watts');
roar=1.724*1e-8;
Rcoil=roar*Lpp/Alconduc; % roar =roa of cu at particular temp
and resis=roa*len/area
Rphase=Rcoil; % bcos here we have R of phase=
2*Rcoil parallel with 2*Rcoil
Rphase
Rcoil

Pcu=m*Rphase*(Ispphase)^2; % m pahses and I^2*R is used
disp('total copper loss in the conductors');
Pcu
disp('');
% core losses

```

```

%Kc=.5e-1;
%alpha=1.7;
%beta=1.9;           % all constants for cal core loss
Bteeth=1.5;
Byoke=0.8;

%Pcore=Kc*(f^alpha)*(Bav^beta); %W/kg of core
%Pcore;

%TPcore=(Wteeth+Wyoke)*Pcore; % Watts of loss at the core
Pcoreyoke=Kc*(f^alpha)*(Byoke^beta); %W/kg of cor
Pcoreyoke;

Pcoreteeth=Kc*(f^alpha)*(Bteeth^beta); %W/kg of cor
Pcoreteeth;
disp('core loss at teeth/kg');
Pcoreteeth
disp('core loss at yoke/kg');
Pcoreyoke

TPcore=(Wteeth*Pcoreteeth)+(Wyoke*Pcoreyoke); % Watts of loss
at the core
TPcore;

disp('total core loss in the machine');
TPcore
TPcoreyoke=Pcoreyoke*Wyoke;
TPcoreyoke

TPcoreteeth=Wteeth*Pcoreteeth;
TPcoreteeth

%Kfb=2; % 1<Kfb<3 constant for frictional loss we choose mean
of 2
Pfric=Kfb*Wrotor*Nspeed*1e-3; %watts frictional loss
Pfric;

Pwind=2*(D)^3*Len*(Nspeed)^3*1e-6; % Watts
Pwind;

TPLoss=Pcu+TPcore+Pfric+Pwind; %Watts
disp('total power loss in the machine');
TPLoss

effi2=(Pg-TPLoss)/Pg*100;
disp('');
disp('efficiency of machine considering all losses');

```

```

effi2
disp('');
Loseffi=Pcu+TPcore;

effi=(Pg-Loseffi)/Pg*100;
disp('efficiency of the machine considering just copper and core
loss');
effi
TPsupp=Pg-TPLoss;
disp('');
disp('total power supplied by the machine for use ie Pgenerated-
Plosses');
TPsupp
disp('');
% costfunction which is to be minimised
%gama1= factor for TPLoss      &      gama2=factor for TWmac these
can be varied
gama1=0.5;
gama2=0.5;
costfunc=gama1*TPLoss+gama2*TWmac;    %

```

APPENDIX- A8

Matlab Programs used in the Linear Reluctance Model of P.M.Machines

```
%*****  
*****  
% linear reluctance model for the Delphi steering motor  
%*****  
*****  
  
clear;  
format long e;  
  
%stator parameters  
%*****  
Ns=18; % #slots  
LOD=70e-3; % lamination outer dia  
Ds=LOD;  
yt=4.65e-3; % yoke thickness  
LID=33.9e-3; % Lamination inner dia  
D=LID;  
%ds= ((LOD-2*yt)-LID)/2; % slot depth  
ds=13.4e-3;  
wt=3.15e-3; % tooth width  
wo=0.08e-2; % slot opening  
Lstk=31.0e-3; % stack length of long stack  
lstk=3.9e-2; % stack length of short stack  
%slamda=pi*D/Ns % stator slot pitch  
%wt=slamda/2 % tooth width =slot pitch /2  
  
%winding parameters  
%*****  
Ncp=4; % #coils per phase  
Nc=12; % #coils  
Ntc=54; % #turns/coil  
Tauwind=3; % winding pitch  
kw=0.9 ; % winding factor  
  
%rotor parameters  
%*****  
ROD=32.45e-3; % rotor outer dia  
Dr=ROD;  
Drc=26.60e-3; % rotor core dia  
%yrc=Drc/2; % rotor core thickness  
yrc=8.3e-3;  
lm=2.925e-3; %magnet thickenss
```

```

ge=.725e-3;          %air gap length g'

% magnet parameters
%*****
P=6;p=P/2;          %#poles=P or pole pairs=p
alpha=0.966;       %magnet coverage alpha
Br=1.2;            %magnet remanent flux density
mumag=1.1;        %relative permeability of magnet

% general constants
%*****
mu=4e-7*pi;        %permeability of vaccumm
musteel=4e3;       %permeability of steel
Bsat=1.7;          %saturation flux density of the stators

% motor ratings
%*****

power=1372 ;%W
Ip=10.7;%A
Irms=sqrt(2/3)*Ip;%A

Nsin=4/pi*kw*Ntc;
Ks=3*Nsin*Ip/(4*p);
Taus=Ks;           % stator back emf in AT

Nsp=Ns/P;
Nsp=2*Nsp;
deltetaks=2*pi/Ns;
deltetakr=2*pi*alpha/P;
S_mnc_r=(pi/12)-(deltetaks*Nsp-deltetakr);
S_mnc_c=D/2*((pi/12)-(deltetaks*Nsp-deltetakr));

%fi of the magnet at full coverage and partial coverage
fimsf=Br*Lstk*deltetaks*(Dr-lm)/2;
fimps=Br*Lstk*S_mnc_r*(Dr-lm)/2;

% RELUCTANCES AT VARIOUS PARTS OF
%STATOR

Ry= (deltetaks*(Ds-yt)/2)/(mu*musteel*yt*Lstk); %yoke

Rt=ds/(mu*musteel*wt*Lstk); %teeth

w_avg= (pi*D/Ns)-wt;
spr=(1/w_avg)*(.1+1.225/3)*1e-2;

```

```

Rsl=1/(Lstk*spr*mu); % slot leakage

Rpl=(D/2)*deltetaks/(Lstk*mu*ge); % half peripheral
leakage

Rspl=Rsl+Rpl/2;
Rmpl=Rpl/2;

Rag= ge/(mu*Lstk*Dr/2*deltetaks); %air gap

%ROTOR

% magnet at full coverage of slot
Rmf=lm/(mu*mumag*Lstk*Dr/2*deltetaks);

% magnet at partial coverage of slot
Rmp=lm/(mu*mumag*Lstk*Dr/2*S_mnc_r);

Rc= yrc/(mu*musteel*(Drc-yrc)/2*Lstk*deltetaks); % core

Taumf=fimsf*Rmf; %tau of magnet at full coverage
Taump=fimsp*Rmp; %tau of magnet at partial coverage

T=Taumf;

%diary resulmac2.m

Ry
Rt
Rsl
Rpl
Rspl
Rmpl
Rc
Rag
Rmf
Rmp
fimsp
fimsf
Taumf
Taump

```

```

At=wt*Lstk;
Ag=Lstk*(D/2)*deltetaks;
Amf=Lstk*deltetaks*(Dr)/2;
Amp=Lstk*S_mnc_r*(Dr)/2;
Arc=(Drc-yrc)/2*Lstk*deltetaks;

At
Ag
Amf
Amp
Arc

stau=pi*D/24;
stau
tw=stau/2;
tw
yt
ds

%formation of reluctances in matrix form

for i=1:Nsp,
    for j=1:Nsp,
        R(i,j)=0;
    end
end

% formation of reluc matrix and calculation of the coresponding
flux densities
num=0;
angle=0;
Rtsl=Rspl*Rt/(Rspl+Rt);

roa=lm/(mu*mumag*Lstk*Dr/2*pi/180)

for angle=0:20:20,
    num=num+1;
    nmacTRmtaucall    %calling func tau

for i=1:Nsp,

    if i==1
        j=Nsp;
        R(i,j)=-Rr(j);
        R(i,i+1)=-Rr(i);

```

```

        R(i,i)=Ry+Rc+Rr(i)+Rr(j);

elseif i==Nspp
    j=1;
    R(i,j)=-Rr(i);
    R(i,i-1)=-Rr(i-1);
    R(i,i)=Ry+Rc+Rr(i)+Rr(i-1);

else
    R(i,i+1)=-Rr(i);
    R(i,i-1)=-Rr(i-1);
    R(i,i)=Ry+Rc+Rr(i)+Rr(i-1);
end

end
num;
Rr
Tauloop(:,num)=tau';
R;
fi=inv(R)*tau';
FIloop(:,num)=fi;

Fi=fi;
FIbranch(:,num)=[fi(1)-fi(2) fi(2)-fi(3) fi(3)-fi(4) fi(4)-
fi(5)...
                fi(5)-fi(6) fi(6)-fi(1)]';
%fimag(:,num)=fi';
taubbranch(:,num)=tauu';
end

%BB
taubbranch
FIloop
Tauloop
FIbranch
fimag

Bairgap=FIbranch/Ag;
Bairgap

fiteeth=FIbranch*Rtsl/Rt;
fiteeth
Bteeth=fiteeth/At;
Bteeth

```

```

% printing of all the values on calculation
%diary off;

nmacTRmtaucall      %calling func tau

if (angle==0)
    Rm1=roa/20;  Rm2=roa/20;  Rm3=roa/20;

    Rmml1=Rm1*Rmpl/(Rm1+Rmpl);
    Rmml2=Rm2*Rmpl/(Rm2+Rmpl);
    Rmml3=Rm3*Rmpl/(Rm3+Rmpl);

    Rr(1)=Rtssl+Rag+Rmml1;
    Rr(2)=Rtssl+Rag+Rmml2;
    Rr(3)=Rtssl+Rag+Rmml3;
    Rr(4)=Rr(1);
    Rr(5)=Rr(2);
    Rr(6)=Rr(3);

    Almag=lm/(mu*mumag*Rm1);
    fi1=Br*Almag;          % 0.9 is to accomodate fringing of
flux lines
    tau1=fi1*Rmml1;

    A2mag=lm/(mu*mumag*Rm2);
    fi2=Br*A2mag;
    tau2=fi2*Rmml2;

    A3mag=lm/(mu*mumag*Rm3);
    fi3=Br*A3mag;
    tau3=fi3*Rmml3;

    fi4=-fi1;
    fi5=-fi2;
    fi6=-fi3;
    tau4=-tau1;
    tau5=-tau2;
    tau6=-tau3;

    tau(1)=tau1-tau6;
    tau(2)=tau2-tau1;
    tau(3)=tau3-tau2;
    tau(4)=tau4-tau3;
    tau(5)=tau5-tau4;

```

```

tau(6)=tau6-tau5;

elseif (angle==7.5)
    Rm1=roa/20; Rm2=roa/20; Rm3=roa/20;
    Rmml1=Rm1*Rmpl/(Rm1+Rmpl);
    Rmml2=Rm2*Rmpl/(Rm2+Rmpl);
    Rmml3=Rm3*Rmpl/(Rm3+Rmpl);

    Rr(1)=Rts1+Rag+Rmml1;
    Rr(2)=Rts1+Rag+Rmml2;
    Rr(3)=Rts1+Rag+Rmml3;
    Rr(4)=Rr(1);
    Rr(5)=Rr(2);
    Rr(6)=Rr(3);

    A1mag=lm/(mu*mumag*Rm1);
    fi1=Br*A1mag;
    tau1=fi1*Rmml1;

    A2mag=lm/(mu*mumag*Rm2);
    fi2=Br*A2mag;
    tau2=fi2*Rmml2;

    A3mag=lm/(mu*mumag*Rm3);
    fi3=Br*A3mag;
    tau3=fi3*Rmml3;

    fi4=-fi1;
    fi5=-fi2;
    fi6=-fi3;

    tau4=-tau1;
    tau5=-tau2;
    tau6=-tau3;

    tau(1)=tau1-tau6;
    tau(2)=tau2-tau1;
    tau(3)=tau3-tau2;
    tau(4)=tau4-tau3;
    tau(5)=tau5-tau4;
    tau(6)=tau6-tau5;

else
    Rm1=roa/20; Rm2=roa/20; Rm3=roa/20;

```

```

Rmml1=Rm1*Rmpl/(Rm1+Rmpl);
Rmml2=Rm2*Rmpl/(Rm2+Rmpl);
Rmml3=Rm3*Rmpl/(Rm3+Rmpl);

Rr(1)=Rtsl+Rag+Rmml1;
Rr(2)=Rtsl+Rag+Rmml2;
Rr(3)=Rtsl+Rag+Rmml3;
Rr(4)=Rr(1);
Rr(5)=Rr(2);
Rr(6)=Rr(3);

Almag=lm/(mu*mumag*Rm1);
fi1=-Br*Almag;
tau1=fi1*Rmml1;

A2mag=lm/(mu*mumag*Rm2);
fi2=Br*A2mag;
tau2=fi2*Rmml2;

A3mag=lm/(mu*mumag*Rm3);
fi3=Br*A3mag;
tau3=fi3*Rmml3;

fi4=-fi1;
fi5=-fi2;
fi6=-fi3;
tau4=-tau1;
tau5=-tau2;
tau6=-tau3;

tau(1)=tau1-tau6;
tau(2)=tau2-tau1;
tau(3)=tau3-tau2;
tau(4)=tau4-tau3;
tau(5)=tau5-tau4;
tau(6)=tau6-tau5;

end
fi=[fi1 fi2 fi3 fi4 fi5 fi6];
fi;
tauu=[tau1 tau2 tau3 tau4 tau5 tau6];
tauu;
fimag(:,num)=fi';

```

Appendix – B1

PERMANENT MAGNET PROPERTIES

The magnetic characteristics of permanent magnets [3]

	B_r (kG)	H_c (Oersted)	Intrinsic H_c (Oersted)	$(B \times H)_{max}$ MGOe	Permeability at $(B \times H)_{max}$	Average Recoil Permeability
3½% Chrome Steel	9.7	60	60	0.30	171	35
38% Cobalt steel	10.4	230	230	0.38	45	12
Alnico 1	7.0	440	450	1.4	14	14
Alnico 2 (sintered)	7.1	550	570	1.5	12	12
Alnico 5 DG	13.3	670	670	6.5	17	17
Alnico 6	10.5	780	800	3.9	13	13
Alnico 8 HC	7.8	1,900	2,170	6.0	-	5
Alnico 9	10.6	1,500	1,500	9.0	-	-
Ceramic 1 (Ba Ferrite)	2.3	1,860	3,250	1.05	1.2	1.2
Ceramic 2 (Ba Ferrite)	2.9	2,400	3,000	1.8	1.3	1.1
Rubber Ceramic (YRM-2B)	2.2	2,000	-	1.1	-	-
Molded Ceramic 2	2.8	2,400	2,500	1.96	-	-
Ceramic 5 (Ba Ferrite)	3.8	2,400	2,500	3.4	1.3	1.1
Ceramic 8B	4.0	2,800	2,900	4.1	-	-
Cunife 1	5.5	530	540	1.4	12	3.7

	B _r (kG)	H _c (Oersted)	Intrinsic H _c (Oersted)	(B×H) _{max} MGOe	Permeability at (B×H) _{max}	Average Recoil Permeability
ESD 31 (Fe-Co-Pb)	5.0	1,000	1,000	2.3	5.3	1.9
ESD 32	6.8	960	960	3.0	8.2	2.6
FECCO (Fe-Cr-Co)	13.5	600	605	5.25	-	-
Manganese – Aluminum	5.45	2,550	3,150	5.0	-	-
Nd-Fe-B (NelGT-24K)	10.2	9,800	19,000	25	-	1.05
Nd-Fe-B (Neomax 27H)	10.8	8,500- 10,200	>17,000	25-28	1.1	1.05
Nd-Fe-B (Neomax 35)	12.1	10,000- 11,500	10,500- 13,000	33-36	1.1	1.05
Nd-Fe-B (Magnaquench I)	6.1	5,300	15,000	8.0	-	1.15
Nd-Fe-B (Magnaquench II)	8.0	6,500	16,000	13.0	-	1.15
Nd-Fe-B (Magnaquench III)	11.75	10,500	13,000	32	-	1.05
Platinum-Cobalt	6.4	5,000	7,200	9.5	-	1.2
Remalloy	9.7	250	250	1.1	43	13
Samarium-Cobalt (Hicorex 22A)	9.0	8,750	15,000	18-22	-	-
Samarium-Cobalt (Hicorex 26A)	10.1	9,500	10,000	24-27	-	-
SMCO 31	11.3	8,000	8,000	31	-	-
Vicalloy 1	7.5	250	250	0.8	-	-

The physical characteristics of permanent magnets

	Density (g/cm ³)	Thermal Conductivity (W/cm-°C)	Hardness	Maximum Operating Temp. (°C)	Curie Temp. (°C)	Electrical Resistivity (μΩ-cm)	Coefficient of Thermal Expansion (1/°C)
Cast Alnicos	7.3	-	45-60 R _c	550	850-890	50-75	12×10 ⁻⁶
Sintered Alnicos	6.7	-	50-65 R _c	-	-	50-68	-
Ceramic Magnets	4.6-5.1	0.0126	-	350	450	> 10 ¹⁰	13×10 ⁻⁶
SUMCO (H22)	8.3	0.104	600 (Hv)	210	710	50	66×10 ⁻⁶
ESD	7.6	0.163	350 (Hv)	500	640	68	11.3×10 ⁻⁶
Nd-Fe-B (Neomax 35)	7.4	-	600 (Hv)	-	-	144	3.4×10 ⁻⁶
Nd-Fe-B (Magnaquench I)	6.0	-	37 R _c	125	312	18,000	3.8×10 ⁻⁶
Nd-Fe-B (Magnaquench II)	7.5	-	60 R _c	150	312	160	Nonlinear
Nd-Fe-B (Magnaquench III)	7.5	-	60 R _c	150	315	160	Nonlinear